

**ACCOUNTING FOR ADSORBED GAS AND ITS EFFECT ON  
PRODUCTION BEHAVIOR OF SHALE GAS RESERVOIRS**

A Thesis

by

SALMAN AKRAM MENGAL

Submitted to the Office of Graduate Studies of  
Texas A&M University  
in partial fulfillment of the requirements for the degree of

MASTER OF SCIENCE

August 2010

Major Subject: Petroleum Engineering

**ACCOUNTING FOR ADSORBED GAS AND ITS EFFECT ON  
PRODUCTION BEHAVIOR OF SHALE GAS RESERVOIRS**

A Thesis

by

SALMAN AKRAM MENGAL

Submitted to the Office of Graduate Studies of  
Texas A&M University  
in partial fulfillment of the requirements for the degree of

MASTER OF SCIENCE

Approved by:

Chair of Committee,	Robert A. Wattenbarger
Committee Members,	J.Bryan Maggard
	Yuefeng Sun
Head of Department,	Stephen A.Holditch

August 2010

Major Subject: Petroleum Engineering

## ABSTRACT

Accounting for Adsorbed Gas and Its Effect on Production Behavior of Shale

Gas Reservoirs. (August 2010)

Salman Akram Mengal, B.Sc., University of Engineering and Technology, Lahore,

Pakistan

Chair of Advisory Committee: Dr. Robert Wattenbarger

Shale gas reservoirs have become a major source of energy in recent years. Developments in hydraulic fracturing technology have made these reservoirs more accessible and productive. Apart from other dissimilarities from conventional gas reservoirs, one major difference is that a considerable amount of gas produced from these reservoirs comes from desorption. Ignoring a major component of production, such as desorption, could result in significant errors in analysis of these wells. Therefore it is important to understand the adsorption phenomenon and to include its effect in order to avoid erroneous analysis.

The objective of this work was to imbed the adsorbed gas in the techniques used previously for the analysis of tight gas reservoirs. Most of the desorption from shale gas reservoirs takes place in later time when there is considerable depletion of free gas and the well is undergoing boundary dominated flow (BDF). For that matter BDF methods, to estimate original gas in place (OGIP), that are presented in previous literature are reviewed to include adsorbed gas in them. More over end of the transient time data can

also be used to estimate OGIP. Kings modified  $z^*$  and Bumb and McKee's adsorption compressibility factor for adsorbed gas are used in this work to include adsorption in the BDF and end of transient time methods.

Employing a mass balance, including adsorbed gas, and the productivity index equation for BDF, a procedure is presented to analyze the decline trend when adsorbed gas is included. This procedure was programmed in *EXCEL VBA* named as shale gas PSS with adsorption (SGPA). SGPA is used for field data analysis to show the contribution of adsorbed gas during the life of the well and to apply the BDF methods to estimate OGIP with and without adsorbed gas. The estimated OGIP's were then used to forecast future performance of wells with and without adsorption.

OGIP estimation methods when applied on field data from selected wells showed that inclusion of adsorbed gas resulted in approximately 30% increase in OGIP estimates and 17% decrease in recovery factor (RF) estimates. This work also demonstrates that including adsorbed gas results in approximately 5% less stimulated reservoir volume estimate.

## **DEDICATION**

The work is dedicated to my parents for their love, kindness, and support for what I am today. They provided me with true guidance and knowledge and determination at every step. I would also want to dedicate this work to my wife for her patience and my extended family members for their continuous support.

## **ACKNOWLEDGEMENTS**

I would like to thank Almighty Allah for all His blessings. I would also like to express my thanks from core of my heart to Dr Robert A. Wattenbarger, chair of my committee, for his dedicated guidance. His commitment, friendly nature and support made my job easy. It was a great honor to have worked under the supervision of Dr. Robert A. Wattenbarger and the knowledge he gave me will always be a part of me. I would also like to thank Dr. J. Bryan Maggard and Dr. Yuefeng Sun, members of my committee, for their continuous contribution.

I am also grateful to Fulbright for giving me the opportunity to complete my M.S. degree at the Harold Vance Department of Petroleum Engineering, allowing me to be part of such great educational environment.

I give special thanks to the faculty members, my colleagues, and friends for their help and support.

## TABLE OF CONTENTS

	Page
ABSTRACT .....	iii
DEDICATION.....	v
ACKNOWLEDGEMENTS .....	vi
TABLE OF CONTENTS .....	vii
LIST OF TABLES .....	x
LIST OF FIGURES .....	xi
 CHAPTER	
I      INTRODUCTION .....	1
1.1    Background .....	1
1.2    Problem Description .....	2
1.3    Research Objectives.....	3
II      LITERATURE REVIEW .....	5
III     DEVELOPMENT AND VALIDATION OF MASS BALANCE EQUATION FOR SHALE GAS INCLUDING ADSORPTION .....	10
3.1    Adsorption in Shale Gas Reservoirs (Barnett) .....	10
3.2    Mass Balance for Shale Gas Including Adsorption (SGPA) .....	12
3.3    Validation of Our Approach (Kings $z^*$ ) .....	17
3.4    Validation of Our Approach (Bumb & McKee's Compressibility Expression for Adsorption) .....	19
3.5    Validation of Our Approach (Unconventional Reservoir Simulator).....	20
IV     OGIP ESTIMATION METHODS (INCLUDING ADSORBED GAS).....	21

CHAPTER	Page
4.1 Review of BDF Methods .....	21
4.2 Palacio and Blasingame's Method Including Adsorbed Gas.....	27
4.3 Ibrahim, Wattenbarger and Helmy's Method Including Adsorbed Gas .....	30
4.4 Anderson et al.'s Method Including Adsorbed Gas .....	31
4.5 OGIP Estimation from Transient Flow Data.....	32
V FIELD CASES .....	35
5.1 BDF in Shale Gas Reservoirs .....	35
5.2 Field Data Analysis.....	36
5.3 Well 137 .....	39
5.4 Well 257 .....	43
5.5 Well 285 .....	47
5.6 Well 314.....	51
5.7 Results.....	55
5.8 Discussion .....	57
VI CONCLUSIONS AND RECOMMENDATIONS.....	60
6.1 Conclusions .....	60
6.2 Recommendations for Future Work .....	61
NOMENCLATURE .....	62
REFERENCES .....	66
APPENDIX A DERIVATION OF KINGS $z^*$ FOR DESORBED GAS AND COMPARISON WITH SGPA RESULTS.....	69
APPENDIX B BUMB & MCKEE'S COMPRESSIBILITY EXPRESSION FOR ADSORBED GAS AND COMPARISON WITH SGPA RESULTS .....	76
APPENDIX C COMPARISON OF SGPA RESULTS WITH NUMERICAL SIMULATOR (URS 01.2009) .....	84
APPENDIX D BOUNDARY DOMINATED FLOW METHODS (INCLUDING ADSORPTION) .....	91
APPENDIX E SIMULATED DATA ANALYSIS .....	104

	Page
VITA.....	111

## LIST OF TABLES

TABLE	Page
5.1 Summary of Results, Well 137 .....	42
5.2 Summary of Results, Well 257 .....	46
5.3 Summary of Results, Well 285 .....	50
5.4 Summary of Results, Well 314 .....	54
5.5 OGIP, SRV and RF Ratio .....	56
A.1 Match cases: Comparison of SGPA Results with King's Modified Material Balance Equation.....	71
B.1 Match cases: Bumb & McKee's Compressibility Expression Applied Results with SGPA Results.....	79
C.1 Match cases: Comparison of SGPA and Numerical Simulator (URS 01.2009) Results.....	84
E.1 Synthetic Data Used in Numerical Simulator (URS 01.2009) Without Adsorption.....	104
E.2 Synthetic Data Used in Numerical Simulator (URS 01.2009) With Adsorption.....	104
E.3 Match Points ( <i>M.P</i> ) from Fig. E.1.....	106
E.4 End of Transient Time and Slopes of Straight Lines Exhibited by Transient Flow Data With and Without Adsorbed gas. ....	108
E.5 Summary of OGIP Estimates.....	110

## LIST OF FIGURES

FIGURE	Page
3.1 Free, adsorbed and total gas content (scf / rcf ) vs pressure for Barnett shale.....	11
3.2 Fraction of Adsorbed gas, free gas to total gas vs pressure for Barnett shale.....	12
3.3 Shale gas PSS with adsorption (SGPA) program input data and plots of results.....	14
3.4 SGPA results on decline curve for free, desorbed and total gas .....	15
3.5 SGPA results on $\log q_g / [m(p_i) - m(p_{wf})]$ vs log time plot for free, desorbed and total gas (SGPA) .....	16
3.6 SGPA results on plot of fraction of adsorbed gas, free gas to total gas vs time .....	16
3.7 $p/z^*$ and $p/z$ vs $G_p$ ( $p/z^*$ values do not resemble $p/z$ values).....	17
3.8 $p/z^*$ vs $G_p$ and $p/z$ vs $G_p$ ( $p/z^{**}$ values similar to $p/z$ values).....	18
4.1 Plot of $[p_i - p_{wf}(t)] / q_o$ vs actual time, constant rate liquid BDF giving a straight line with slope $m_{BDF}$ to calculate $V_p$ .....	21
4.2 Plot of $[p_i - p_{wf}] / q_o(t)$ vs actual time, variable rate liquid exhibiting exponential decline ( $b = 0$ ). .....	22
4.3 Plot of $[p_i - p_{wf}] / q_o(t)$ vs material balance time $t_c$ variable rate liquid BDF shifting variable rate solution to constant rate solution with slope $m_{BDF}$ to calculate $V_p$ .....	23
4.4 Plot of $[m(p_i) - m(p_{wf})(t)] / q_g$ vs pseudo time $t_n^*$ constant rate gas BDF including adsorbed gas with slope $m_{BDF}$ to calculate $G$ .....	25
4.5 Plot of $[m(p_i) - m(p_{wf})(t)] / q_g$ vs pseudo time $t_n^*$ variable rate gas BDF including adsorbed gas exhibiting exponential decline ( $b = 1$ ).....	25
4.6 Plot of $[m(p_i) - m(p_{wf})] / q_g(t)$ vs material balance pseudo time $t_{ca}^*$ ,	

FIGURE	Page
variable rate gas BDF including adsorbed gas, shifting variable rate gas solution to constant rate solution with slope $m_{BDF}$ to calculate G.....	26
4.7 Matching plot of $\log q_g / [m(p_i) - m(p_{wf})]$ vs $\log t_{cz}^*$ on harmonic decline ( $b = 1$ ) stem of Fetkovich's (1980) type curves to establish match points. ....	29
4.8 Ibrahim, Wattenbarger and Helmy's plot $[m(p_i) - m(p_{wf})] / q_g(t)$ vs $Super-t_n^*$ with and without adsorbed gas BDF with slope $m_{BDF}$ used to calculate OGIP. ....	30
4.9 Anderson et al.'s plot normalized rate vs normalized cumulative with and without adsorbed gas showing OGIP on x-axis .....	32
4.10 Ibrahim & Wattenbarger. (2005) plot of $[m(p_i) - m(p_{wf})] / q_g(t)$ vs $\sqrt{t}$ to establish end of transient time $t_{esr}$ and slope of line exhibited by transient flow .....	33
5.1 Slab model (Al-Ahmadi et al. 2010) showing BDF and stimulated reservoir volume (SRV).....	35
5.2 Square root of time plot to determine end of transient time and slope of straight line exhibited by transient flow, Well 137.. ....	39
5.3 Matching plot of $\log q_g / [m(p_i) - m(p_{wf})]$ vs $\log t_{ca}^*$ on harmonic decline ( $b = 1$ ) stem of Fetkovich's (1980) Type curve to establish match points used to calculate OGIP with and without adsorbed gas by Palacio & Blasingame's (1993) method, Well 137.....	40
5.4 Plot of $[m(p_i) - m(p_{wf})] / q_g$ vs $t_{ca}^*$ showing with and without adsorbed gas BDF with slope $m_{BDF}$ used to calculate OGIP, Well 137 .....	41
5.5 Normalized rate vs normalized cumulative with and without adsorbed gas showing OGIP on x-axis, Well 137. ....	41
5.6 Decline curve: Forecast results for 50 years with and without adsorbed gas, Well 137.....	42
5.7 Square root of time plot to determine end of transient time and slope of straight line exhibited by transient flow, Well 257.. ....	43
5.8 Matching plot of $\log q_g / [m(p_i) - m(p_{wf})]$ vs $\log t_{ca}^*$ on harmonic	

FIGURE	Page
decline ( $b = 1$ ) stem of Fetkovich's (1980) type curve to establish match points used to calculate OGIP with and without adsorbed gas by Palacio and Blasingame's (1993) method, Well 257 .....	44
5.9 Plot of $[m(pi) - m(pwf)] / q_g$ vs $t_{ca}^*$ showing with and without adsorbed gas BDF with slope $m_{BDF}$ used to calculate OGIP, Well 257. ....	45
5.10 Normalized rate vs Normalized Cumulative with and without adsorbed gas showing OGIP on x-axis, Well 257. ....	45
5.11 Decline curve: Forecast results for 50 years with and without adsorbed gas, Well 257.....	46
5.12 Square root of time plot to determine end of transient time and slope of straight line exhibited by transient flow, Well 285.. ....	47
5.13 Matching plot of $\log q_g / [m(pi) - m(pwf)]$ vs $\log t_{ca}^*$ on harmonic decline ( $b = 1$ ) stem of Fetkovich's (1980) Type curve to establish match points used to calculate OGIP with and without adsorbed gas by Palacio and Blasingame's (1993) method, Well 285 .....	48
5.14 Plot of $[m(pi) - m(pwf)] / q_g$ vs $t_{ca}^*$ showing with and without adsorbed gas BDF with slope $m_{BDF}$ used to calculate OGIP, Well 285 .....	49
5.15 Normalized rate vs Normalized Cumulative with and without adsorbed gas showing OGIP on x-axis, Well 285. ....	49
5.16 Decline curve: Forecasting results for 50 years with and without adsorbed gas, Well 285.....	50
5.17 Square root of time plot to determine end of transient time and slope of straight line exhibited by transient flow, Well 314.. ....	51
5.18 Matching plot of $\log q_g / [m(pi) - m(pwf)]$ vs $\log t_{ca}^*$ on harmonic decline ( $b = 1$ ) stem of Fetkovich's (1980) Type curve to establish match points used to calculate OGIP with and without adsorbed gas by Palacio and Blasingame's (1993) method, Well 314 .....	52
5.19 Plot of $[m(pi) - m(pwf)] / q_g$ vs $t_{ca}^*$ showing with and without adsorbed gas BDF with slope $m_{BDF}$ used to calculate OGIP, Well 314 .....	53
5.20 Normalized rate vs Normalized Cumulative with and without adsorbed	

FIGURE	Page
gas showing OGIP on x-axis, Well 314. ....	53
5.21 Decline curve: Forecasting results for 50 years with and without adsorbed gas, Well 314.....	54
5.22 Comparison of OGIP without adsorption estimates from transient data, BDF Ibrahim, Wattenbarger & Helmy's and BDF Palacio & Blasingame's methods for all the wells.....	55
5.23 Comparison of OGIP without adsorption estimates from transient data, BDF Ibrahim, Wattenbarger & Helmy's and BDF Palacio & Blasingame's methods for all the wells.....	56
5.24 OGIP, SRV and RF ratios for all the wells.....	57
A.1 Case 1: $p/z^{**}$ and $p/z$ vs $G_p$ (% adsorbed = 0).....	72
A.2 Case 1: $G_p$ vs time (% adsorbed = 0).....	72
A.3 Case 2: $p/z^{**}$ and $p/z$ vs $G_p$ (% adsorbed = 50).....	73
A.4 Case 2: $G_p$ vs time (% adsorbed = 50).....	73
A.5 Case 3: $p/z^{**}$ and $p/z$ vs $G_p$ (% adsorbed = 0).....	74
A.6 Case 3: $G_p$ vs time (% adsorbed = 0).....	74
A.7 Case 4: $p/z^{**}$ and $p/z$ vs $G_p$ (% adsorbed = 50).....	75
A.8 Case 4: $G_p$ vs time (% adsorbed = 50).....	75
B.1 Case 1: Decline curve (% adsorbed = 0) .....	80
B.2 Case 1: Compressibility vs pressure (% adsorbed = 0) .....	80
B.3 Case 2: Decline curve (% adsorbed = 50) .....	81
B.4 Case 2: Compressibility vs pressure (% adsorbed = 50) .....	81
B.5 Case 3: Decline curve (% adsorbed = 0) .....	82
B.6 Case 3: Compressibility vs pressure (% adsorbed = 0) .....	82

FIGURE	Page
B.7 Case 4: Decline curve (% adsorbed = 50) .....	83
B.8 Case 4: Compressibility vs pressure (% adsorbed = 50) .....	83
C.1 Case 1c: Decline curve (% adsorbed = 0).....	85
C.2 Case 1c: log $q$ vs time (% adsorbed = 0) .....	85
C.3 Case 1c: $G_p$ vs time (% adsorbed = 0).....	86
C.4 Case 2c: Decline curve (% adsorbed = 50).....	86
C.5 Case 2c: log $q$ vs time (% adsorbed = 50) .....	87
C.6 Case 2c: $G_p$ vs time (% adsorbed = 50).....	87
C.7 Case 3c: Decline curve (% adsorbed = 0).....	88
C.8 Case 3c: log $q$ vs time (% adsorbed = 0) .....	88
C.9 Case 3c: $G_p$ vs time (% adsorbed = 0).....	89
C.10 Case 4c: Decline curve (% adsorbed = 50).....	89
C.11 Case 4c: log $q$ vs time (% adsorbed = 50) .....	90
C.12 Case 4c: $G_p$ vs time (% adsorbed = 50).....	90
E.1 Matching plot of Log $q_g / [m(pi) - m(pwf)]$ vs Log $t_{ca}^*$ on harmonic decline ( $b = 1$ ) stem of Fetkovich's (1980) Type curve to establish match points used to calculate OGIP with and without adsorbed gas by Palacio & Blasingame's (1993) method, simulated data.....	105
E.2 Plot of $[m(pi) - m(pwf)] / q_g$ vs $t_{ca}^*$ showing with and without adsorbed gas BDF with slope $m_{BDF}$ used to calculate OGIP, simulated data .....	107
E.3 Normalized rate vs Normalized Cumulative with and without adsorbed gas showing OGIP on x-axis, Simulated data.....	108
E.4 Square of time Plot to determine end of transient time and slope of	

	Page
straight line exhibited by transient flow, simulated data.....	109

## CHAPTER I

### INTRODUCTION

Unconventional gas reservoirs are expected to play a vital role in satisfying the demand for gas in future. The major component of Unconventional gas reservoirs comprises of shale gas. It is evident from the recent year activities in shale gas plays that in future shale gas will constitute the largest component in gas production. The stimulation techniques, to achieve better production rates from shale gas reservoirs have brought shale gas reserves in the spot light. These stimulation techniques are expected to improve with time, however as better stimulation techniques are becoming attainable it is important to have better understanding of shale gas reservoir behavior in order to apply these techniques in an efficient fashion.

#### 1.1 Background

Unlike conventional gas reservoirs, shale gas reservoirs have very low permeability, and are economical only when hydraulically fractured. One important aspect of the shale gas reservoirs which needs special consideration is the adsorption phenomenon. In the past adsorption in coal bed methane (CBM) reservoirs is studied extensively. Gas is adsorbed on the surface of the pores instead of occupying them. The gas desorbs or is produced as the reservoir pressure declines during production and becomes part of the free gas in natural fractures. Langmuir's isotherm is normally used to define the amount of gas desorbed as the pressure declines. Flow from the matrix to

---

This thesis follows the style of *SPE Journal*.

natural fractures are defined by Flick's law of diffusion instead of Darcy's law. In CBM reservoirs all the gas produced comes from desorption which is not the case in shale gas reservoirs where the natural fractures are already occupied by free gas.

A survey of literature shows that currently there is no way of distinguishing desorbed gas from free gas. All the methods (decline curves etc) do predict the total gas produced from the reservoir but do not show the percentage of desorbed gas contributing to total production. It is also important to note that desorption being an independent phenomenon has a completely different response to pressure. Which means that with declining pressure the contribution of desorbed gas will vary and will effect the decline trend accordingly.

## **1.2 Problem Description**

The ability to predict flow rates corresponding to bottom hole pressure ( $p_{wf}$ ) is the basis of all forecasting techniques. The methods applied for forecasting on conventional gas reservoirs can not be applied to shale gas reservoirs as it is not possible to measure the average reservoir pressures ( $\bar{p}$ ) by conventional well tests due to very low permeabilities. Decline curves for conventional gas, when applied on shale gas reservoirs, can not be validated by material balance due to unavailability of average reservoir pressure. However number of techniques have been proposed and applied to obtain type curves for shale gas reservoirs. The phenomenon of desorption adds further complexity to the problem.

It is estimated that desorbed gas contributes around 30 to 50 % of the gas produced by shale gas reservoirs. In this respect it becomes crucial to have accurate estimates of the desorbed gas and its effect on the decline behavior of the reservoir.

### **1.3 Research Objectives**

The objectives of this thesis are as follows.

- To develop a simple method, employing conventional techniques, which include desorbed gas to accurately estimate the amount of desorbed gas contributing to total production. Using our method we will be able to show the amount of desorbed gas produced with respect to the pressure decline in presence of free gas.
- To develop a mass balance equation incorporating both free gas and adsorbed gas. The mass balance equation and stabilized flow equation can then be used to calculate the average reservoir pressures iteratively. This way rate and cumulative production for free gas, desorbed gas and total gas will be generated.
- To validate our method by comparing with results using modified material balance equations and compressibility expression for desorbed gas introduced in previous works.
- Using our method to analyze the effect of desorption on estimated ultimate recovery (RF) in shale gas reservoirs, in order to show the amount of gas desorbed gas that is ignored.

- Assess the influence of desorbed gas on the decline behavior of shale gas. Our target is to see the effect of desorption on the decline curves and to apply a correction that would account for it.

The expected outcomes from this research will be as follows.

- Better understanding of desorption in shale gas reservoirs.
- Use of diagnostic plots to differentiate between the produced free gas and desorbed gas.
- Technique to forecast shale gas production which comprises the free as well as the desorbed gas.
- Assess contribution of desorbed gas towards total production over the life of the well.
- Recommendations for better performance of shale gas wells keeping in view results of this work.

## CHAPTER II

### LITERATURE REVIEW

Most of the early work done on desorption is on coal bed methane (CBM) reservoirs. Desorption phenomenon was not given much importance during early discovery and production phases of shale gas reservoirs. Several authors have presented different type of approaches to try and define the behavior of shale gas reservoirs with respect to desorption.

Fraim & Wattenbarger in their work published in 1987 modified pseudo time function in order to correct for gas properties that change with pressure.

$$t_n = \int_0^t \frac{(\mu c_t)_i}{\mu(\bar{p})c_t(\bar{p})} d\tau \dots\dots\dots 2.1$$

They demonstrated that when normalized pseudo time and pseudo pressure are used, for Boundary dominated flow (BDF) and constant ( $p_{wf}$ ) decline for gas, it matches exactly with Arps's (1944) exponential type decline ( $b=0$ ), regardless of the reservoir shape.

In 1986 Bumb and McKee derived an approximate analytic solution for single phase gas flow which included the adsorbed gas. Using Langmuir isotherm for desorption of gas in a conservation of mass equation they showed desorption as an additional compressibility factor. The differential equation governing the flow for radial case is given as follows.

$$\frac{\phi \mu_g}{k} \left[ c_g + \frac{\alpha c_m}{\phi} + \frac{\rho_{gsc} V_L p_L}{\phi \rho_g (p_L + \bar{p})^2} \right] \frac{\partial \Delta m(p)}{\partial t} = \frac{1}{r} \frac{\partial}{\partial r} \left( r \frac{\partial \Delta m(p)}{\partial r} \right) \dots\dots\dots 2.2$$

where

$$\left[ c_g + \frac{\alpha c_m}{\phi} + \frac{\rho_{gsc} V_L p_L}{\phi \rho_g (p_L + \bar{p})^2} \right] \dots\dots\dots 2.3$$

Eq. 2.3 is the total compressibility and Eq. 2.4 is the desorption factor which shows the

$$\frac{\rho_{gsc} V_L p_L}{\phi \rho_g (p_L + p)^2} = \frac{p_{sc} T \bar{z}}{\bar{p} T_{sc} \bar{z}_{sc}} \frac{V_L p_L}{\phi (p_L + \bar{p})^2} = \frac{B_g V_L p_L}{\phi (p_L + \bar{p})^2} \dots\dots\dots 2.4$$

additional compressibility due to desorption. They verified their approximate analytic solution against numerical simulator results.

In 1990 King presented a modified material balance technique to estimate the original gas in place and to predict the future performance of the well for coal seams and Devonian shale. The technique works just like the conventional material balance, where the  $p/z$  straight line plot is used to estimate original gas in place. King's method assumes equilibrium condition for free and adsorbed gasses. The desorption from the matrix to fractures is assumed to be in pseudo steady state. The material balance equation given by King is as follows.

$$\frac{\bar{p}}{\bar{z}^*} = \frac{p_i}{z_i^*} \left[ 1 - \frac{G_p}{G} \right] \dots\dots\dots 2.5$$

Assuming negligible rock and water compressibilities, and constant water saturation,  $z^*$  for unconventional gas reservoirs is given as

$$z^* = \frac{z}{S_g + \frac{V_L T p_{sc} z}{\phi (p + p_L) T_{sc} z_{sc}}} \dots\dots\dots 2.6$$

Similar to conventional  $p/z$  A plot of  $p/z^*$  vs cumulative production is a straight line and can be extrapolated to estimate OGIP.

Palacio and Blasingame in 1993 introduced material balance time which can be used to analyze variable rate as well as variable pressure production data.

$$t_c = \frac{G_p}{q_g} \dots\dots\dots 2.7$$

For BDF material balance time, when coupled with normalized pseudo time, shifts the gas production data to match Arps's (1944) harmonic type depletion ( $b = 1$ ).

$$t_{ca} = \frac{\mu_{gi} c_{ti}}{q_g} \int_0^t \frac{q_g}{\mu_g(\bar{p}) c_t(\bar{p})} d\tau \dots\dots\dots 2.8$$

In 1991 Seidle, using Al-Hussainy et al.'s (1996) approach, used real gas pseudo pressure and Langmuir's isotherm to define a equation for flow of gas in coal cleats.

$$\nabla^2 m(p) = \frac{\phi \mu_g S_g}{k_g} [c_g + c_d] \frac{\partial m(p)}{\partial t} \dots\dots\dots 2.9$$

where  $c_d$ , the adsorbed gas compressibility, is given as

$$c_d = 1.7525 \times 10^{-4} \frac{B_g V_m \rho_B p_L}{\phi (p + p_L)^2} \dots\dots\dots 2.10$$

Seidle defined the dimensionless time and dimensionless  $m(p)$  for coal gas. By comparing his results with liquid analytical solution, which were found to be in agreement except at large dimensionless times, Seidle showed that real gas pseudo pressure can be used for coal beds. Seidle than used  $m(p)$  in a gas deliverability equation and a mass balance, which included the desorbed gas (defined by Langmuir's isotherm) to calculate average reservoir pressure iteratively and to predict gas production.

In 2009 Moghadam, Jeje and Mattar presented a advanced material balance equation applicable to all kinds of reservoirs be they un conventional, over pressured or

water driven. Their  $p/z^{**}$  vs Gp plotting function is similar to conventional  $p/z$  plot.  $z^{**}$  is related to King's  $z^*$  as follows.

$$z^{**} = z^* \left( \frac{z_i}{z_i^*} \right) \dots\dots\dots 2.11$$

King's  $p/z^*$  values barely had any resemblance with the conventional  $p/z$ . The advantage of  $p/z^{**}$  is that it has values which are similar to the conventional  $p/z$ .

Ibrahim, Wattenbarger and Helmy in 2003 showed their method to estimate OGIP for gas wells. They modified the definition of pseudo time including porosity in it.

$$t_n = (\phi \mu c_i)_i \int_0^t \frac{1}{\phi(\bar{p}) \mu(\bar{p}) c_i(\bar{p})} d\tau \dots\dots\dots 2.12$$

They used normalized pseudo time to calculate super position time in order to analyze gas production data at variable rate / variable pressure. When  $[m(pi) - m(pwf)] / qg$  vs  $Super-t_n$  (Normalized pseudo super position time) is plotted on Cartesian co-ordinates a straight line is obtained. The slope of the straight line is used than to calculate the OGIP.

$$G = \frac{2 p_i S_{gi}}{m_{BDF} z_i \mu_i c_{ti}} \dots\dots\dots 2.13$$

The pseudo time however requires the knowledge of average reservoir pressure which is than used to calculate  $Super-t_n$  and ultimately OGIP. The authors suggested a iterative procedure where OGIP is assumed and average reservoir pressure is updated accordingly. The new slope obtained is than used to calculate OGIP. This procedure is repeated until the assumed OGIP matches the calculated OGIP.

Ibrahim and Wattenbarger in 2005 demonstrated that analytical solution can be applied on tight gas (permeability of less than 0.1 md) reservoirs which exhibit transient

linear gas flow just as they can be applied to transient radial gas flow accurately if a correction factor is applied. The square root of time plot (  $[m(p_i) - m(p_{wf})] / qg$  vs  $\sqrt{t}$  is used to determine end of transient time ( $t_{esr}$ ) and slope of straight line exhibited by transient flow data. This information can then be used to estimate OGIP as follows.

$$OGIP = f_{CP} \frac{200.8 T S_{gi}}{(\mu_g c_t B_g)_i} \left( \frac{\sqrt{t_{esr}}}{\tilde{m}_{CPL}} \right) \dots\dots\dots 2.14$$

Anderson et al. in 2010 showed that a boundary dominated signal on a plot of normalized rate versus normalized cumulative will be a straight line giving the hydrocarbon pore volume (HCPV), where normalized rate and normalized cumulative are given as.

$$q_g / [m(p_i) - m(p_{wf})] \dots\dots\dots 2.15$$

$$\frac{2 p_i q_g}{z_i \mu_i c_{ti} [m(p_i) - m(p_{wf})]} t_{ca} \dots\dots\dots 2.16$$

They claimed that this HCPV is representative of the stimulated reservoir volume (SRV).

## CHAPTER III

### DEVELOPMENT AND VALIDATION OF MASS BALANCE EQUATION FOR SHALE GAS INCLUDING ADSORPTION

#### 3.1 Adsorption in Shale Gas Reservoirs (Barnett)

Adsorbed gas present in shales is molecularly adsorbed on the surface of the shale. In order to measure the amount of adsorbed gas, gas content (scf/ton) and sorption isotherm are measured in lab using core samples. Gas content is the amount of total gas adsorbed on the surface of the reservoir rock, whereas sorption isotherm is the capacity of the reservoir rock to hold adsorbed gas with respect to pressure at constant temperature. Langmuir's isotherm (1918) can also be used to define the relationship of pressure and gas storage capacity of the reservoir rock. Langmuir's isotherm is given as

$$V_E = V_L \frac{p}{(p + p_L)} \dots\dots\dots 3.1$$

$$V_L = 0.031214 \rho_B V_m \dots\dots\dots 3.2$$

where  $V_L$  is the gas content in scf/rcf and  $p_L$  (Langmuir's pressure) is the pressure at which 50% of the gas is desorbed. Looking at previous literature (eg., Wang & Reed. 2009, Jacobi et al. 2008 and Lewis & Hughes. 2008 ) we decided to use approximate values of  $V_m$  (96 scf/ton),  $\rho_B$  (2.38 gm/cc) and  $p_L$  (650 psi) for Barnett shale. A Langmuir isotherm can be constructed using these approximate values as shown in Fig. 3.1. The Langmuir Isotherm for Barnett shale gives us an idea of how the adsorbed gas, free gas and total gas capacity of the reservoir relate with the pressure in terms of gas content.

It should be noted that in Fig. 3.1 the adsorbed gas curve follows the Langmuir isotherm and the free gas curve is constructed using the volumetric gas capacity of reservoir with respect to pressure. Fig 3.2 shows the ratio of adsorbed and free gas varying with respect to pressure. An important observation from Fig 3.2 is that the adsorbed gas is the dominant contributor to gas production below 2000 psi, 50 to more than 80 %, where as above 2000 psi it is still significant 50 to 30 %. We can safely deduce that at low reservoir pressures most of the gas production comes from desorbed gas. In this respect ignoring desorbed gas when doing decline curve or material balance analysis will definitely result in serious errors.

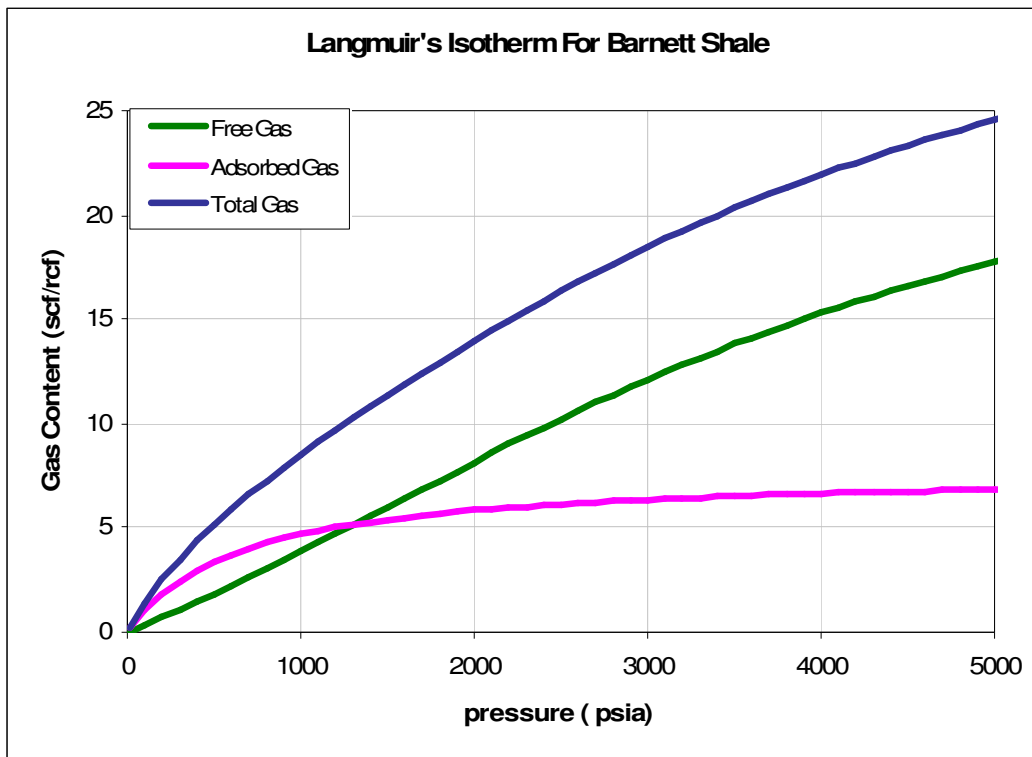


**Fig. 3.1 —Free, adsorbed and total gas content (scf / rcf ) vs pressure for Barnett shale.**

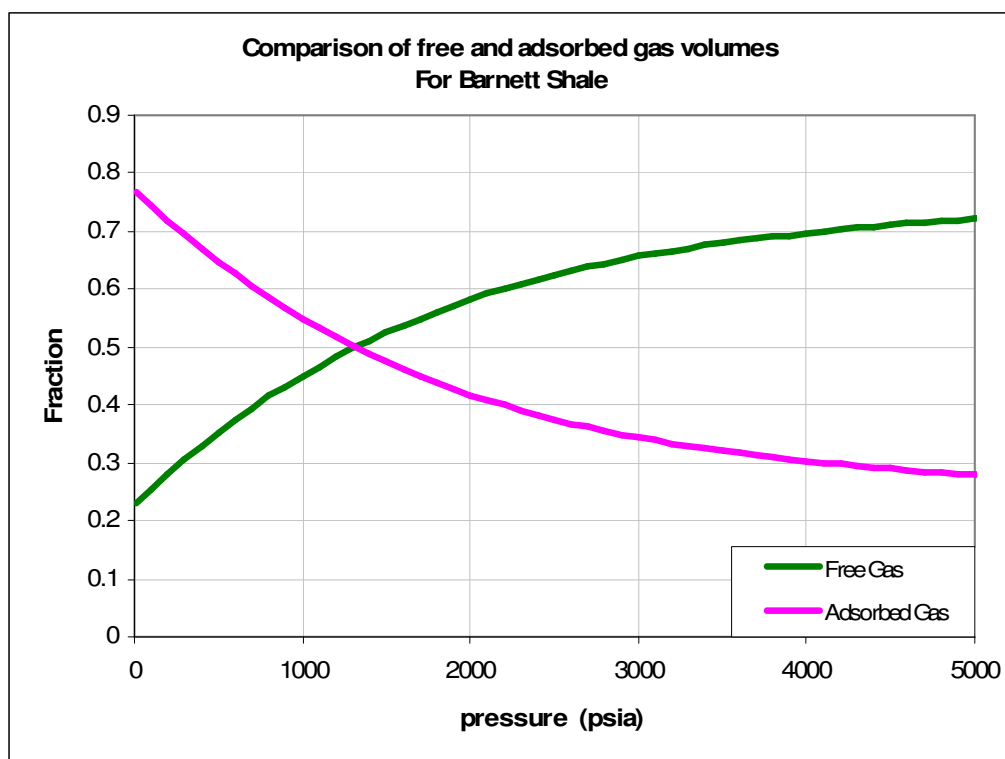


**Fig. 3.2 —Fraction of adsorbed gas, free gas to total gas vs pressure for Barnett shale.**

### 3.2 Mass Balance for Shale Gas Including Adsorption (SGPA)

In order to observe the decline trends and make analysis in presence of desorbed gas we need to obtain average reservoir pressures, rate and cumulative gas produced for free as well as desorbed gas. A mass balance is derived to obtain average reservoir pressures at each time step.

The Original gas in Place including the adsorbed gas, at initial pressure is given by

$$G = V_B \left[ \left( \frac{\phi S_g}{B_{gi}} \right) + \left( V_L \frac{p_i}{(p_i + p_L)} \right) \right] \dots\dots\dots 3.3$$

The productivity index equation at constant bottom hole pressure, to calculate rate ( $q_g$ ) at any pressure is given as

$$q_g = J_g [m(\bar{p}) - m(p_{wf})] \dots\dots\dots 3.4$$

$G_p$  at the end of first time step is equal to the initial gas in place minus the current Gas in place.

$$G_p = G - V_B \left[ \left( \frac{\phi S_{gi}}{\bar{B}_g} \right) + \left( V_L \frac{\bar{p}}{(\bar{p} + p_L)} \right) \right] \dots\dots\dots 3.5$$

Since  $G_p$  is equal to the product of rate and time at the end of first time step, Eq. 3.5 can be used to calculate average reservoir pressure ( $\bar{p}$ ) iteratively. The new  $\bar{p}$  leads us to the new average pseudo pressure  $m(\bar{p})$  and new  $q_g$  which will be an increment to current  $G_p$ . The new  $G_p$  is then used in Eq. 3.5 to calculate the next  $\bar{p}$  etc. Using mass balance equation, the total, free gas and adsorbed gas as well as the cumulative production from total, free and desorbed gas are obtained as a function of time (Fig 3.3).

This technique was used in previous works (Seidle, 1991) as well and gives a easy and simple way to carry out basic analysis. It differs from the conventional material balance as it includes the adsorbed gas. Another advantage of this technique is that the desorbed gas and free gas rates can be obtained separately. Apart from the conventional assumptions that hold for the material balance the additional assumptions for this technique are as follows.

- The desorbed gas and pressure relationship is defined by the Langmuir's isotherm
- Free gas and desorbed gas are in equilibrium. i.e. desorption of gas is completely pressure dependent.
- Flow of desorbed gas from the matrix into the fractures follows the Darcy's Law.

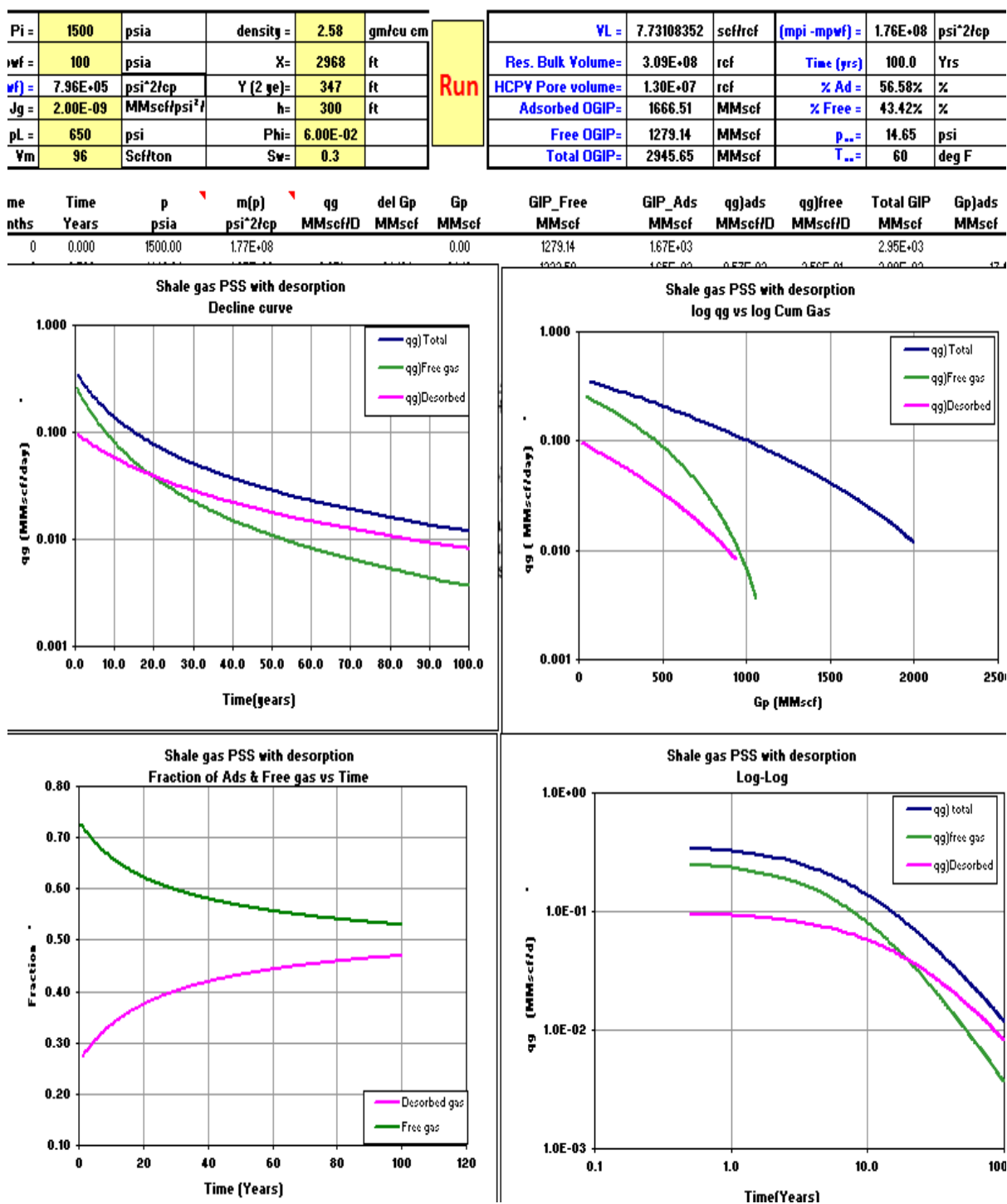


Fig. 3.3 —Shale gas PSS with adsorption (SGPA) program input data and plots of results.

- Rock and water compressibilities are negligible.

- Water saturation is constant and water remains immobile.
- The desorbed gas does not interact with the matrix.
- Free gas and the desorbed gas have the same composition and there is no difference in the specific gravities of the two gasses.

The material balance calculations can be programmed in Excel VBA to calculate the above mentioned parameters in order to generate plots such as decline curves,  $\log q$  vs Cumulative  $G_p$ ,  $\log q$  vs  $\log$  time and ratio of adsorbed and free gas to total gas vs time or pressure (Figs. 3.4-3.6). These plots show the curves for free, desorbed and total gas. The program is named as shale gas pseudo state with adsorption (SGPA).

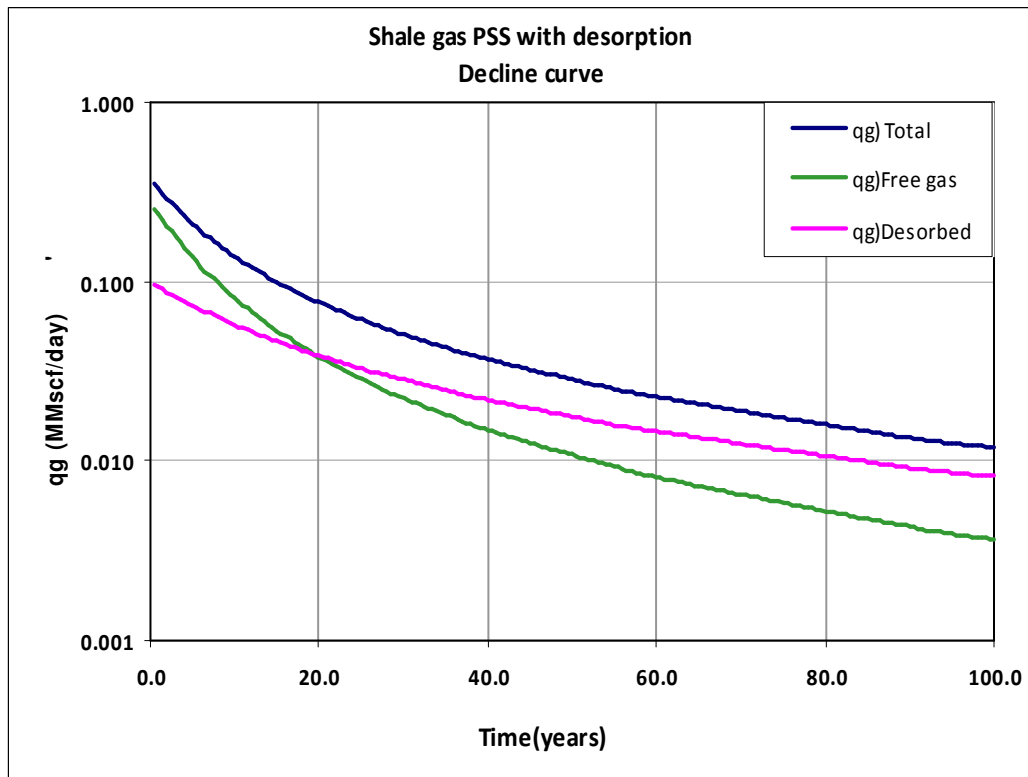


Fig. 3.4 — SGPA results on decline curves for free, desorbed and total gas.

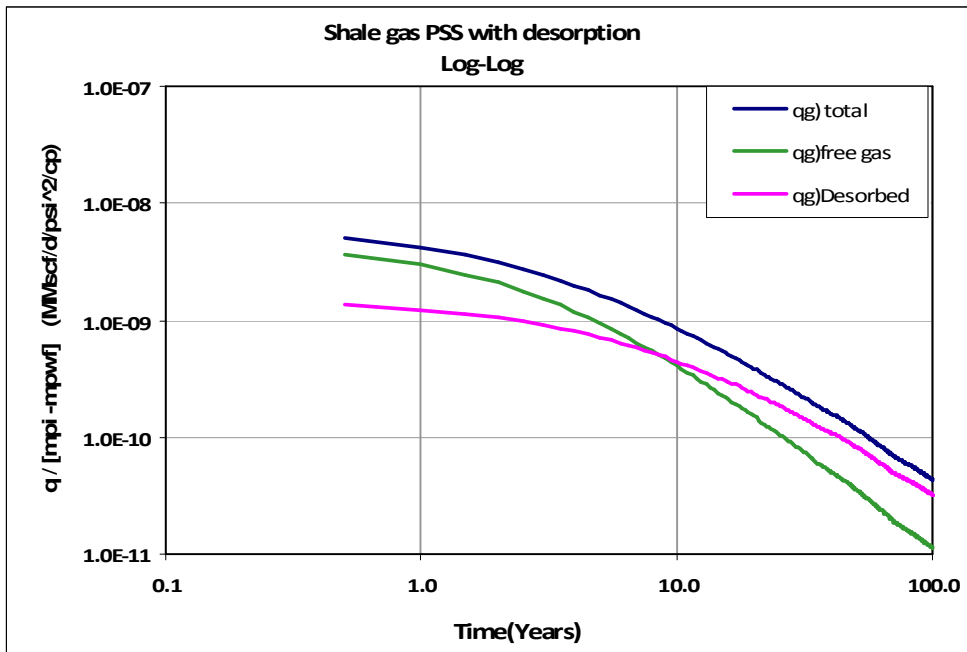


Fig. 3.5 — SGPA results on  $\log q_g / [m(p_i) - m(p_{wf})]$  vs log time plot for free, desorbed and total gas (SGPA).

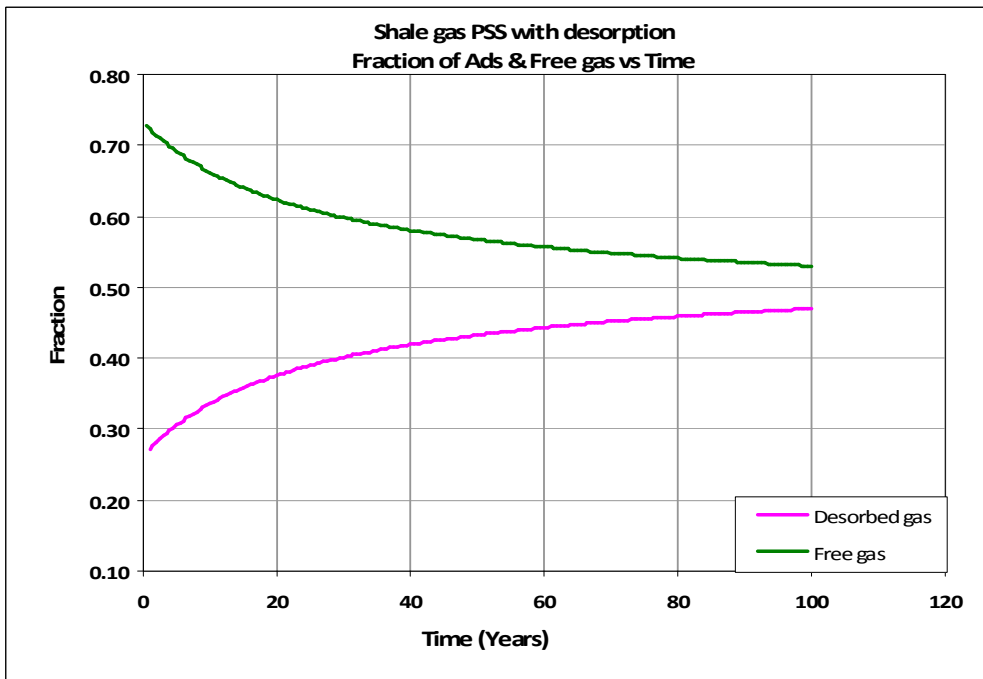


Fig. 3.6 —SGPA results on plot of fraction of adsorbed gas , free gas to total gas vs time.

### 3.3 Validation of Our Approach ( King's $z^*$ )

King presented a modified material balance equation to incorporate adsorbed gas.

$$\frac{\bar{p}}{z^*} = \frac{p_i}{z_i^*} \left[ 1 - \frac{G_p}{G} \right] \dots\dots\dots 3.6$$

where  $z^*$  at constant water saturation and negligible water and gas compressibility is defined as.

$$z^* = \frac{z}{S_g + \frac{V_L T p_{sc} z}{\phi (p + p_L) T_{sc} z_{sc}}} \dots\dots\dots 3.7$$

Following King's method and using our mass balance equation we derived the modified material balance equation similar to King with same  $z^*$  (Appendix A). In order to validate our results we used King's  $z^*$  to calculate  $G_p$  at different pressures. These  $G_p$

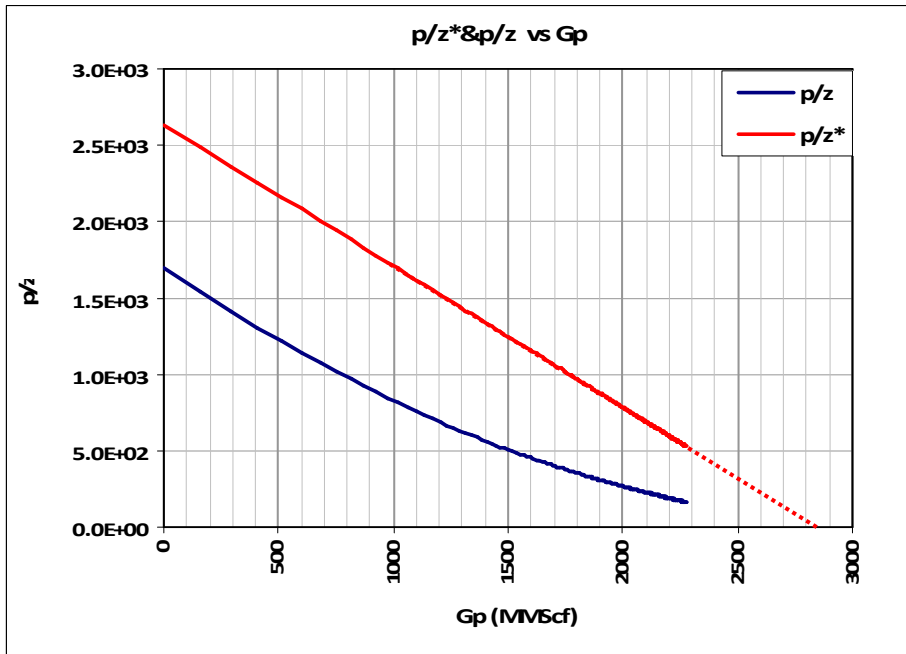


Fig. 3.7 — $p/z^*$  and  $p/z$  vs  $G_p$  plot ( $p/z^*$  values do not resemble  $p/z$  values).

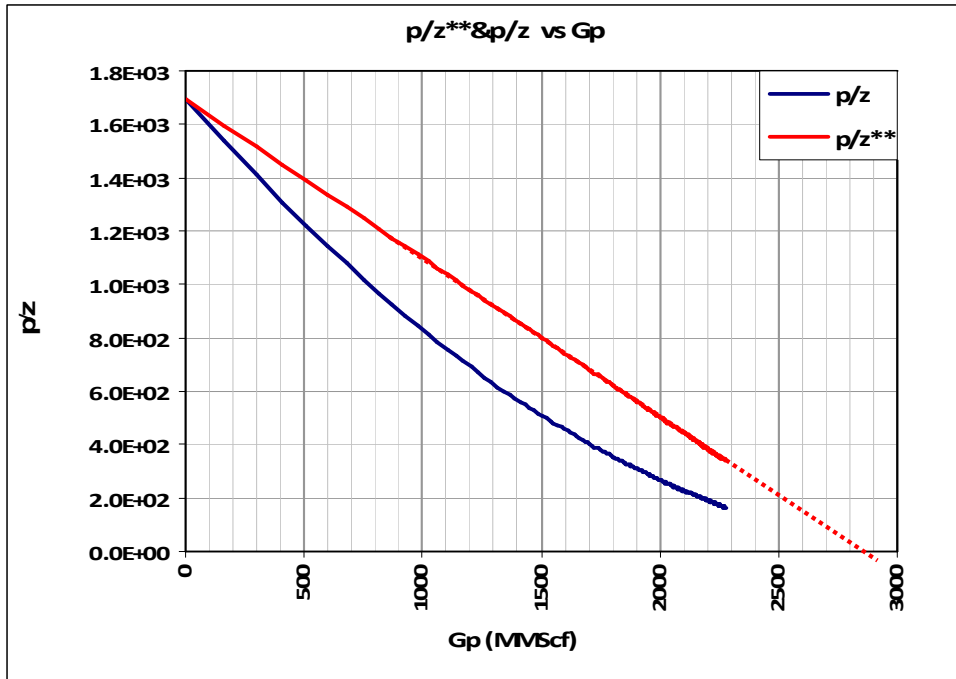


Fig. 3.8 — $p/z^{**}$  vs  $G_p$  and  $p/z$  vs  $G_p$  ( $p/z^{**}$  values similar to  $p/z$  values).

values were then compared with SGPA results (Appendix A).

It should be noted here the  $z^*$  values do not resemble the  $z$  values (Fig. 3.7). The normalized  $z^*$  (S.Moghadam et al. 2009) denoted as  $z^{**}$  was used in the material balance equation to obtain realistic values of  $z^*$  which resemble the actual  $z$  values (Fig 3.8).  $z^{**}$  is given as.

$$z^{**} = z^* \left( \frac{z_i}{z_i^*} \right) \dots\dots\dots 3.8$$

$G_p$  using  $z^{**}$  can be calculated as follows

$$G_p = \frac{\phi V_B z_i^2}{B_{gi} p_i z_i^*} \left[ \frac{p_i}{z_i^{**}} - \frac{\bar{p}}{\bar{z}^{**}} \right] \dots\dots\dots 3.9$$

The calculated  $G_p$  were then compared with  $G_p$  results from SGPA for different cases. The plotting functions  $p/z$  vs  $G_p$  and  $G_p$  vs time were used to compare the results. The results were an exact match. Table A.1 in Appendix A shows the match cases followed by match plots.

### 3.4 Validation of Our Approach (Bumb & McKee's Compressibility Expression for Adsorption)

In order to apply Bumb & McKee's compressibility expression to find out gas rate an equation was derived which relates gas rate with the total compressibility in the form of an exponential decline equation. We begin by differentiation of our mass balance equation with respect to pressure to get  $G_p$  in terms of total compressibility including free and desorbed gases.

$$\frac{dG_p}{dp} = -\frac{\phi V_B S_g}{B_g} [c_g + c_d] \dots\dots\dots 3.10$$

Derivation of Eq. 3.10 and using chain rule we get an expression on form of  $q_g$

$$q_g = -\frac{\phi V_B S_g}{B_g} [c_g + c_d] \frac{dp}{dt} \dots\dots\dots 3.11$$

Similarly differentiating productivity index equation (Assuming constant  $p_{wf}$ ) with respect to pressure will yield.

$$dq_g = 2J_g \frac{\bar{p}}{\bar{z} \bar{\mu}} d\bar{p} \dots\dots\dots 3.12$$

Dividing Eq. 3.12 with Eq. 3.11 and Integrating will give us  $q_g$  in terms of Bumb and McKee's (1986) compressibility expression as under.

$$q_g = q_0 e^{-\frac{2 J_g}{\phi V_B (1-S_w)} \left[ \frac{B_g \bar{p}}{c_g + c_d} \right] \frac{t}{\bar{z} \bar{\mu}}} \dots\dots\dots 3.13$$

Using Eq. 3.13 we can calculate the gas rate which is then matched with the gas rates from SGPA on decline curve plots. Table B.1 in Appendix B shows the match cases followed by match plots for different cases.

### 3.5 Validation of Our Approach (Unconventional Reservoir Simulator)

SGPA results were matched with URS 01 (2009) assuming that the saturation of water is zero. The Input data for URS 01 (2009) was set up such that PSS flow starts on day one. The Langmuir's constants and other data were same as used in SGPA. Table C.1 in Appendix C shows the match cases followed by the match plots .

## CHAPTER IV

### OGIP ESTIMATION METHODS (INCLUDING ADSORBED GAS)

Derivations of the given solutions in this chapter are presented in detail in Appendix D.

#### 4.1 Review of BDF Methods

The fundamental relations of volumetric expansion and productivity index for BDF liquids are given as:

$$\frac{d\bar{p}}{dt} = -\frac{q_o B_o}{V_p c_t} \dots\dots\dots 4.1$$

$$q_o = J(\bar{p} - p_{wf}) \dots\dots\dots 4.2$$

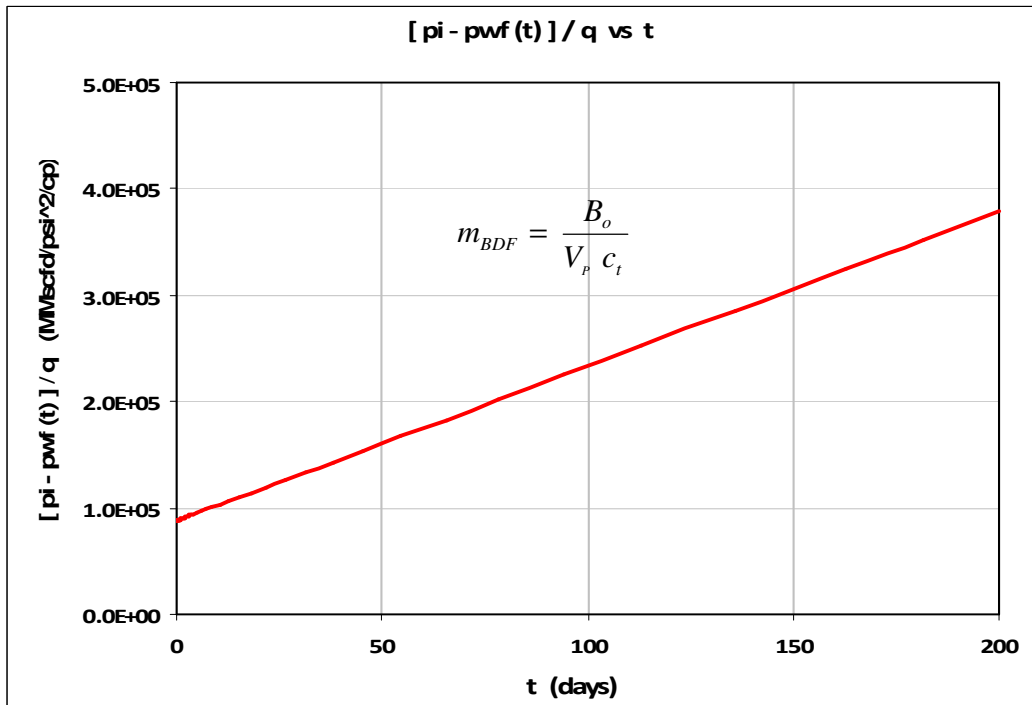


**Fig. 4.1 — Plot of  $[p_i - p_{wf}(t)] / q_o$  vs time for constant rate liquid BDF giving a straight line with slope  $m_{BDF}$  to calculate  $V_p$ .**

Eq.'s. 4.1 and 4.2 are used to drive BDF equation for constant rate.

$$\frac{[p_i - p_{wf}(t)]}{q_o} = \frac{B_o}{V_p c_t} t + \frac{[p_i - p_{wf}(t)]}{q_{oi}} \dots\dots\dots 4.3$$

Graphically a plot of  $[p_i - p_{wf}(t)] / q_o$  vs *time* (Fig 4.1) is a straight line with slope  $B_o / V_p c_t$ . The slope can be used to estimate the  $V_p$ .

Eq. 4.3 for variable rate liquid is of the form

$$\frac{(p_i - p_{wf})}{q_o(t)} = \frac{(p_i - p_{wf})}{q_{oi}} e^{\frac{J B_o}{V_p c_t} t} \dots\dots\dots 4.4$$

The plot of  $[p_i - p_{wf}] / q_o(t)$  vs *time* is no longer a straight line (Fig. 4.2) and can be traced back to Arps's exponential type decline ( $b=0$ ).

$$q_o(t) = q_{oi} e^{-D_i t} \dots\dots\dots 4.5$$

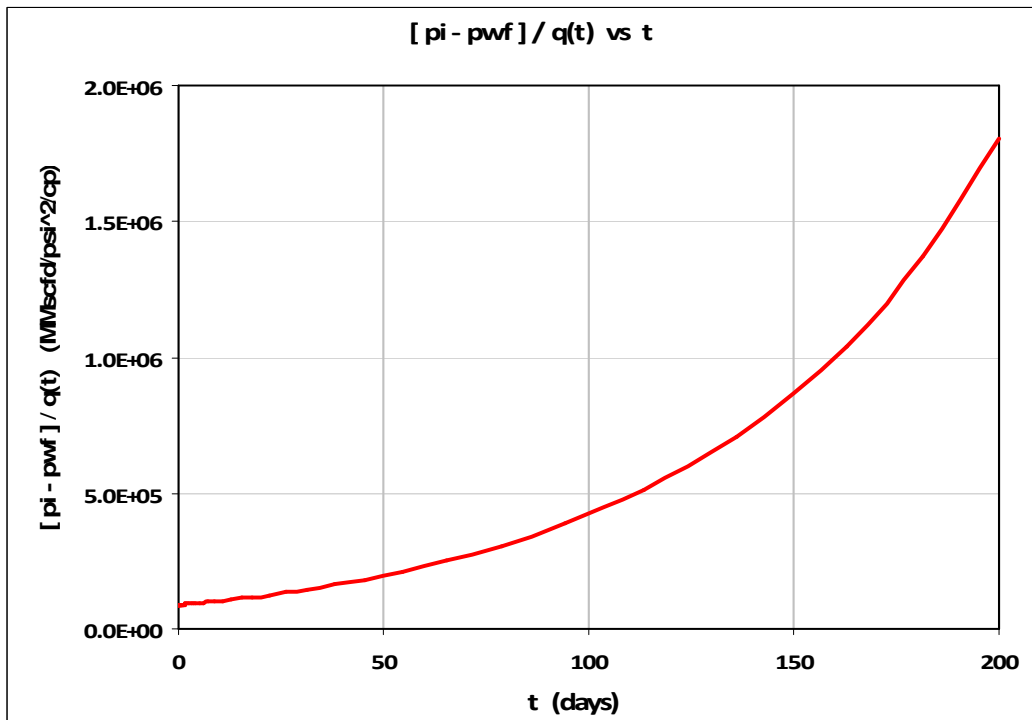


**Fig. 4.2 —Plot of  $[p_i - p_{wf}] / q_o(t)$  vs time variable rate liquid BDF exhibiting exponential decline ( $b = 0$ ).**

where

$$D_i = \frac{J B_o}{V_p \bar{c}_t}$$

Material balance time (Palacio & Blasingame. 1993), when used instead of actual time, will shift the variable rate liquid solution to a constant rate liquid solution (Fig 4.3).

$$t_c = \frac{N_p(t)}{q_o(t)} \dots\dots\dots 4.6$$

$$\frac{(p_i - p_{wf})}{q_o(t)} = \frac{B_o}{V_p \bar{c}_t} t_c + \frac{(p_i - p_{wf})}{q_{oi}} \dots\dots\dots 4.7$$

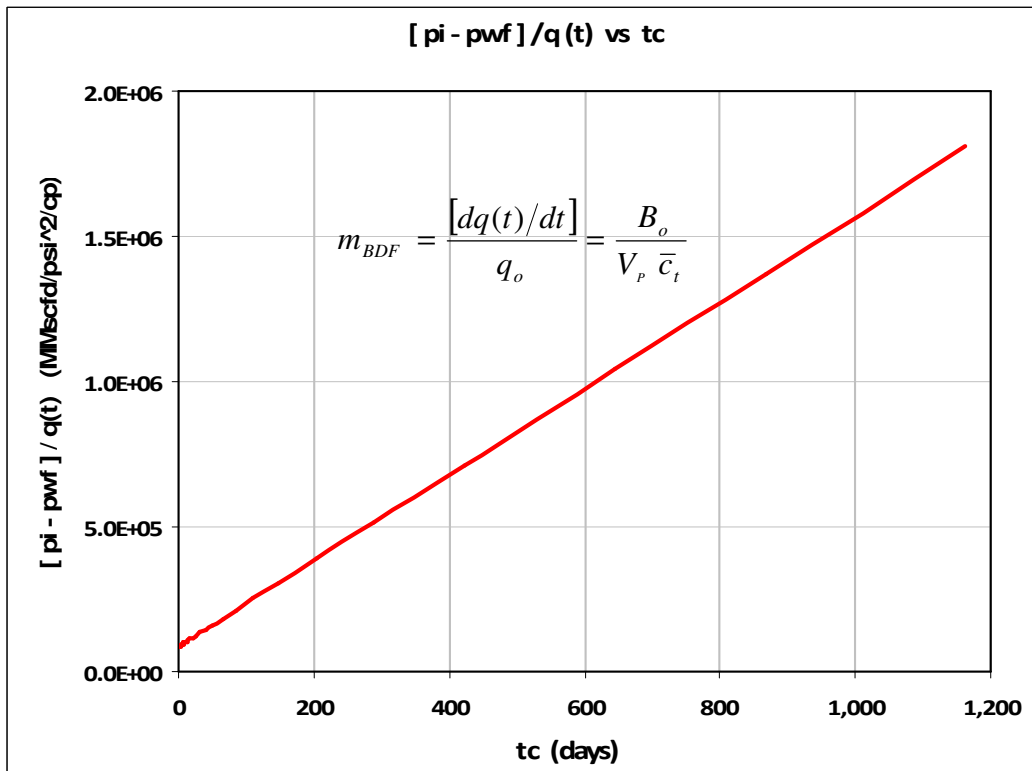


**Fig. 4.3 —Plot of  $[p_i - p_{wf}] / q_o(t)$  vs material balance time  $t_c$  variable rate liquid BDF shifting variable rate solution to constant rate solution with slope  $m_{BDF}$  to calculate  $V_p$ .**

Eq. 4.7 can be traced back to Arps's harmonic type decline ( $b=1$ ).

$$q_o(t) = \frac{q_{oi}}{[1 + D_i t_c]} \dots\dots\dots 4.8$$

where

$$D_i = \frac{J B_o}{V_p c_t}$$

The fundamental relations of volumetric expansion and productivity index can be applied on BDF gas if pseudo pressure and normalized pseudo time (Fraim & Wattenbarger, 1987) are used. To include adsorbed gas  $z^*$  (King, 1990) and compressibility  $c_t = S_g [c_g + c_d]$  (Bumb & McKee 1986) are incorporated in the solutions.

$$\frac{dm(\bar{p})}{dt_n^*} = -\frac{2 p_i}{G z_i^* \mu_i c_{ti}^*} \frac{q_g}{\dots\dots\dots} 4.9$$

$$q_g = J [m(\bar{p}) - m(p_{wf})] \dots\dots\dots 4.10$$

Similar to liquid case the corresponding, constant rate BDF gas equation including adsorbed gas, is of the form.

$$\frac{[m(p_i) - m(p_{wf})(t)]}{q_g} = \frac{[m(p_i) - m(p_{wf})(t)]}{q_{gi}} + \frac{2 p_i}{G z_i^* \mu_i c_{ti}^*} t_n^* \dots\dots\dots 4.11$$

A plot of  $[m(p_i) - m(p_{wf})(t)] / q_o$  vs  $t_n^*$  is a straight line (Fig. 4.4) with slope

$2p_i / G z_i^* \mu_i c_{ti}^*$ . The slope can be used to calculate OGIP.

Eq. 4.11 for variable rate Gas including adsorbed gas is of the form

$$\frac{[m(p_i) - m(p_{wf})]}{q_o(t)} = \frac{[m(p_i) - m(p_{wf})]}{q_{oi}} e^{\frac{2J p_i}{G z_i^* \mu_i c_{ti}^*} t_n^*} \dots\dots\dots 4.12$$

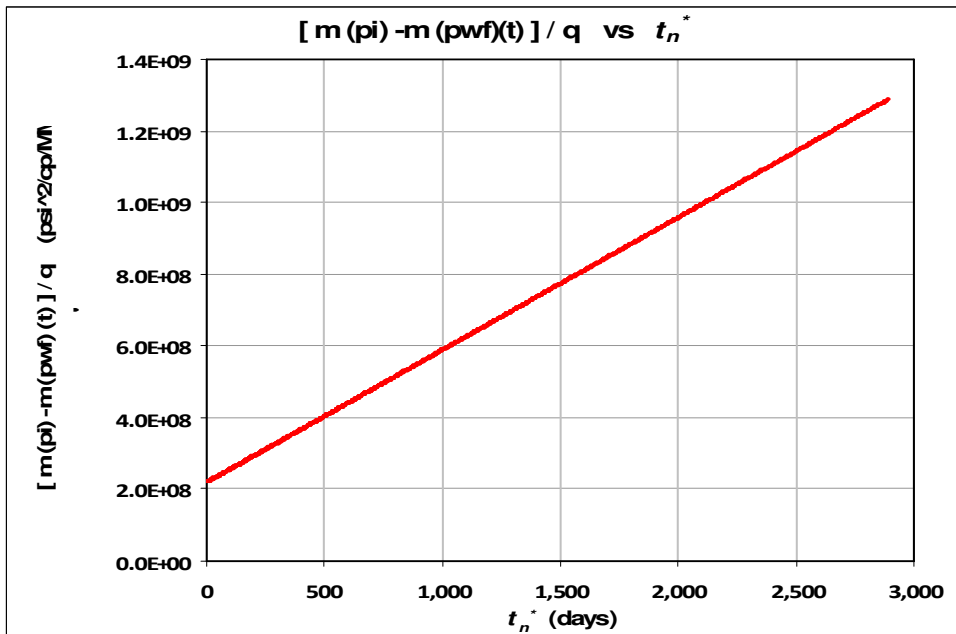


Fig. 4.4 —Plot of  $[m(p_i) - m(p_{wf})(t)] / q_g$  vs pseudo time  $t_n^*$  constant rate gas BDF including adsorbed gas with slope  $m_{BDF}$  to calculate  $G$ .

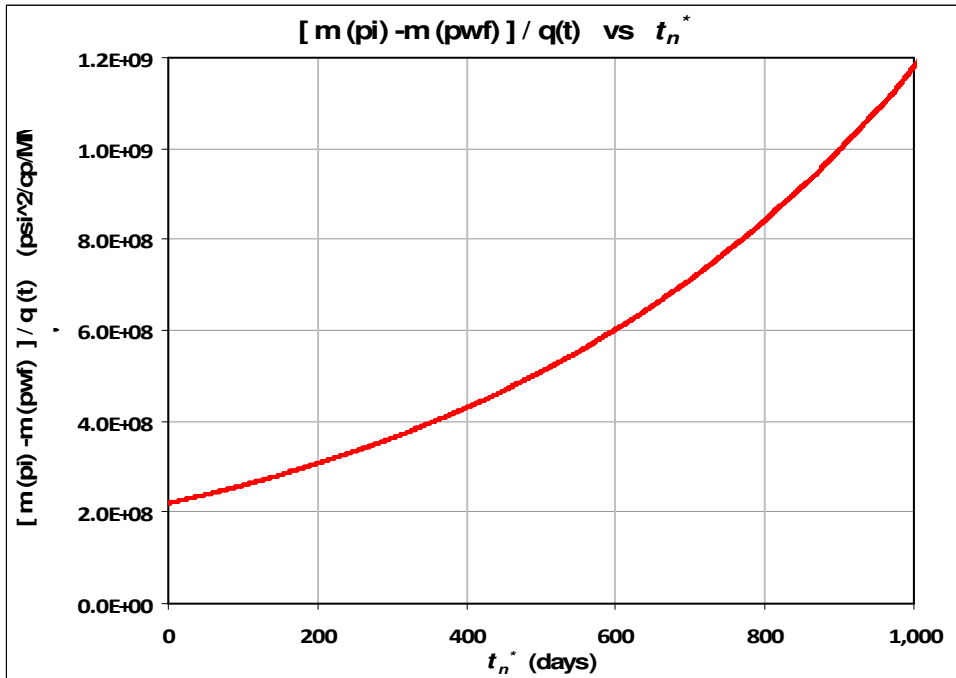


Fig. 4.5 —Plot of  $[m(p_i) - m(p_{wf})(t)] / q_g$  vs pseudo time  $t_n^*$  variable rate gas BDF including adsorbed gas exhibiting exponential decline ( $b = 1$ ).

The plot of  $[m(p_i) - m(p_{wf})(t)] / q_o$  vs  $t_n^*$  is no longer a straight line (Fig. 4.5) and can be traced back to Arps's (1944) exponential type decline ( $b=0$ ).

$$q_o(t) = q_{oi} e^{-D_i t} \dots\dots\dots 4.13$$

where

$$D_i = \frac{2 J p_i}{G z_i^* \mu_i c_{ti}^*}$$

Material balance pseudo time when used instead of normalized pseudo time shifts the variable rate gas solution to constant rate gas solution giving a straight line (Fig. 4.6), where material balance pseudo time including adsorbed gas is given as:

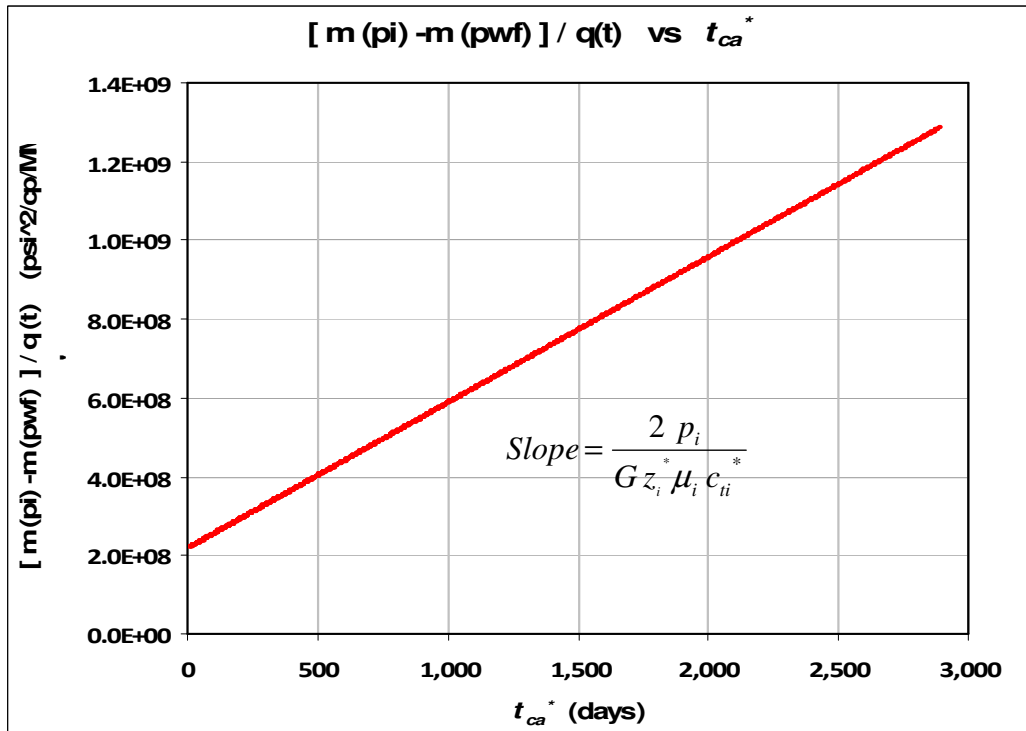


**Fig. 4.6 —Plot of  $[m(p_i) - m(p_{wf})] / q_g(t)$  vs material balance pseudo time  $t_{ca}^*$ , variable rate gas BDF including adsorbed gas, shifting variable rate gas solution to constant rate solution with slope  $m_{BDF}$  to calculate  $G$ .**

$$t_{ca}^* = \frac{1}{q_g(t)} \int_0^{t_n^*(t)} q_g(t_n^*) \frac{\mu_i c_{ti}^*}{\bar{\mu} \bar{c}_t^*} dt \dots\dots\dots 4.14$$

The solution for BDF variable rate gas is as under

$$\frac{[m(p_i) - m(p_{wf})]}{q_g(t)} = \frac{2 p_i}{G z_i^* \mu_i c_{ti}^*} t_{ca}^* + \frac{[m(p_i) - m(p_{wf})]}{q_{gi}} \dots\dots\dots 4.15$$

Eq. 4.15 can be traced back to Arps's (1944) harmonic type decline ( $b=1$ ).

$$q_g(t) = \frac{q_{gi}}{[1 + D_i t_{ca}^*]} \dots\dots\dots 4.16$$

where

$$D_i = \frac{2 J p_i}{G z_i^* \mu_i c_{ti}^*} = J m_{BDF} \dots\dots\dots 4.17$$

as

$$m_{BDF} = \frac{2 p_i}{G z_i^* \mu_i c_{ti}^*} \dots\dots\dots 4.18$$

## 4.2 Palacio and Blasingame's Method Including Adsorbed Gas

Palacio & Blasingame (1993) showed that if material pseudo time is used in analysis it is possible to model variable rate and variable pressure production for single phase gas using Fetkovich's (1980) harmonic decline ( $b=1$ ). The author's showed that OGIP can be calculated by using match points. Eq. 4.16 in Fetkovich's (1980) in dimensionless form is given as:

$$q_{dD} = \frac{1}{[1 + t_{dD}]} \dots\dots\dots 4.19$$

Recalling Eq. D.66 (Appendix D)

$$\frac{[m(p_i) - m(p_{wf})]}{q_g(t)} = \frac{2 p_i}{G z_i^* \mu_i c_{ii}^*} t_{ca}^* + \frac{[m(p_i) - m(p_{wf})]}{q_{gi}} \dots\dots\dots D.66$$

Substituting Eq. 4.18 and Eq. D.50 in D.66

$$\frac{[m(p_i) - m(p_{wf})]}{q_g(t)} = \frac{1}{J} (J m_{BDF} t_{ca}^* + 1) \dots\dots\dots 4.20$$

Taking inverse of Eq. 4.20 and re arranging

$$\frac{q_g(t)}{J [m(p_i) - m(p_{wf})]} = \frac{1}{(J m_{BDF} t_{ca}^* + 1)} \dots\dots\dots 4.21$$

$$\frac{q_g(t)}{q_{gi}} = \frac{1}{[1 + J m_{BDF} t_{ca}^*]}$$

$$q_{dD} = \frac{1}{[1 + t_{dD}]} \dots\dots\dots 4.22$$

where

$$q_{dD} = \frac{q_g(t)}{q_{gi}} = \frac{q_g(t)}{J [m(p_i) - m(p_{wf})]} \dots\dots\dots 4.23$$

$$t_{dD} = D_i t_{ca}^* = J m_{BDF} t_{ca}^* \dots\dots\dots 4.24$$

$$J = \frac{q_g(t)}{[m(p_i) - m(p_{wf})]} \bigg/ q_{dD} \dots\dots\dots 4.25$$

Eq.4.22 is similar to Eq.4.19.as suggested by Palacio and Blasingame when  $q_g(t) / [m(p_i) - m(p_{wf})]$  vs  $t_{ca}^*$  is plotted on a log-log scale exactly overlays Fetkovich's harmonic decline ( $b=1$ ) curve (Fig 4.7). Substituting Eq.4.25 and Eq. 4.18 in Eq.4.24 and rearranging

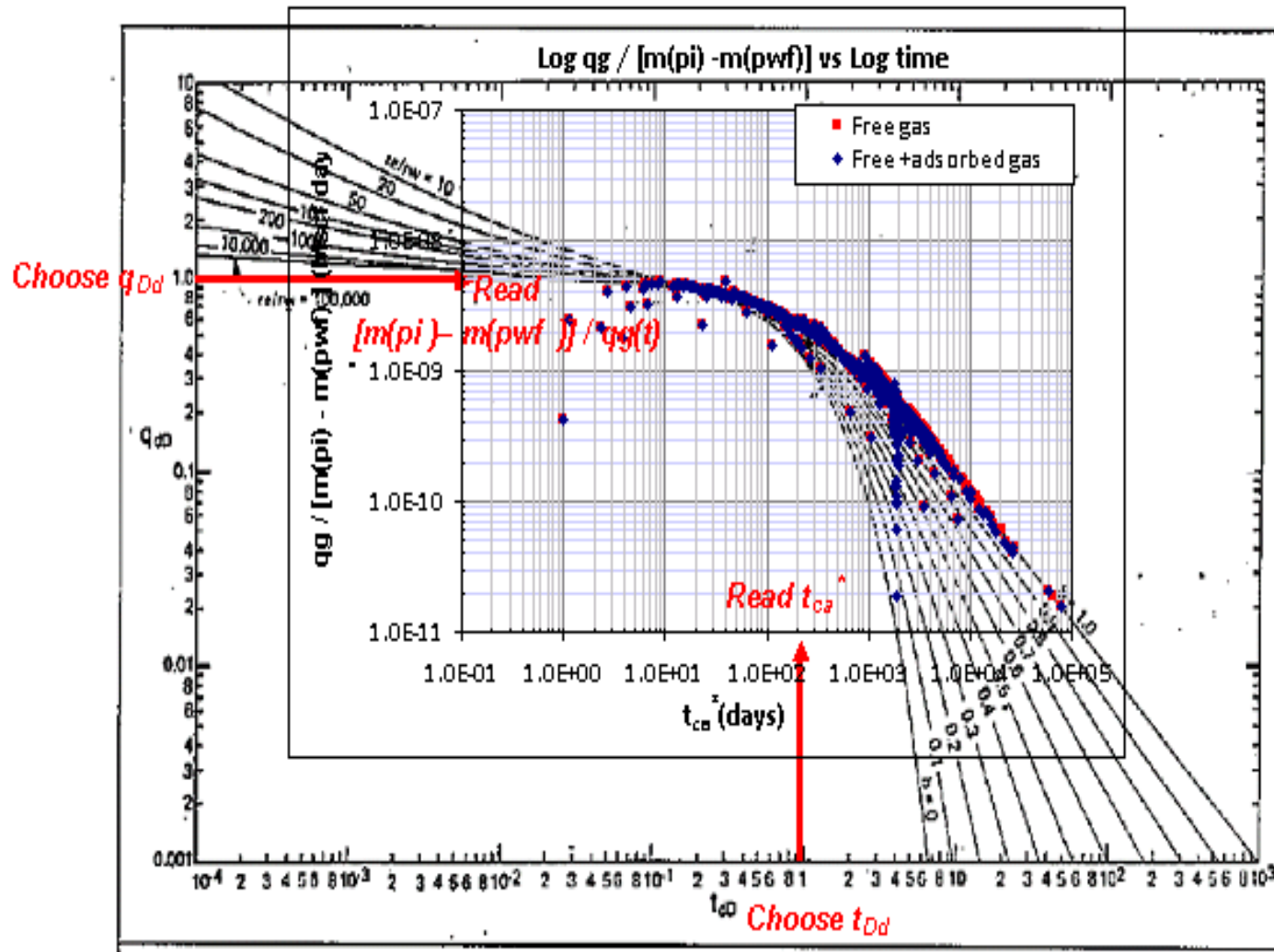


Fig. 4.7 — Matching plot of  $\log q_g / [m(p_i) - m(p_{wf})]$  vs  $\log t_{ca}^*$  on harmonic decline ( $b = 1$ ) stem of Fetkovich's (1980) type curves to establish match points.

$$G = \frac{\left( \frac{q_g(t)}{[m(p_i) - m(p_{wf})]} \right)_{M.P.}}{(q_{Dd})_{M.P.}} \frac{2 p_i}{z_i * \mu_i c_{ti} *} \frac{(t_{ca}^*)_{M.P.}}{(t_{Dd})_{M.P.}} \dots\dots\dots 4.26$$

where *M.P* stands for match point. The match points permit us to calculate OGIP with and without adsorbed gas using Eq.4.26.

### 4.3 Ibrahim, Wattenbarger and Helmy's Method Including Adsorbed Gas

Ibrahim, Wattenbarger and Helmy showed that Eq. D.66 can be used to estimate OGIP by using normalized superposition pseudo time (*Super-t<sub>n</sub>*) instead of *t<sub>ca</sub>*\*. To account for the adsorbed gas *Super-t<sub>n</sub>*\* instead of *Super-t<sub>n</sub>* is used (Fig.4.8).

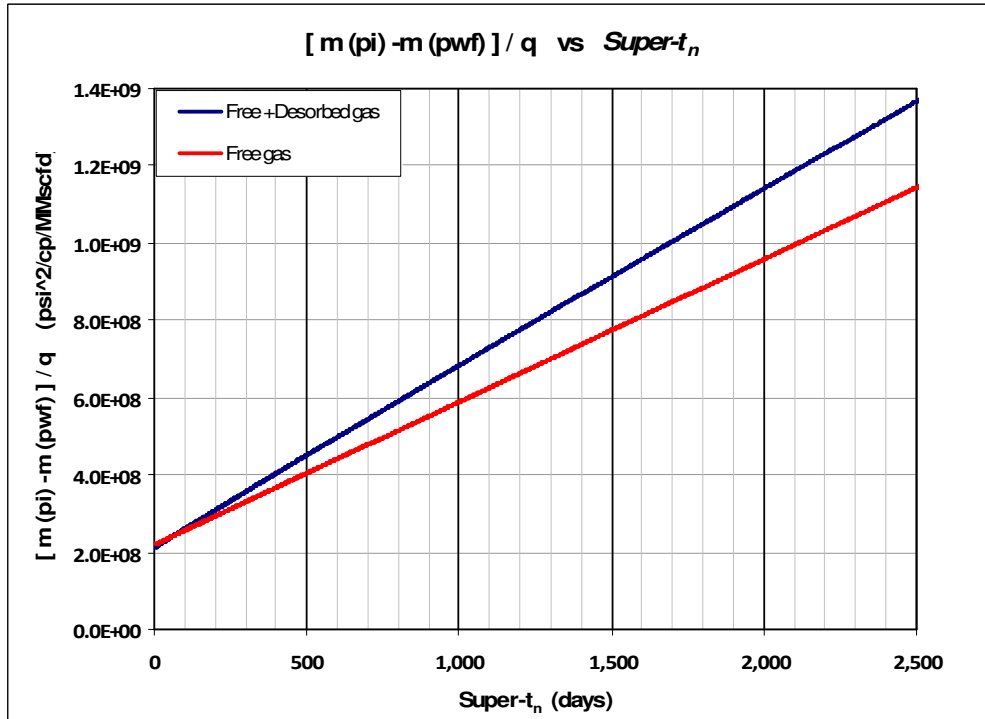


**Fig. 4.8 —Ibrahim, Wattenbarger and Helmy's plot  $[m(p_i) - m(p_{wf})] / q_g$  vs  $Super-t_n^*$  with and without adsorbed gas BDF with slope  $m_{BDF}$  used to calculate OGIP.**

Rewriting equation Eq. 4.15 with *Super-t<sub>n</sub>*\*

$$\frac{[m(p_i) - m(p_{wf})]}{q_g(t)} = \frac{2 p_i}{G z_i^* \mu_i c_{ti}^*} Super-t_n^* + \frac{[m(p_i) - m(p_{wf})]}{q_{gi}} \dots\dots\dots 4.27$$

where (*Super-t<sub>n</sub>*<sup>\*</sup>) and Slope are given as

$$(Super-t_n^*) = \left[ \sum_{i=1}^n \frac{\Delta q_{qi}}{q_{gn}} (t_n^* - t_{i=1}^*) \right]$$

$$m_{BDF} = \frac{2 p_i}{G z_i^* \mu_i c_{ti}^*}$$

Ibrahim, Wattenbarger and Helmy et al used plotting functions  $[m(p_i) - m(p_{wf})]/q_g$  vs *Super-t<sub>n</sub>*<sup>\*</sup>. OGIP is than calculated as

$$G = \frac{2 p_i}{m_{PSS} z_i^* \mu_i c_{ti}^*}.$$

It should be noted here that *Super-t<sub>n</sub>*<sup>\*</sup> is equivalent to the Palacio and Blasingame's pseudo material balance *t<sub>ca</sub>*<sup>\*</sup> (Eq. 4.14).

#### 4.4 Anderson et al.'s Method Including Adsorbed Gas

Anderson et al. (2010) used a similar form of equation

$$\frac{q_g(t)}{[m(p_i) - m(p_{wf})]} = \frac{2 J p_i q_g(t)}{G z_i^* \mu_i c_{ti}^* [m(p_i) - m(p_{wf})]} t_{ca}^* + \frac{q_{gi}}{[m(p_i) - m(p_{wf})]} \dots\dots\dots 4.28$$

This equation is a equation of a straight line with slope *J/G*. Anderson et al used plotting functions (normalized rate) vs (normalized cumulative production) on Cartesian co-ordinates to obtain OGIP directly (Fig 4.9).

Normalized rate and normalized cumulative production are given as

$$\text{Normalized rate} = q_g / [m(p_i) - m(p_{wf})]$$

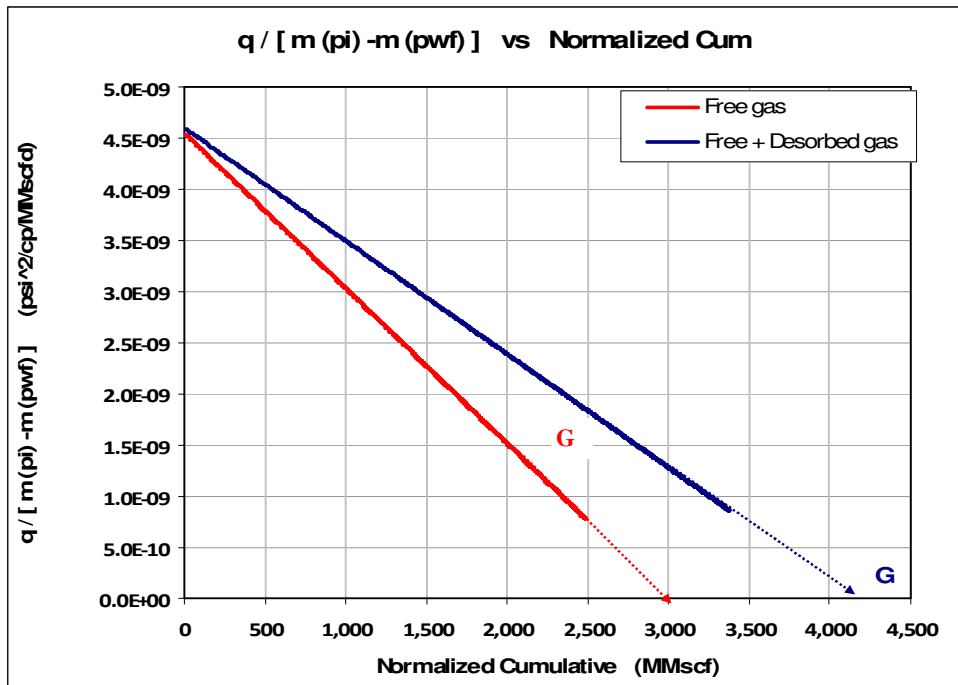


**Fig. 4.9 —Anderson et al.'s plot normalized rate vs normalized cumulative with and without adsorbed gas showing OGIP on x-axis.**

$$\text{Normalized cumulative production} = \frac{2 p_i q_g}{z_i * \mu_i c_{ti} * [m(p_i) - m(p_{wf})]} t_{ca} *$$

Anderson et al.'s plot (Fig. 4.9) shows the OGIP directly on the x-axis when extrapolated.

#### 4.5 OGIP Estimation from Transient Flow Data

Due to very low permeability the shale gas reservoirs are found to exhibit transient linear flow for very long period. Analytical solutions are applied on transient linear flow to estimate OGIP. The equation to estimate pore volume using end of transient time ( $t_{esr}$ ) is presented (Ibrahim & Wattenbarger 2005) previously as

$$V_p = f_{CP} \frac{200.8 T}{(\mu c_t)_i} \left( \frac{\sqrt{t_{esr}}}{\tilde{m}_4} \right) \dots\dots\dots 4.29$$

where  $\sqrt{t_{esr}}$  and  $\tilde{m}_4$  are the end of transient flow time and slope of the straight line exhibited by transient flow on a plot of  $[m(p_i) - m(p_{wf})]/q_g$  vs  $\sqrt{t}$  (Fig. 4.10).

As

$$V_p = \phi V_B$$

Substituting  $V_p$  in Eq. 4.29 results in

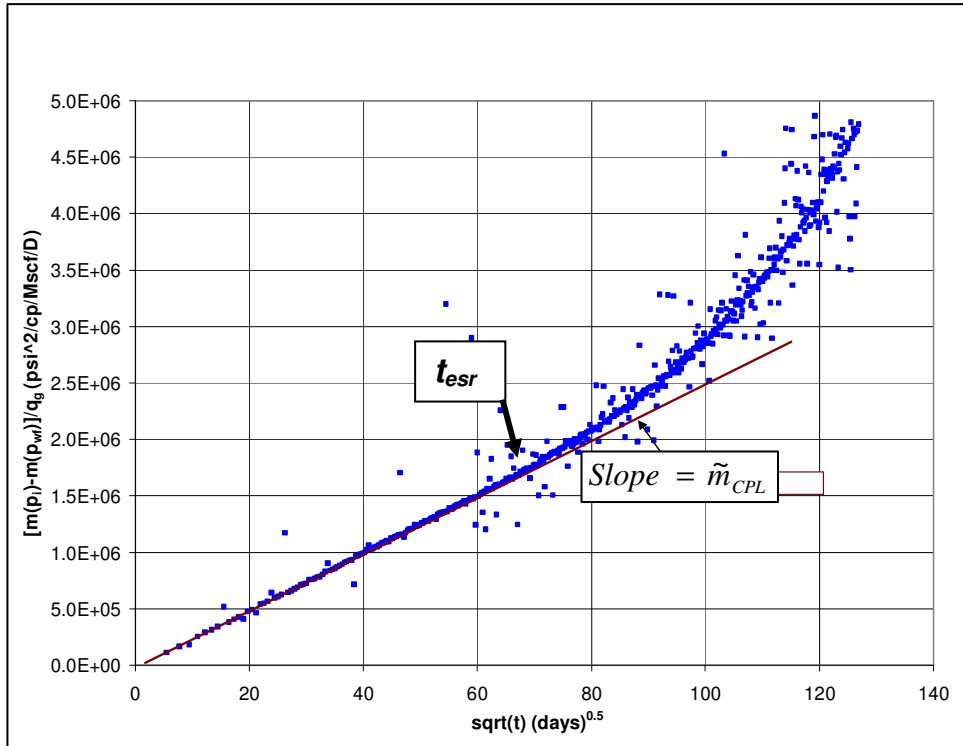


**Fig. 4.10 — Ibrahim and Wattenbarger (2005) plot of  $[m(p_i) - m(p_{wf})]/q_g$  vs  $\sqrt{t}$  to establish end of transient time  $t_{esr}$  and slope of line exhibited by transient flow.**

$$V_B = f_{CP} \frac{200.8 T}{\phi(\mu c_t)_i} \left( \frac{\sqrt{t_{esr}}}{\tilde{m}_{CPL}} \right) \dots\dots\dots 4.30$$

OGIP including adsorbed gas is given by Eq.3.3 as

$$G = V_B \left[ \left( \frac{\phi S_{gi}}{B_{gi}} \right) + \left( V_L \frac{p_i}{(p_i + p_L)} \right) \right] \dots\dots\dots 3.3$$

Substituting Eq. 4.30 in Eq. 3.3

$$G = f_{CP} \frac{200.8 T}{\phi(\mu c_t^*)_i} \left( \frac{\sqrt{t_{esr}}}{\tilde{m}_{CPL}} \right) \left[ \left( \frac{\phi S_{gi}}{B_{gi}} \right) + \left( V_L \frac{p_i}{(p_i + p_L)} \right) \right] \dots\dots\dots 4.31$$

Eq.4.31 can be used to calculate OGIP with and without adsorbed gas. Where  $c_t^*$  is given as

$$c_t^* = S_g [c_g + c_d]$$

$f_{CP}$  in Eq. 4.31 is the correction factor which corrects the error in slope due to draw down effect and is given as

$$f_{CP} = 1 - 0.0852(D_D) - 0.0857(D_D)^2$$

where  $D_D$  is the dimensionless draw down given as

$$D_D = \frac{m(p_i) - m(p_{wf})}{m(p_i)}$$

## CHAPTER V

### FIELD CASES

In order to demonstrate the effect of adsorbed gas, four Barnett shale wells which show BDF flow were selected to perform our analysis. Production data from these wells is used to estimate OGIP using SGPA. The OGIP is then used to forecast the 50 years production with and without adsorbed gas using the numerical simulator (URS 01.2009).

#### 5.1 BDF in Shale Gas Reservoirs

Fig. 5.1 (Al-Ahmadi et al. 2010) showed a conceptual model representing a shale gas horizontal well with hydraulic fractures. Gas drains from the matrix in the hydraulic fractures and then to the well.  $L$  is the spacing between the hydraulic fractures. As the

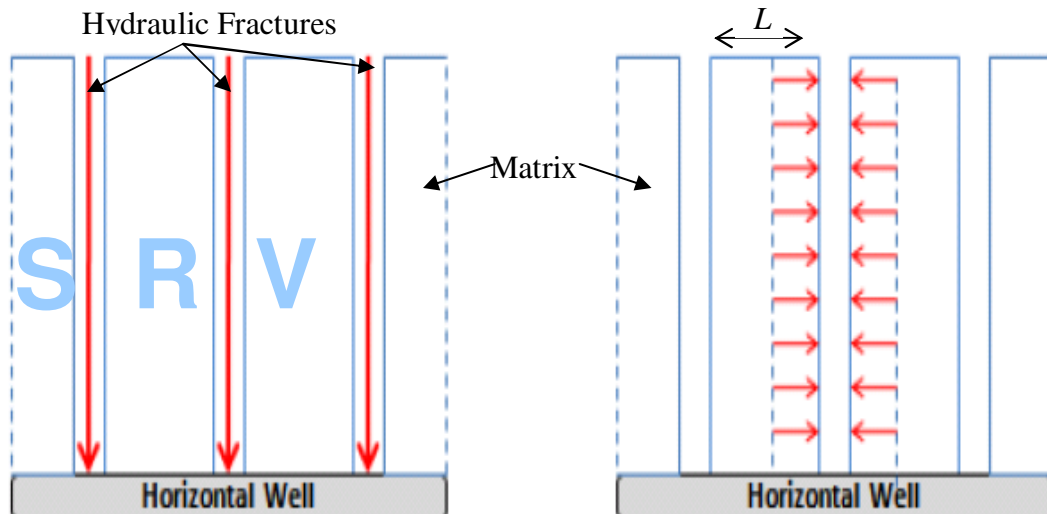


**Fig. 5.1 —Slab model (Al-Ahmadi et al. 2010) showing BDF and stimulated reservoir volume (SRV).**

pressure declines and the matrix is drained to the half of fracture spacing ( $L$ ) BDF will start. It is assumed that only the stimulated reservoir volume (SRV) which is the matrix volume open to hydraulic fractures contributes to the flow. Our analysis techniques require that the start of BDF flow may be recognized accurately. In this work we used square root of time plot as diagnostic plot to distinguish end of transient flow period. Transient flow signal on square root of time plot will as a straight line.

## 5.2 Field Data Analysis

Field data from the selected wells was analyzed in the following order.

### a. Estimation of OGIP (End of Transient data)

1. Use production data to plot  $[m(p_i) - m(p_{wf})] / qg$  vs  $Sqrt (time)$  to determine end of transient flow period ( $t_{esr}$ ).
2. Calculate slope of straight line (transient flow data) from square root of time plot.
3. Calculate OGIP with and without adsorption using Eq. 4.31

### b. Estimation of OGIP (Palacio & Blasingame)

1. Use production data to plot  $\text{Log } [m(p_i) - m(p_{wf})] / qg$  vs  $\text{Log } t_{ca}^*$ .
2. Match plot  $\text{Log } qg / [m(p_i) - m(p_{wf})]$  vs  $\text{Log } t_{ca}^*$  on harmonic stem ( $b = 1$ ) of Fetkovich's decline curve to establish match points.
3. Use match points to calculate OGIP with and without adsorption using equation

$$G = \frac{\left( \frac{q_g(t)}{[m(p_i) - m(p_{wf})]} \right)_{M.P.}}{(q_{Dd})_{M.P.}} \frac{2 p_i}{z_i * \mu_i c_{ti} *} \frac{(t_{ca}^*)_{M.P.}}{(t_{Dd})_{M.P.}}$$

### c. Estimation of OGIP (BDF Ibrahim, Wattenbarger and Helmy)

1. Use production data to plot  $[m(p_i) - m(p_{wf})] / qg$  vs  $\sqrt{time}$  to determine start of BDF flow.
2. Plot  $[m(p_i) - m(p_{wf})] / qg$  vs  $t_{ca}$  on Cartesian co-ordinates and calculate Slope (PSS).
3. Calculate OGIP using equation

$$G = \frac{2 p_i q}{m_{BDF} z_i \mu_i c_{ti}}$$

4. Using calculated OGIP, calculate  $p/z$  for each data point using MB equation

$$\frac{\bar{p}}{\bar{z}} = \frac{p_i}{z_i} \left[ 1 - \frac{G_p}{G} \right]$$

5. Calculate average reservoir pressure at each data point and update gas properties.
6. Repeat step 2 & 3.
7. If new OGIP is equal to previous OGIP than stop, otherwise repeat steps 2 to 6 until OGIP converges.

In order to demonstrate the effect of adsorption we need to estimate OGIP separately first assuming that all the production is coming from free gas only and then assuming that produced gas comprises of both free gas and adsorbed gas. In this way we will have two estimated OGIPs one without adsorbed gas and one with adsorbed gas. While estimating OGIP for free + adsorbed gas  $z$  is replaced by modified  $z^*$  (King, 1990) and  $c_g$  is replaced by  $[c_g + c_d]$  (Bumb & McKee, 1986) at each time step. Also Langmuir's approximate constants for Barnett shale are used to determine the amount of adsorbed gas. All these calculations are performed using SGPA.

d. *Comparison of results with and without adsorbed gas*

Using the estimated OGIP's for with and without adsorbed gas we can plot the results on  $[m(p_i) - m(p_{wf})] / qg$  vs  $t_{ca}$  and Anderson et al.'s plot and compare the results.

e. *Verification of SGPA results using numerical simulator (URS 01.2009)*

The SGPA results for with and without adsorbed gas are then verified by matching SGPA and numerical simulator (URS 01.2009) results.

f. *Forecasting*

Once the OGIP for both with and without adsorbed gas cases are determined and verified by simulation, the results are then used to forecast the production for 50 years. We have compared the results of produced gas with and without adsorption at the end of 50 years.

g. *Summary of results*

The results from each well are summarized in form of table following the plots.

The rest of this chapter consists of plots followed by summary of results of each of the four wells

### 5.3 Well 137

Following figures (5.2 – 5.6) and Table 5.1 show the OGIP estimation methods applied to field data from a Barnett shale well as discussed in section 5.2 of this chapter.

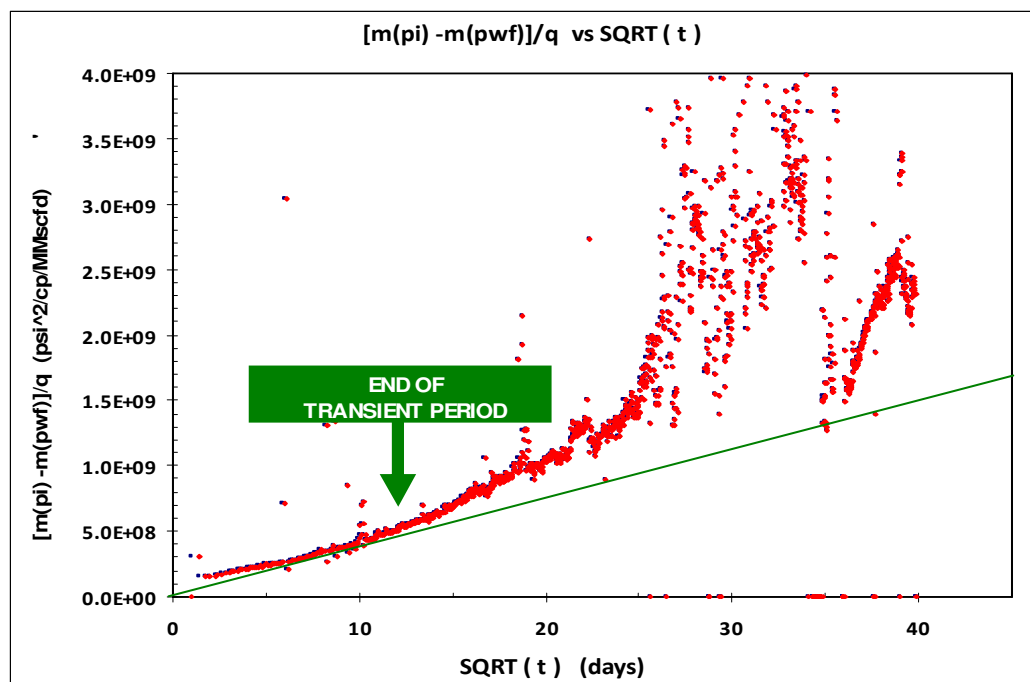


**Fig. 5.2** —Square of time plot to determine end of transient time and slope of straight line exhibited by transient flow, Well 137.

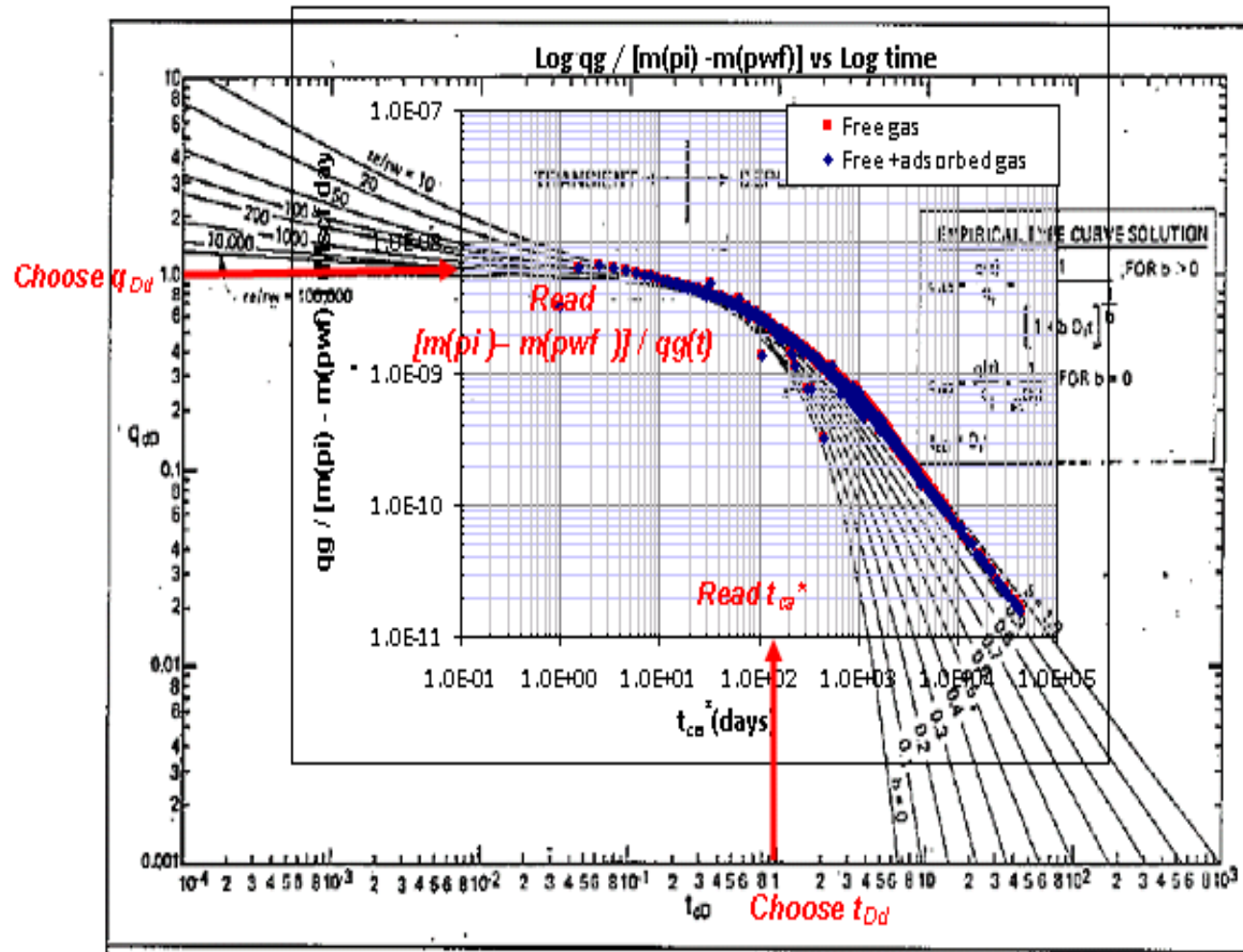


Fig. 5.3 — Matching plot of  $\log q_g / [m(p_i) - m(p_{wf})]$  vs  $\log t_{ca}^*$  on harmonic decline ( $b = 1$ ) stem of Fetkovich's (1980) type curve to establish match points used to calculate OGIP with and without adsorbed gas by Palacio & Blasingame's (1993) method, Well 137.

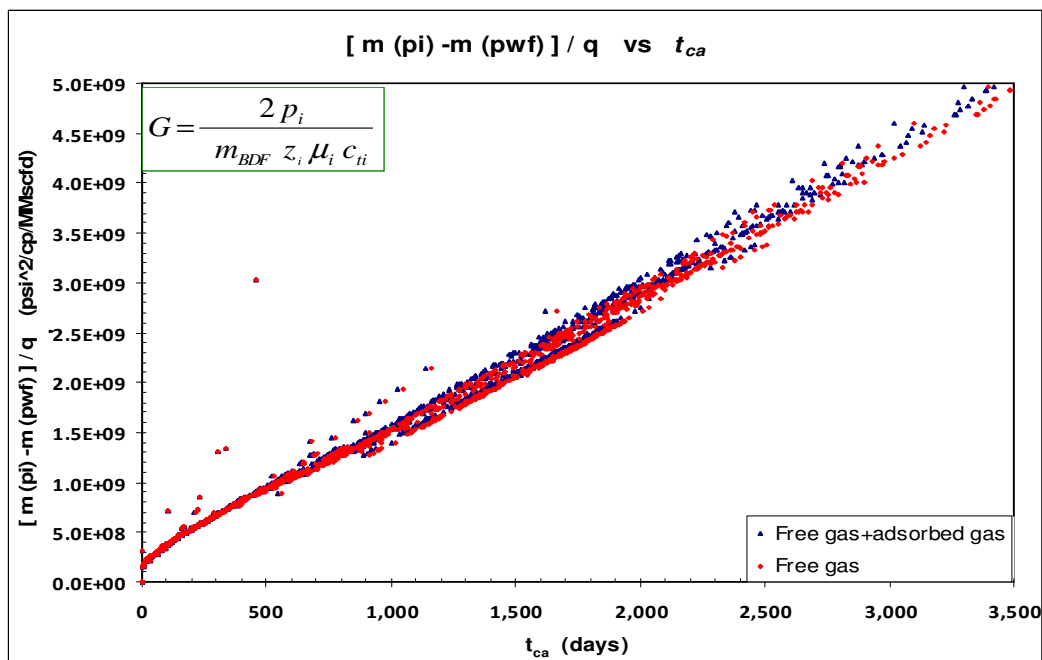


Fig. 5.4 —Plot of  $[m(p_i) - m(p_{wf})] / q_g$  vs  $t_{ca}^*$  showing with and without adsorbed gas BDF with slope  $m_{BDF}$  used to calculate OGIP, Well 137.

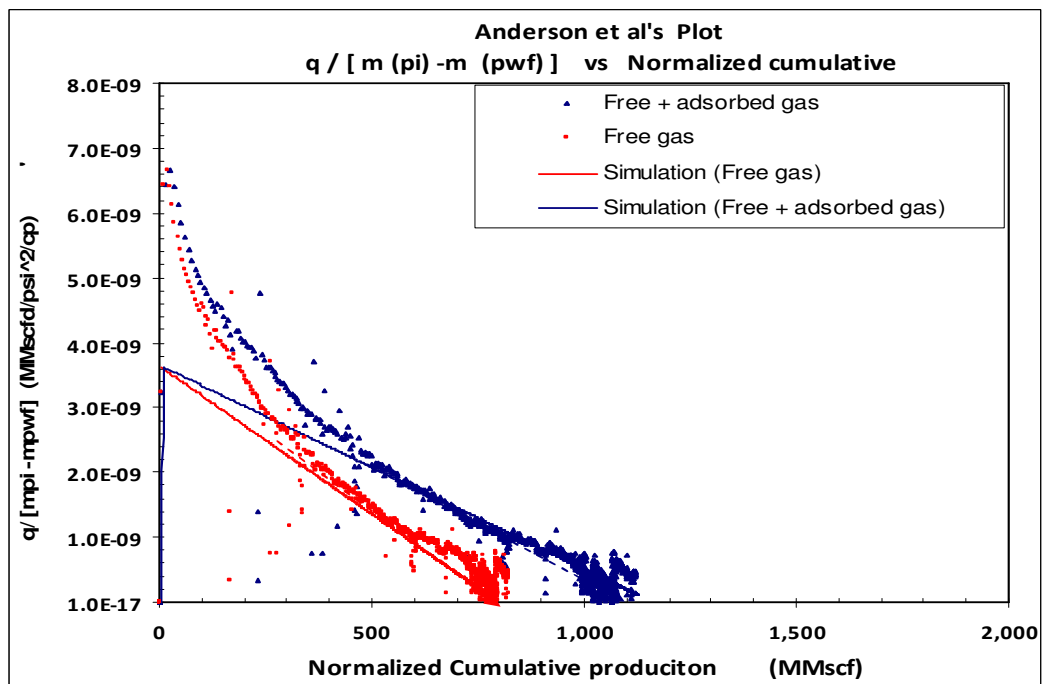
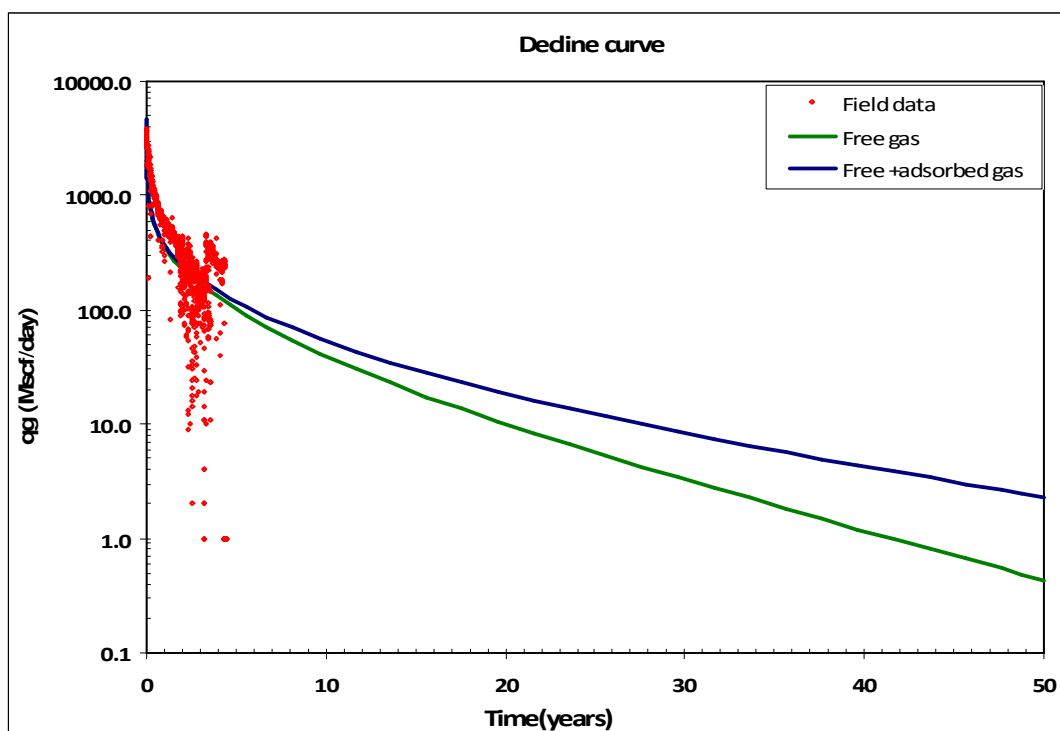


Fig. 5.5 —Normalized rate vs normalized cumulative with and without adsorbed gas showing OGIP on x-axis, Well 137.



**Fig. 5.6 —Decline curve: forecast results for 50 years with and without adsorbed gas, Well 137.**

<b>Table 5.1— Summary of Results, Well 137</b>						
<b>Estimated Parameters</b>	<b>OGIP Transient Data</b>		<b>OGIP BDF (Ibrahim, Wattenbarger &amp; Helmy)</b>		<b>OGIP BDF (Palacio &amp; Blasingame)</b>	
	Without Adsorbed Gas	With Adsorbed Gas	Without Adsorbed Gas	With Adsorbed Gas	Without Adsorbed Gas	With Adsorbed Gas
OGIP free, Bscf	0.87	0.79	0.8	0.8	0.83	0.77
OGIP Adsorbed, Bscf	0	0.42	0	0.4	0	0.37
OGIP Total, Bscf	0.87	1.2	0.8	1.2	0.83	1.15
SRV, rcf	$7.28 \times 10^7$	$6.58 \times 10^7$	$6.70 \times 10^7$	$6.43 \times 10^7$	$6.70 \times 10^7$	$6.43 \times 10^7$
$G_p$ (50 yrs) Bscf	-	-	0.68	0.80	-	-
RF (50 yrs)	-	-	0.85	0.67	-	-

## 5.4 Well 257

Following figures (5.7 – 5.11) and Table 5.2 show the OGIP estimation methods applied to field data from a Barnett shale well as discussed in section 5.2 of this chapter.

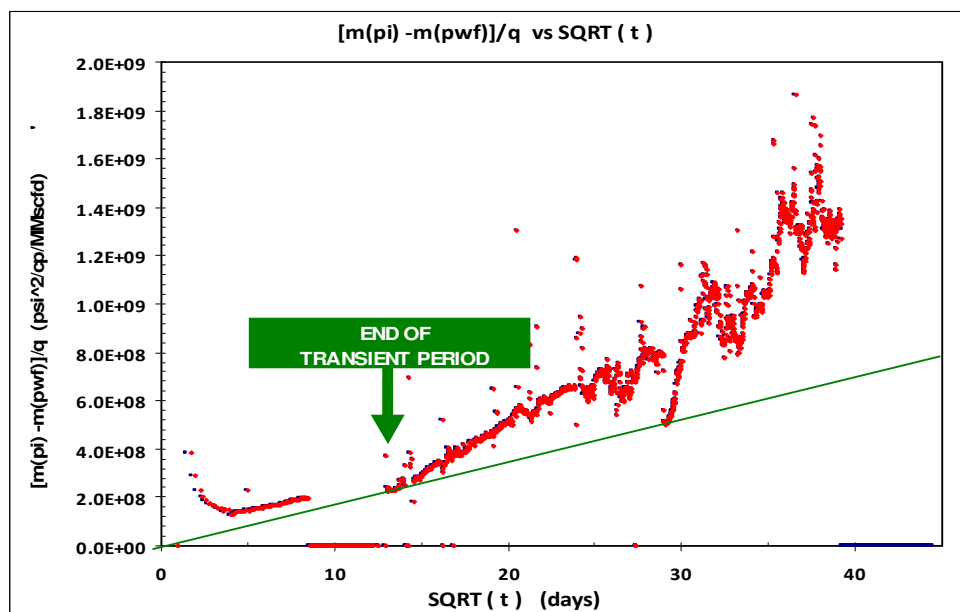


**Fig. 5.7 — Square of time plot to determine end of transient time and slope of straight line exhibited by transient flow, Well 257.**

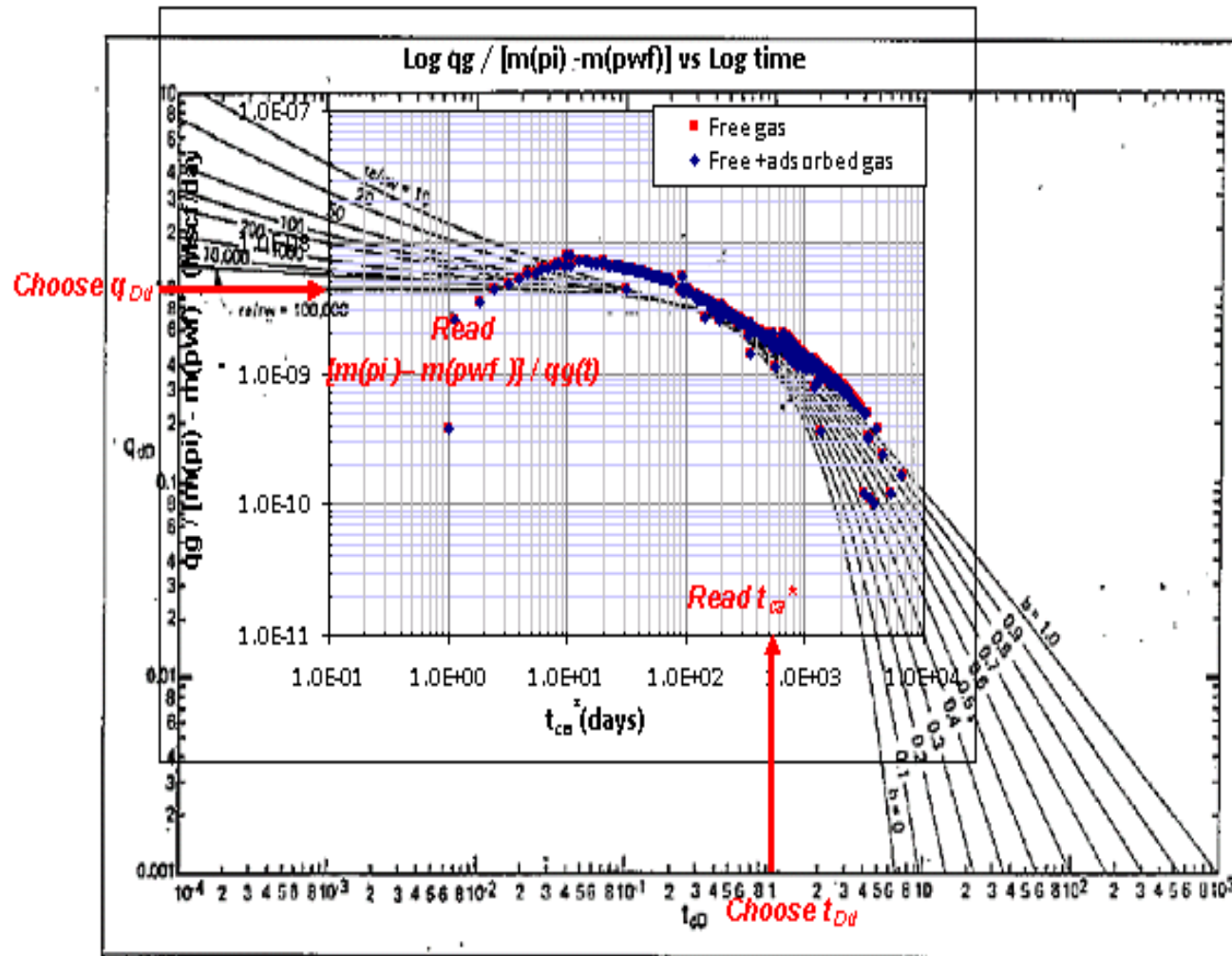


Fig. 5.8 —Matching plot of  $\log [m(p_i) - m(p_{wf})] / q_g$  vs  $\log t_{ca}^*$  on harmonic decline ( $b = 1$ ) stem of Fetkovich's (1980) Type curve to establish match points used to calculate OGIP with and without adsorbed gas by Palacio and Blasingame's (1993) method, Well 257.

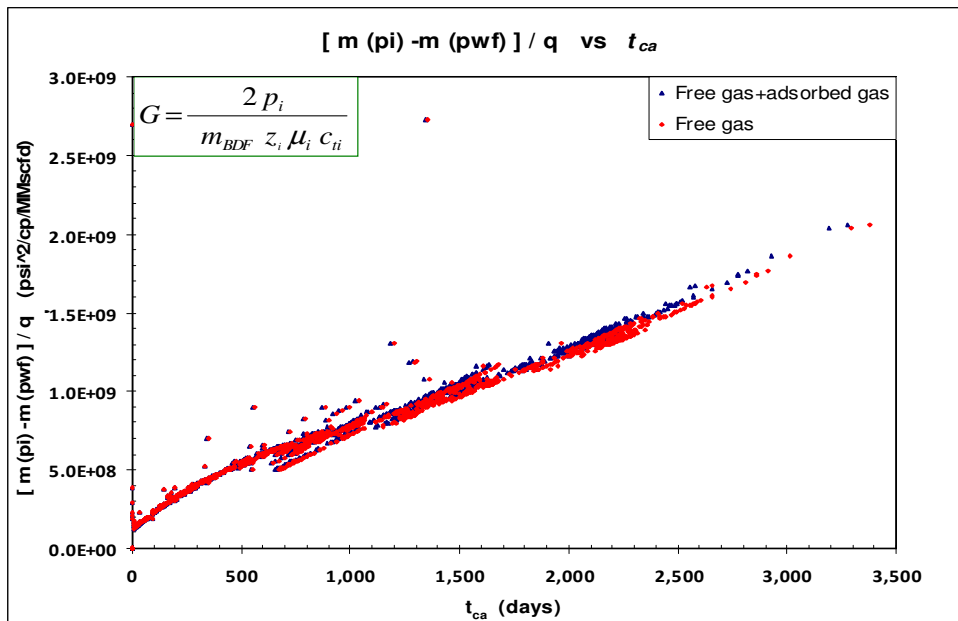


Fig. 5.9 — Plot of  $[m(p_i) - m(p_{wf})] / q_g$  vs  $t_{ca}^*$  showing with and without adsorbed gas BDF with slope  $m_{BDF}$  used to calculate OGIP, Well 257.

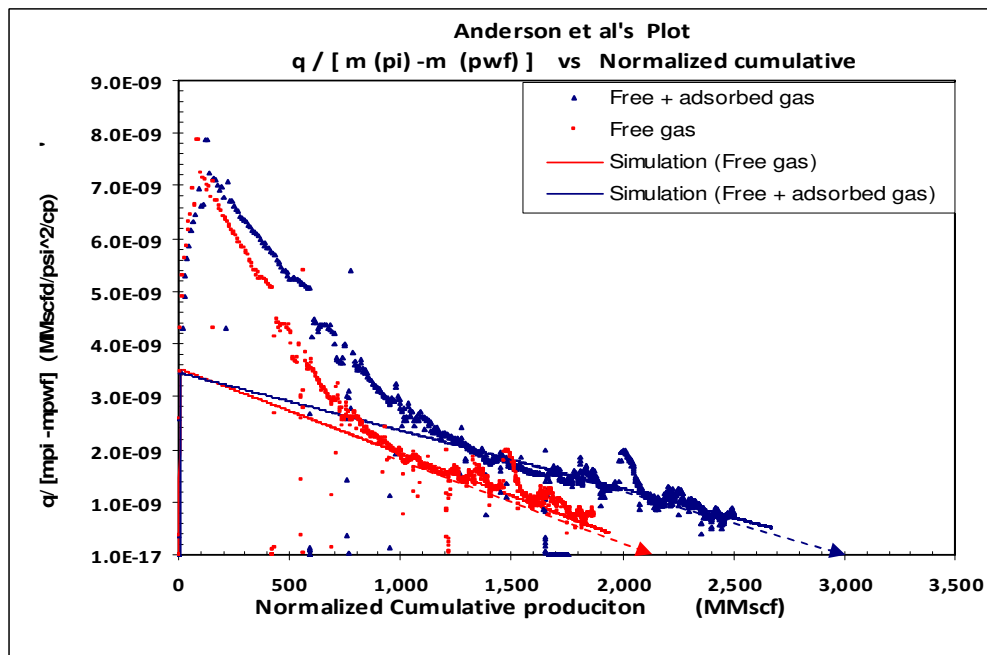


Fig. 5.10 — Normalized rate vs normalized cumulative with and without adsorbed gas showing OGIP on x-axis, Well 257.

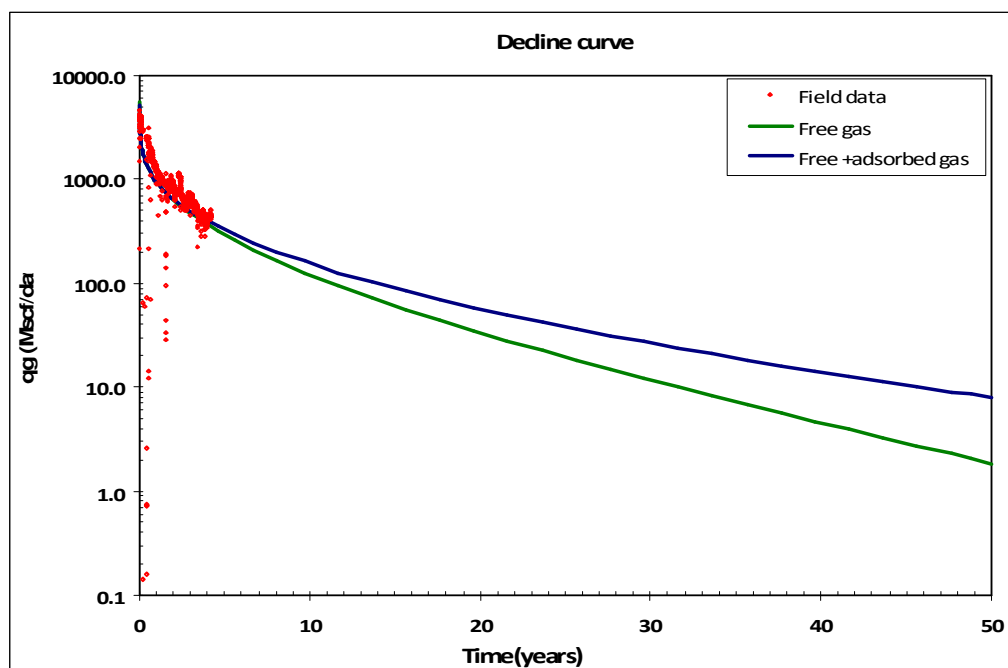
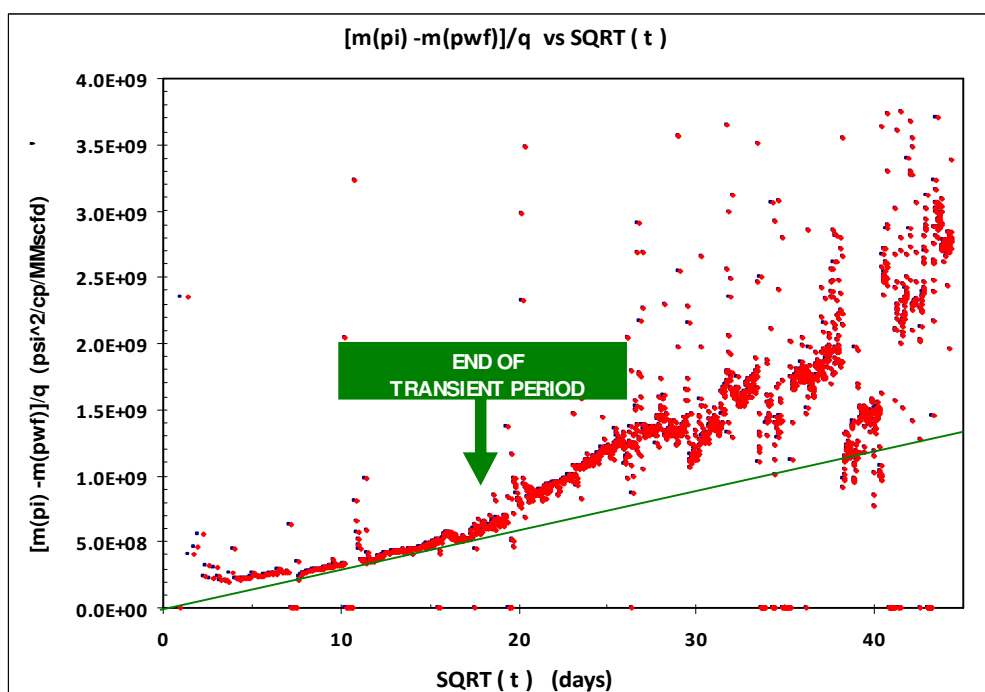


Fig. 5.11 —Decline curve: forecast results for 50 years with and without adsorbed gas, Well 257.

Table 5.2— Summary of Results, Well 257						
Estimated Parameters	OGIP transient Data		OGIP BDF (Ibrahim, Wattenbarger & Helmy)		OGIP BDF (Palacio & Blasingame)	
	Without Adsorbed Gas	With Adsorbed Gas	Without Adsorbed Gas	With Adsorbed Gas	Without Adsorbed Gas	With Adsorbed Gas
OGIP free, Bscf	2.3	2.0	2.2	1.03	2.20	1.02
OGIP Adsorbed, Bscf	0	1.1	0	2.07	0	2.04
OGIP Total, Bscf	2.3	3.1	2.2	3.1	2.20	3.06
SRV, rcf	$1.90 \times 10^8$	$1.72 \times 10^8$	$1.84 \times 10^8$	$1.73 \times 10^8$	$1.86 \times 10^8$	$1.71 \times 10^8$
$G_p$ (50 yrs) Bscf	-	-	1.9	2.2	-	-
RF (50 yrs)	-	-	0.85	0.71	-	-

## 5.5 Well 285

Following figures (5.12 – 5.16) and Table 5.3 show the OGIP estimation methods applied to field data from a Barnett shale well as discussed in section 5.2 of this chapter.



**Fig. 5.12 — Square of time plot to determine end of transient time and slope of straight line exhibited by transient flow, Well 285.**

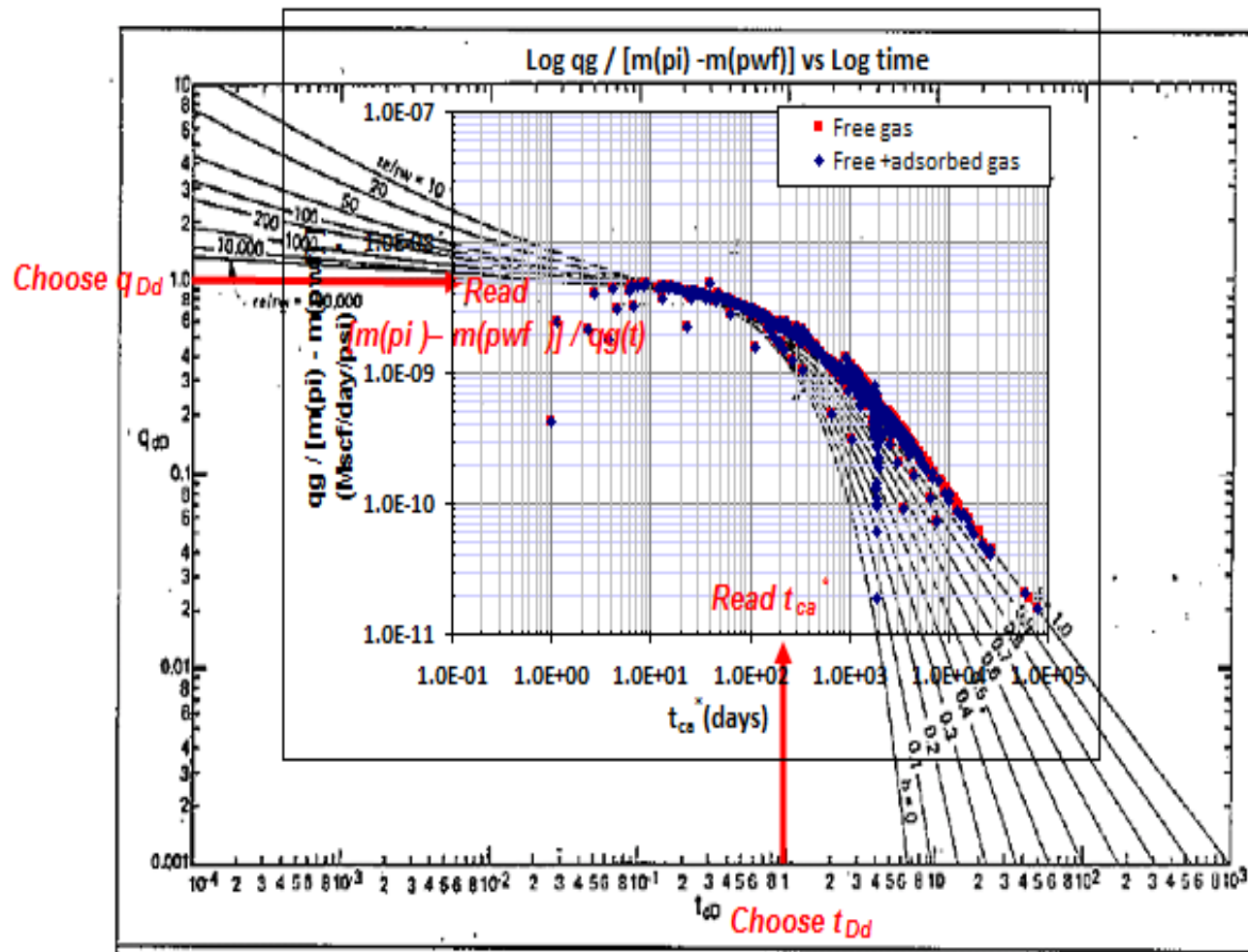


Fig. 5.13 —Matching plot of  $\log [m(p_i) - m(p_{wf})] / q_g$  vs  $\log t_{ca}^*$  on harmonic decline ( $b = 1$ ) stem of Fetkovich's (1980) type curve to establish match points used to calculate OGIP with and without adsorbed gas by Palacio & Blasingame's (1993) method, Well 285.

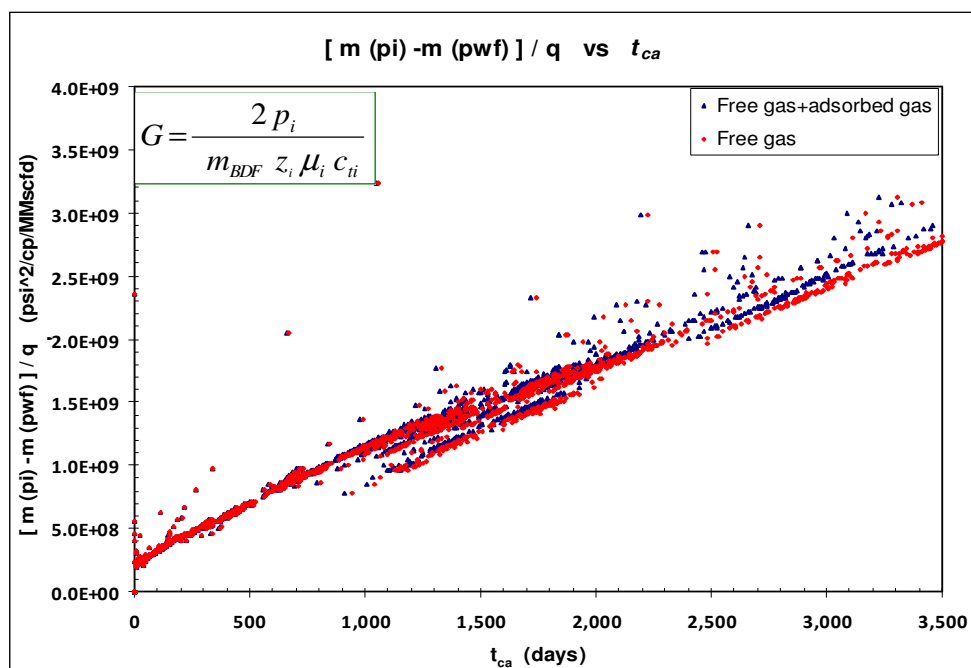


Fig. 5.14 — Plot of  $[m(p_i) - m(p_{wf})] / q_g$  vs  $t_{ca}^*$  showing with and without adsorbed gas BDF with slope  $m_{BDF}$  used to calculate OGIP, Well 285.

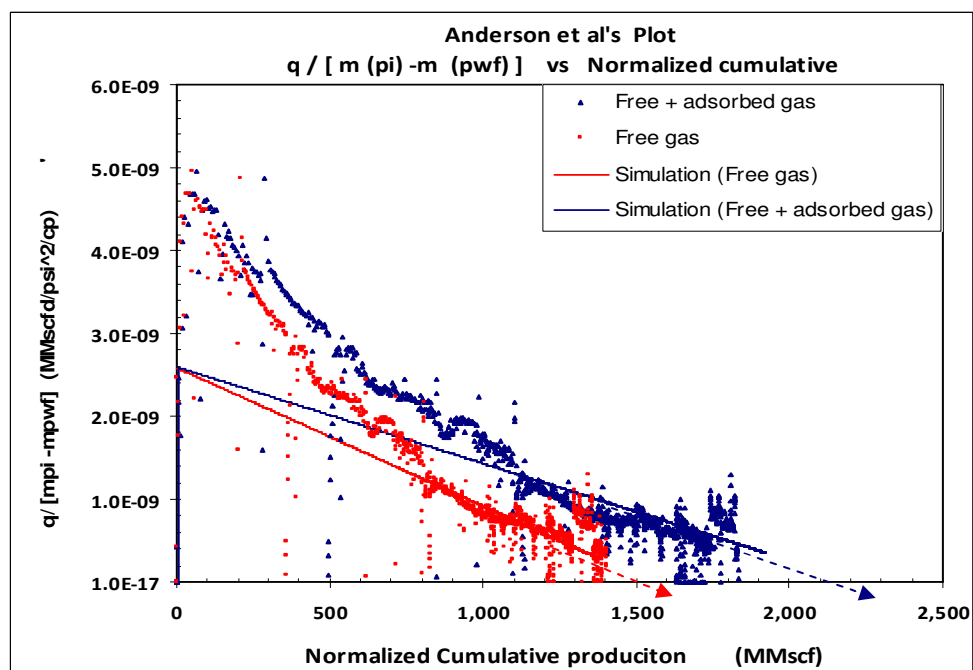


Fig. 5.15 — Normalized rate vs Normalized Cumulative with and without adsorbed gas showing OGIP on x-axis, Well 285.

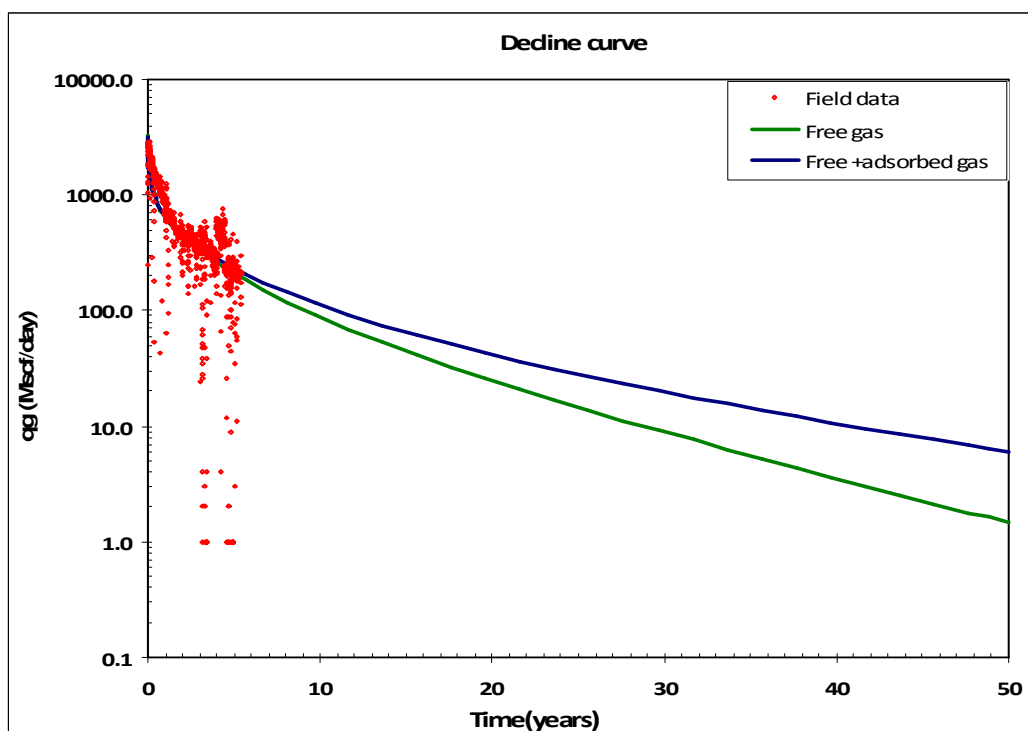
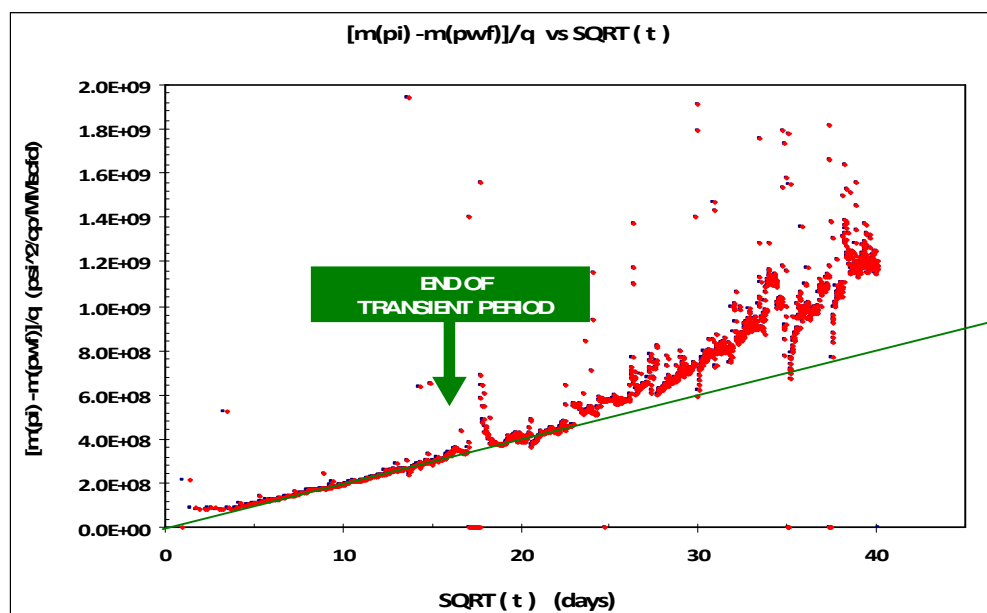


Fig. 5.16 — Decline curve: Forecast results for 50 years with and without adsorbed gas, Well 285.

Table 5.3— Summary of Results, Well 285						
Estimated Parameters	OGIP Transient Data		OGIP BDF (Ibrahim, Wattenbarger & Helmy)		OGIP BDF (Palacio & Blasingame)	
	Without Adsorbed Gas	With Adsorbed Gas	Without Adsorbed Gas	With Adsorbed Gas	Without Adsorbed Gas	With Adsorbed Gas
OGIP free, Bscf	1.58	1.4	1.55	1.5	1.52	1.41
OGIP Adsorbed, Bscf	0	0.8	0	0.7	0	0.70
OGIP Total, Bscf	1.58	2.2	1.55	2.2	1.52	2.11
SRV, rcf	$1.32 \times 10^8$	$1.20 \times 10^8$	$1.3 \times 10^8$	$1.23 \times 10^8$	$1.27 \times 10^8$	$1.18 \times 10^8$
$G_p$ (50 yrs) Bscf	-	-	1.30	1.6	-	-
RF (50 yrs)	-	-	0.84	0.72	-	-

## 5.6 Well 314

Following figures (5.17 – 5.21) and Table 5.4 show the OGIP estimation methods applied to field data from a Barnett shale well as discussed in section 5.2 of this chapter.



**Fig. 5.17 — Square of time plot to determine end of transient time and slope of straight line exhibited by transient flow, Well 314.**

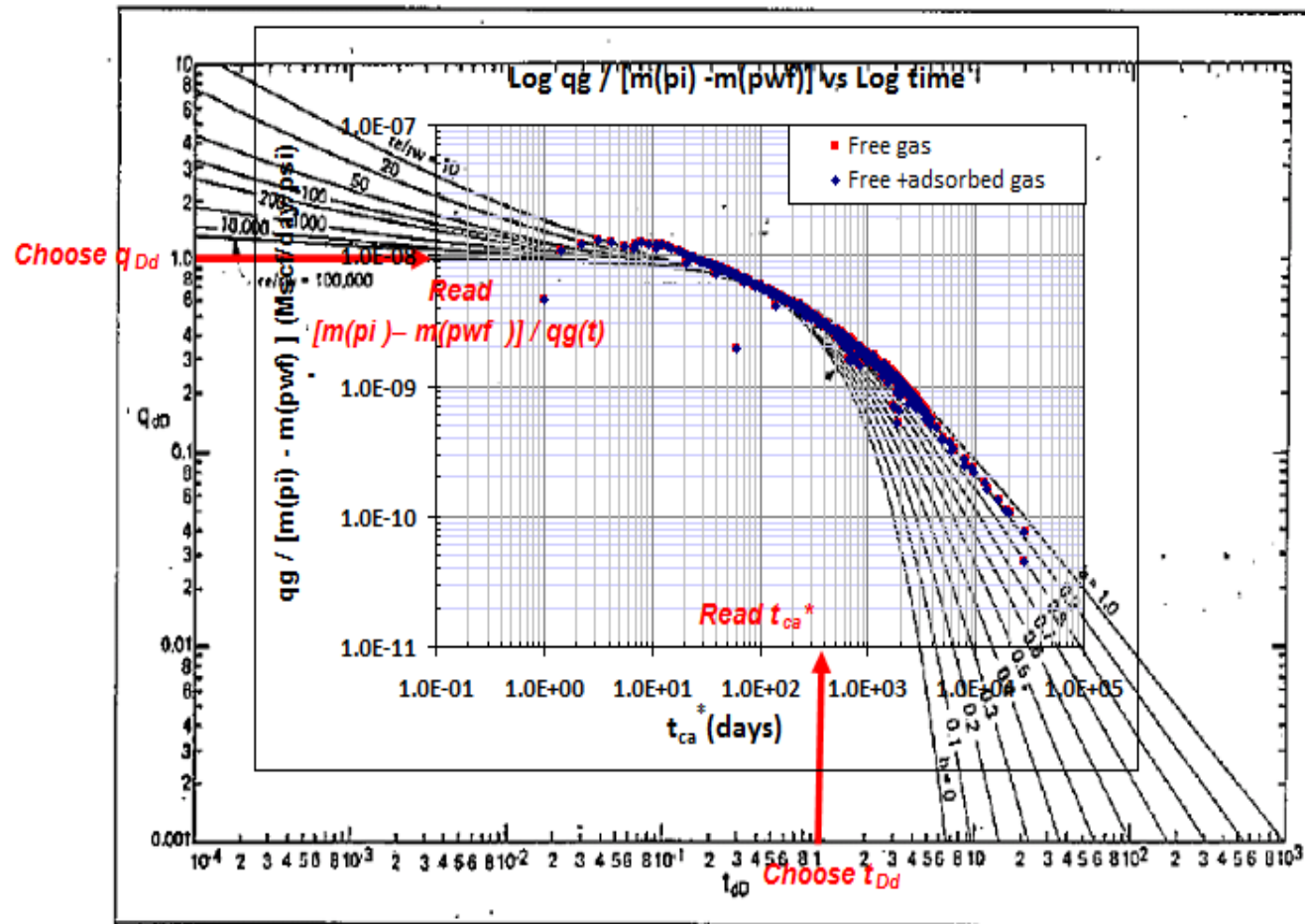


Fig. 5.18 —Matching plot of  $\log [m(p_i) - m(p_{wf})] / q_g$  vs  $\log t_{ca}^*$  on harmonic decline ( $b = 1$ ) stem of Fetkovich's (1980) type curve to establish match points used to calculate OGIP with and without adsorbed gas by Palacio & Blasingame's (1993) method, Well 314.

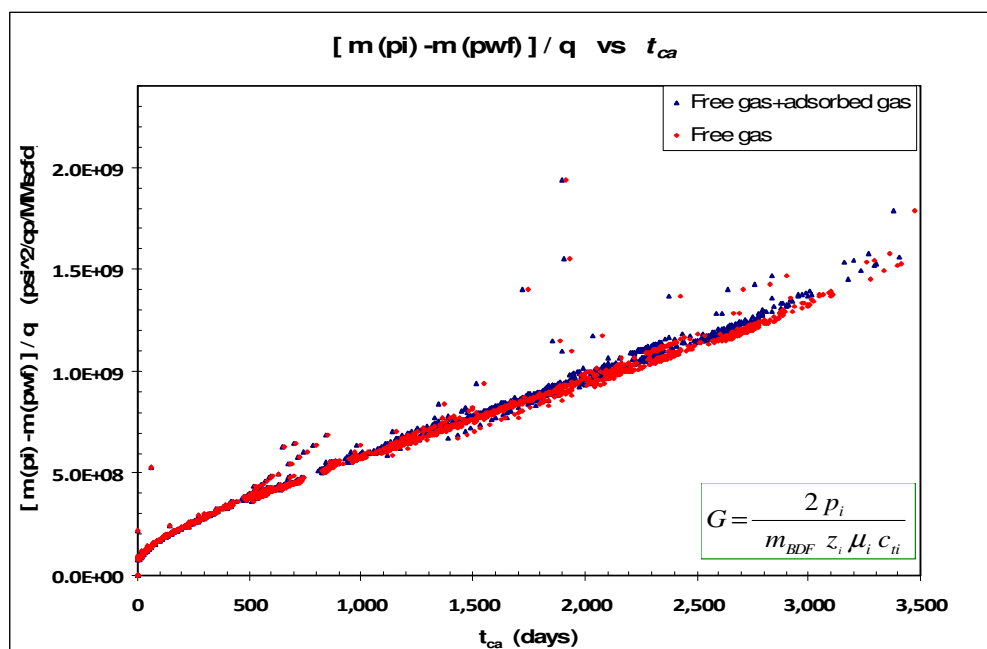


Fig. 5.19 —Plot of  $[m(p_i) - m(p_{wf})] / q_g$  vs  $t_{ca}^*$  showing with and without adsorbed gas BDF with slope  $m_{BDF}$  used to calculate OGIP, Well 314.

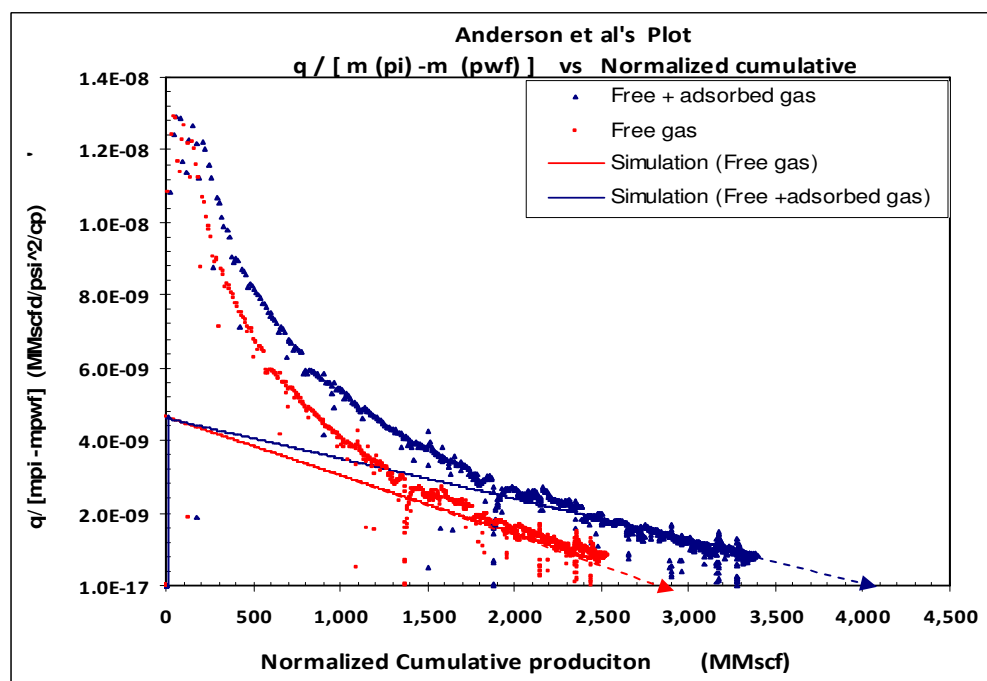


Fig. 5.20 — Normalized rate vs normalized cumulative with and without adsorbed gas showing OGIP on x-axis, Well 314.

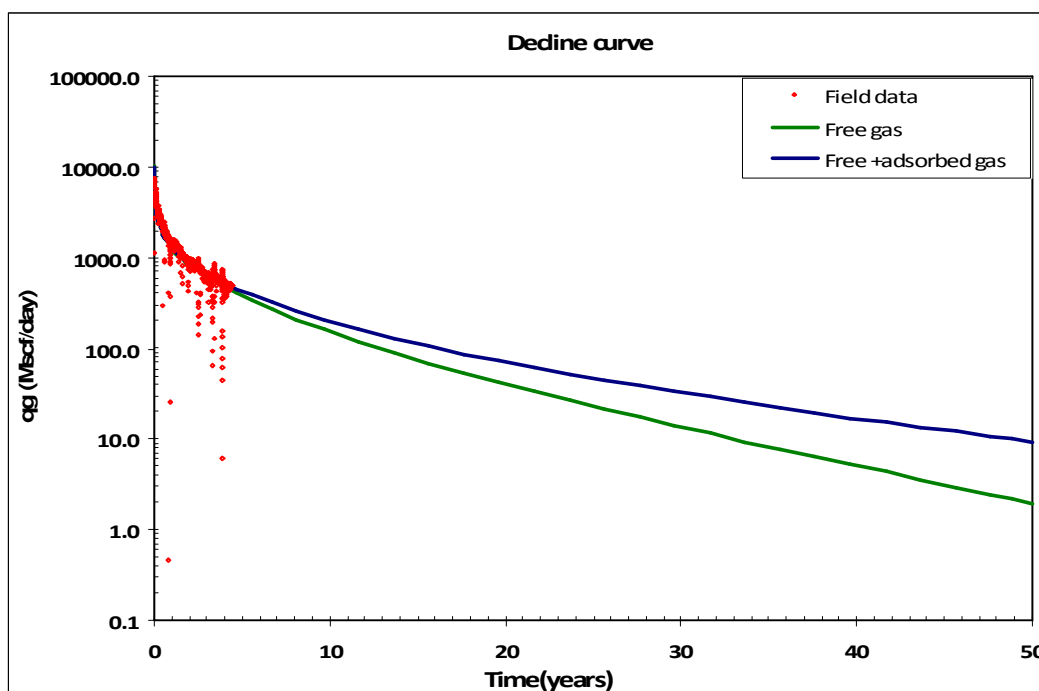


Fig. 5.21 — Decline curve: forecast results for 50 years with and without adsorbed gas, Well 314.

Table 5.4— Summary of Results, Well 314						
Estimated Parameters	OGIP transient Data		OGIP BDF (Ibrahim, Wattenbarger & Helmy)		OGIP BDF (Palacio & Blasingame)	
	Without Adsorbed Gas	With Adsorbed Gas	Without Adsorbed Gas	With Adsorbed Gas	Without Adsorbed Gas	With Adsorbed Gas
OGIP free, Bscf	2.9	2.6	2.9	2.7	1.52	1.36
OGIP Adsorbed, Bscf	0	1.4	0	1.4	0	2.72
OGIP Total, Bscf	2.9	4.0	2.9	4.1	1.52	4.08
SRV, rcf	$2.43 \times 10^8$	$2.20 \times 10^8$	$2.43 \times 10^8$	$2.29 \times 10^8$	$2.47 \times 10^8$	$2.28 \times 10^8$
$G_p$ (50 yrs) Bscf	-	-	2.5	2.9	-	-
RF (50 yrs)	-	-	0.85	0.70	-	-

## 5.7 Results

Comparing the OGIP with and without adsorbed gas estimated from transient data and BDF methods (Figs.5.22 & 5.23) give approximately the same results. In order to compare OGIP, SRV and Recovery factor (RF) with and without adsorption for all the wells we used OGIP, SRV and RF ratios :

$$\text{OGIP Ratio} = \text{OGIP without adsorbed gas} / \text{OGIP with adsorbed gas}$$

$$\text{SRV Ratio} = \text{Adsorbed gas SRV} / \text{Free gas SRV}$$

$$\text{RF Ratio} = \text{Adsorbed gas RF} / \text{Free gas RF.}$$

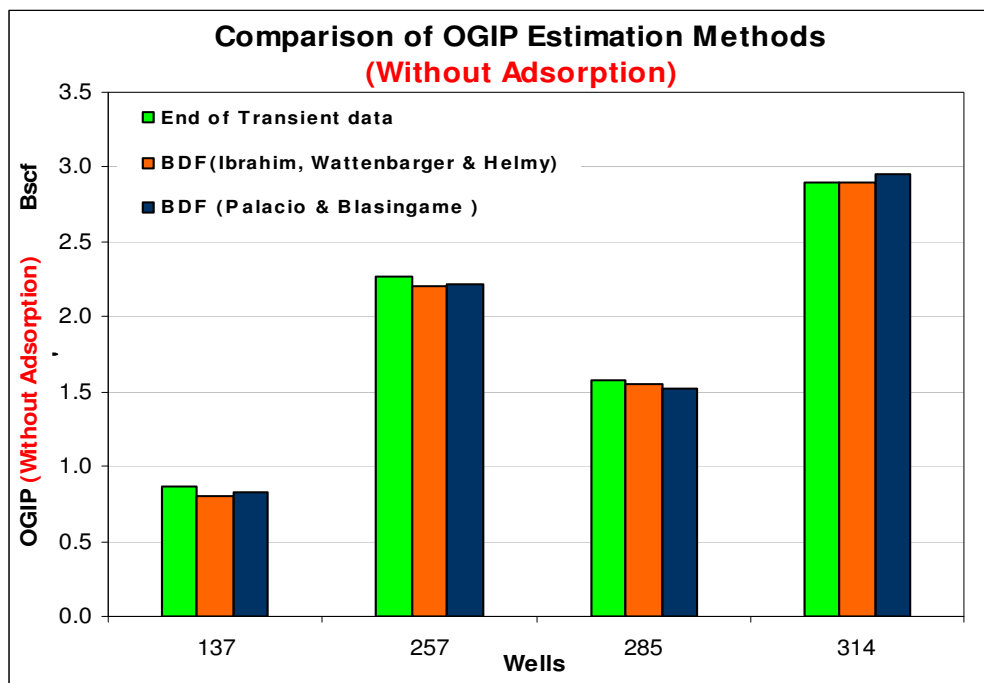


**Fig. 5.22 — Comparison of OGIP without adsorption estimates from transient data, BDF Ibrahim, Helmy & Wattenbarger and BDF Palacio & Blasingame's methods for all the wells.**

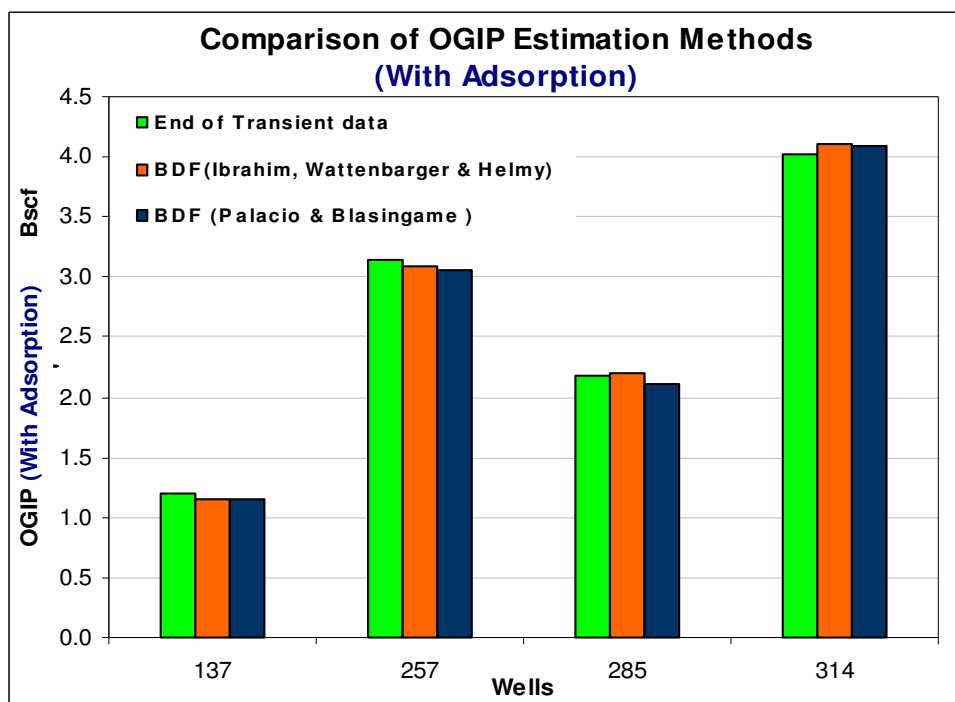


**Fig. 5.23 — Comparison of OGIP without adsorption estimates from transient data, BDF Ibrahim, Helmy & Wattenbarger and BDF Palacio & Blasingame's methods for all the wells.**

<b>Well</b>	<b>OGIP Ratio</b>	<b>SRV ratio</b>	<b>RF Ratio</b>
137	0.67	0.96	0.79
257	0.71	0.94	0.84
285	0.70	0.95	0.86
314	0.71	0.93	0.81
AVERAGE	0.70	0.95	0.83

The average values of OGIP,SRV and RF ratios for these wells (Fig 5.24 & Table. 5.5) is 0.70, 0.95 and 0.83 respectively which shows that ignoring adsorbed gas results in

30% under estimation of OGIP, 5 % over estimation of SRV and 17 % over estimation of RF.

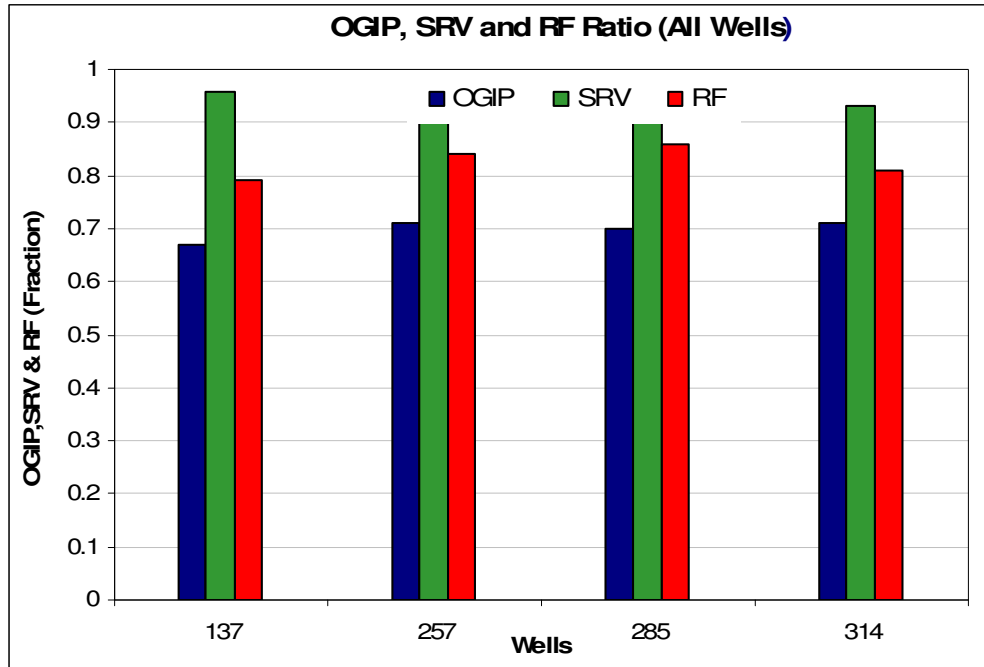


Fig. 5.24 —OGIP, SRV and RF ratios for all the wells.

## 5.8 Discussion

A mass balance equation using the Langmuir's isotherm relation was developed to incorporate the adsorbed gas.

$$G = V_B \left[ \left( \frac{\phi S_{gi}}{B_{gi}} \right) + \left( V_L \frac{p_i}{(p_i + p_L)} \right) \right] \dots\dots\dots 3.3$$

Using the mass balance and the productivity index equation for BDF a iterative process is defined to find average reservoir pressure at every time step. The process is programmed in *EXCEL VBA* and named SGPA. SGPA results were validated by comparing with modified material balance, including adsorbed gas, (King. .1990) results.

$$\frac{\bar{p}}{\bar{z}^*} = \frac{p_i}{z_i^*} \left[ 1 - \frac{G_p}{G} \right] \dots\dots\dots 3.6$$

A exponential decline type rate equation was derived using the material balance equation and productivity index equation for constant pressure boundary dominated flow (Appendix B). The total compressibility in the rate equation includes the Adsorbed gas compressibility (Bumb & McKee. 1986).

$$q_g = q_0 e^{-\frac{2 J_g}{\phi V_B S_g} \left[ \frac{B_g \bar{p}}{c_g + c_d} \right] \frac{\bar{p}}{\bar{z} \bar{\mu}} t} \dots\dots\dots 3.13$$

The results from the equation were compared with SGPA and found to be same.

OGIP Estimation methods for BDF Palacio & Blasingame (1993), Ibrahim Wattenbarger and Helmy (2003) /Anderson et al. (2010) and using end of transient data were reviewed to include adsorbed gas by using King's  $z^*$  and Bumb and McKee's adsorption compressibility.

$$G = \frac{\left( \frac{q_g(t)}{[m(p_i) - m(p_{wf})]} \right)_{M.P}}{(q_{Dd})_{M.P}} \frac{2 p_i}{z_i^* \mu_i c_{ti}^*} \frac{(t_{ca}^*)_{M.P}}{(t_{Dd})_{M.P}} \dots\dots\dots 4.26$$

$$\frac{[m(p_i) - m(p_{wf})]}{q_g(t)} = \frac{2 p_i}{G z_i^* \mu_i c_{ti}^*} Super - t_n^* + \frac{[m(p_i) - m(p_{wf})]}{q_{gi}} \dots\dots\dots 4.27$$

$$\frac{q_g(t)}{[m(p_i) - m(p_{wf})]} = \frac{2 J p_i q_g(t)}{G z_i^* \mu_i c_{ti}^* [m(p_i) - m(p_{wf})]} t_{ca}^* + \frac{q_{gi}}{[m(p_i) - m(p_{wf})]} \dots\dots\dots 4.28$$

$$G = f_{CP} \frac{200.8 T}{\phi (\mu c_t^*)_i} \left( \frac{\sqrt{t_{esr}}}{\tilde{m}_{CPL}} \right) \left[ \left( \frac{\phi S_{gi}}{B_{gi}} \right) + \left( V_L \frac{p_i}{(p_i + p_L)} \right) \right] \dots\dots\dots 4.31$$

SGPA was then used to estimate OGIP with and without adsorbed gas for four selected wells from Barnett shale using above mentioned BDF and end of transient methods. OGIP, SRV and RF with and without adsorbed gas for these wells were average difference for with and without adsorbed gas were established.

A method has been presented to analyze field data from shale gas reservoirs for BDF, which incorporates the adsorbed gas. The method assumes that free gas and desorbed gas are in equilibrium. i.e. desorption of gas is completely pressure dependent. Also the method assumes constant water saturation and negligible rock and water compressibility.

## CHAPTER VI

### CONCLUSIONS AND RECOMMENDATIONS

#### 6.1 Conclusions

Summary of conclusions from this work are as follows:

1. A method is developed to analyze field data to assess the effect of ignoring adsorbed gas in material balance calculations for BDF. Using this method the amount of gas contributed due to desorption can also be calculated at any specific time.
2. Ignoring adsorbed gas results in significant errors in OGIP SRV and RF estimates.
3. We have shown that for the same field data ignoring adsorbed gas will result in over estimation of SRV. This will consequently result in ignoring unstimulated reservoir volume.
4. OGIP estimates increase by 30 % when adsorbed gas is included. Ignoring adsorbed gas will result in low OGIP estimates and consequently serious errors in forecasting.
5. Forecasting results based on our estimates show that ignoring adsorbed gas will result in high RF even for low  $G_p$  where as including adsorbed gas will give higher  $G_p$  and a lower RF.
6. Forecasting results show that adsorption does not have a major contribution at early times but becomes significant at late times and low reservoir pressures.

7. This method can be applied to other shales as well if Langmuir isotherm constants for respective shales are used.
8. It is not possible to get accurate estimations and Forecasting if adsorbed gas in shales is ignored.

### **6.1 Recommendations for Future Work**

Recommendations for future work are as follows:

1. Extending this method to include variable water saturation, water and rock compressibilities.
2. Extending the present method to include sorption time.

## NOMENCLATURE

$B_o$  = liquid formation volume factor, rB/STB

$B_g$  = gas formation volume factor, rcf/scf

$B_{gi}$  = formation volume factor at initial reservoir pressure, rcf/scf

$\bar{B}_g$  = formation volume factor at average reservoir pressure, rcf/scf

$c_d$  = adsorbed gas compressibility,  $\text{psi}^{-1}$

$c_g$  = free gas compressibility,  $\text{psi}^{-1}$

$c_m$  = matrix compressibility,  $\text{psi}^{-1}$

$c_t$  = total compressibility,  $\text{psi}^{-1}$

$c_{ti}$  = total compressibility at initial reservoir pressure,  $\text{psi}^{-1}$

$\bar{c}_t$  = total compressibility at average reservoir pressure,  $\text{psi}^{-1}$

$D_D$  = dimensionless draw down

$D_i$  = Arps's (1944) initial decline rate,  $\text{days}^{-1}$

$f_{cp}$  = slope correction factor, dimensionless

$G$  = original gas in place, scf

$G_p$  = cumulative gas produced, scf

$h$  = reservoir thickness, ft

$J$  = productivity index, scf/psi

$k$  = homogeneous reservoir permeability, md

$m_{BDF}$  = slope of boundary dominated flow region.

$\tilde{m}_{CPL}$  = slope of transient flow region.

$m(p_i)$  = initial pseudopressure (gas), psi<sup>2</sup>/cp

$m(p_{wf})$  = well bore flowing pseudopressure (gas), psi<sup>2</sup>/cp

$m(\bar{p})$  =average reservoir pseudopressure (gas), psi<sup>2</sup>/cp

$N$  = liquid Oil in place, scf

$N_p$  = liquid cumulative production, scf

$p_i$  = initial reservoir pressure, psi

$p_L$  = Langmuir's pressure, psi

$p_{sc}$  = pressure at standard conditions, psi

$p_{wf}$  = wellbore flowing pressure, psi

$\bar{p}$  = average reservoir pressure, psi

$q_{Dd}$  = dimensionless gas rate, dimensionless

$q_g$  = gas rate, scf/day

$q_{gi}$  = initial gas rate, scf/day)

$q_o$  = liquid rate, scf/day

$q_{oi}$  = initial liquid rate, scf/day

$Super-t$  =super position time, days

$Super-t_n$  = normalized pseudo Super position time, days

$S_g$  = water saturation, fraction

$S_w$  = water saturation, fraction

$t$  = time, days

$t_a$  = pseudo time, psi/cp

$t_{ca}$  = normalized pseudo material balance time, days

$\sqrt{t_{esr}}$  = end of transient flow period, days

$t_{Dd}$  = dimensionless time, dimensionless

$T$  = absolute temperature, °R

$T_{sc}$  = temperature at standard conditions, °R

$V_b$  = total matrix bulk volume, ft<sup>3</sup>

$V_L$  = adsorbed gas content, scf/ft<sup>3</sup> =  $0.031297 \rho_B V_m$

$V_m$  = adsorbed gas content, scf/ton

$V_p$  = pore volume, scf

$z_i$  = initial gas deviation factor, dimensionless

$z_{sc}$  = gas deviation factor at standard conditions, dimensionless

$\bar{z}$  = gas deviation factor at average reservoir pressure, dimensionless

$z^*$  = King's gas deviation factor for free + adsorbed gas, dimensionless

### **Greek symbols**

$\alpha$  = effective stress parameter

$\rho$  = density of the matrix, gm/cc

$\mu$  = viscosity, cp

$\phi$  = porosity

### **Superscript**

\* = includes adsorbed gas

### **Subscript**

$b$  = bulk volume

$i$  = initial

$g$  = gas

$sc$  = standard conditions

## REFERENCES

- Al-Ahmadi, Hasan A. Almarzooq, Anas M. and Wattenbarger, R.A. 2010. Application of Linear Flow Analysis to Shale Gas Wells—Field Cases. Paper SPE 130370 presented at the SPE Unconventional Gas Conference, Pittsburgh, Pennsylvania, 23-25 February.
- Al-Hussainy, R., Ramey, H.J. Jr. and Crawford, P.B. 1965. The Flow of Real Gases Through Porous Media. Paper SPE 1243A presented at the SPE Annual Fall Meeting, Denver, Colorado, 3-6 October.
- Anderson, D.M., Nobakht, M., Moghadam, S. and Mattar, L. 2010. Analysis of Production Data From Fractured Shale Wells. Paper SPE 131787 presented at the SPE Unconventional Gas Conference held in Pittsburgh, Pennsylvania, 23-25 February.
- Arps, J.J. 1944. Analysis of Decline Curves. *Trans. AIME*, **160**: 228-247.
- Bumb, A.C., and McKee, C.R. 1986. Gas-Well Testing in the Presence of Desorption for Coal bed Methane and Devonian Shale. Paper SPE 15227 presented at SPE Unconventional Gas Technology Symposium, Louisville, Kentucky, 18-21 May.
- Fraim, M.L., and Wattenbarger, R.A. 1987. Gas Reservoir Decline-Curve Analysis Using Type Curves With Real Gas Pseudopressure and Normalized Time. Paper SPE 14238 presented at SPE Annual Technical Conference and Exhibition, Las Vegas, 22-25 September.
- Fetkovich, M.J. 1980. Decline Curve Analysis Using Type Curves. *Journal of Petroleum Technology*. **June 1980**: 1065-1077.

- Ibrahim, M. and Wattenbarger, R. A. 2005. Analysis of Rate Dependence in Transient Linear Flow in Gases. Paper PETSOC 2005-057 presented at the Petroleum Society's Canadian International Petroleum Conference , Calgary, Alberta, Canada, 7- 9 June.
- Ibrahim, M., Wattenbarger, R. A., and Helmy, W.2003. Determination of OGIP for Tight Gas Wells-New Methods. Paper PETSOC 2003-012 presented at the Petroleum Society's Canadian International Petroleum Conference, Calgary, Alberta, Canada, 10-12 June.
- Jacobi, D., Gladkikh, M., LeCompte, B., Hursan, G., Mendez, F., Longo, J., Ong, S., Bratovich, M. and Patton, G. 2008. Integrated Petrophysical Evaluation of Shale Gas Reservoirs. Paper SPE 114925 presented at the CIPC/SPE Gas Technology Symposium, Calgary, Alberta, Canada, 16-19 June.
- King, G.R. 1990. Material Balance Techniques for Coal Seam and Devonian Shale Gas Reservoirs. Paper SPE 20730 presented at the 65<sup>th</sup> Annual Technical Conference and Exhibition, New Orleans, Louisiana, 23-26 September.
- Lewis, A.M. and Hughes, R.G. 2008. Production Data Analysis of Shale Gas Reservoirs. Paper SPE 116688 presented at the SPE Annual Technical Conference and Exhibition, Denver, Colorado, 21-24 September.
- Moghadam, S., Jeje, O. and Mattar, L. 2009. Advanced Gas Material Balance, in Simplified Format. Paper PETSOC 2009-149 presented at the Canadian International Petroleum Conference (CIPC), Calgary, Alberta, Canada, 16-18 June.

- Palacio, J.C. and Blasingame, T.A. 1993. Decline-Curve Analysis Using Type Curves- Analysis of Gas Well Production Data. Paper SPE 25909 presented at the SPE Joint Rocky Mountain Regional and Low Permeability Reservoir Symposium, Denver, Colorado, 26-29 April.
- Seidle, J.P. 1991. Long-Term Gas Deliverability of a Dewatered Coal bed. Paper SPE 21488 presented at the SPE Gas Technology Symposium, Houston, Texas, 23-25 January.
- Unconventional Reservoir Simulator (URS 01). 2009. Simulator developed by Reservoir Modeling Consortium, Department of Petroleum Engineering Texas A&M University. August
- Wang, F.P. and Reed, R.M. 2009. Pore Networks and Fluid Flow in Gas Shales. Paper SPE 124253 presented at the SPE Annual Technical Conference and Exhibition, New Orleans, Louisiana, 4-7 October.

## APPENDIX A

### DERIVATION OF KING'S $z^*$ FOR DESORBED GAS AND COMPARISON WITH SGPA RESULTS

King defined a material balance equation for unconventional gas reservoirs which included adsorbed gas.

$$\frac{\bar{p}}{z^*} = \frac{p_i}{z_i^*} \left[ 1 - \frac{G_p}{G} \right] \dots\dots\dots A.1$$

where  $z^*$  at constant water saturation and negligible water and gas compressibility is defined as.

$$z^* = \frac{z}{S_g + \frac{V_L T p_{sc} z}{\phi (p + p_L) T_{sc} z_{sc}}} \dots\dots\dots A.2$$

Following King's method

$G_p = OGIP - GIP$  (at current pressure)

$$G_p = \left( \frac{V_B \phi S_g}{B_{gi}} + V_B V_L \frac{p_i}{(p_i + p_L)} \right) - \left( \frac{V_B \phi S_g}{\bar{B}_g} + V_B V_L \frac{\bar{p}}{(\bar{p} + p_L)} \right) \dots\dots\dots A.3$$

Simplifying Eq. A.3

$$G_p = \phi V_B \left[ \left( \frac{S_g}{B_{gi}} + V_L \frac{p_i}{\phi (p_i + p_L)} \right) - \left( \frac{S_g}{\bar{B}_g} + V_L \frac{\bar{p}}{\phi (\bar{p} + p_L)} \right) \right] \dots\dots\dots A.4$$

The formation volume factor for gas,  $B_g$  is defined as

$$B_g = \frac{p_{sc} T z}{p T_{sc} z_{sc}} \Rightarrow \frac{z}{p} B_g = \frac{p_{sc} T}{T_{sc} z_{sc}} \dots\dots\dots A.5$$

Substituting Eq.A.5 in Eq.A.4 we get

$$G_p = \frac{\phi V_B T_{sc} z_{sc}}{p_{sc} T} \left[ \left( \frac{p_i S_g}{z_i} \right) + \left( \frac{V_L T p_{sc} p_i}{\phi T_{sc} z_{sc} (p_i + p_L)} \right) - \left( \frac{\bar{p} S_g}{\bar{z}} \right) - \left( \frac{V_L T p_{sc} \bar{p}}{\phi T_{sc} z_{sc} (\bar{p} + p_L)} \right) \right] \dots\dots\dots A.6$$

Simplifying Eq.A.6

$$G_p = \frac{\phi V_B T_{sc} z_{sc}}{p_{sc} T} \left[ \frac{p_i}{z_i^*} - \frac{\bar{p}}{\bar{z}^*} \right] \dots\dots\dots A.7$$

where

$$z^* = \frac{z}{S_g + \frac{V_L T p_{sc} z}{\phi (p + p_L) T_{sc} z_{sc}}} \dots\dots\dots A.8$$

Eq.A.8 is King's  $z^*$ . Substituting Eq. A.5 in Eq. A.7

$$G_p = \frac{\phi V_B z_i}{p_i B_{gi}} \left[ \frac{p_i}{z_i^*} - \frac{\bar{p}}{\bar{z}^*} \right] \dots\dots\dots A.9$$

Rearranging Eq.A.9

$$\frac{\bar{p}}{\bar{z}^*} = \frac{p_i}{z_i^*} \left[ 1 - \frac{G_p}{(\phi V_B z_i / B_{gi} z_i^*)} \right]$$

$$\text{As } G = \frac{\phi V_B z_i}{B_{gi} z_i^*} \dots\dots\dots A.10$$

$$\frac{\bar{p}}{\bar{z}^*} = \frac{p_i}{z_i^*} \left[ 1 - \frac{G_p}{G} \right] \dots\dots\dots A.11$$

Eq.A.9 is similar to the conventional material balance equation except that it accounts for the desorbed gas in form of  $z^*$ . King's material balance equation works like a conventional material balance where a  $p/z$  and  $G_p$  plot is used to estimate the OGIP by extrapolation. The disadvantage of  $z^*$  material balance is that the  $z^*$  values do not

resemble the actual  $z$  values. Normalized  $z^*$  (S.Moghadam et al. 2009) denoted by  $z^{**}$  is given as

$$z^{**} = z^* \left( \frac{z_i}{z_i^*} \right) \dots\dots\dots A.12$$

Substituting  $z^{**}$  in Eq.A.11 will yield.

$$\frac{\bar{p}}{z^{**}} = \frac{p_i}{z_i^{**}} \left[ 1 - \frac{G_p}{G} \right]$$

$$G_p = G \frac{z_i^{**}}{p_i} \left[ \frac{p_i}{z_i^{**}} - \frac{\bar{p}}{z^{**}} \right] \dots\dots\dots A.13$$

Substituting Eq.A.10 and A.12 we get

$$G_p = \frac{\phi V_B z_i^2}{B_{gi} p_i z_i^*} \left[ \frac{p_i}{z_i^{**}} - \frac{\bar{p}}{z^{**}} \right] \dots\dots\dots A.14$$

The  $z^{**}$  values resemble the  $z$  values which makes it easier for the user to relate with the results. The calculated  $G_p$  from the modified material balance equation was compared with  $G_p$  results from SGPA. The plotting functions  $p/z$  vs  $G_p$  and  $G_p$  vs time

<b>Table A.1— Match cases: Comparison of SGPA Results with King's Modified Material Balance Equation</b>				
<b>Case #</b>	<b>Fig</b>	<b><math>p_i</math> (psi)</b>	<b>% Adsorbed</b>	<b>OGIP (MMscf)</b>
Case 1	A.1 & A.2	1500	0	1279
Case 2	A.3 & A.4	1500	50	1279
Case 3	A.5 & A.6	8000	0	6455
Case 4	A.7 & A.8	8000	50	6455

were used to compare the results. Table A.1 shows different match cases followed by the respective plots.

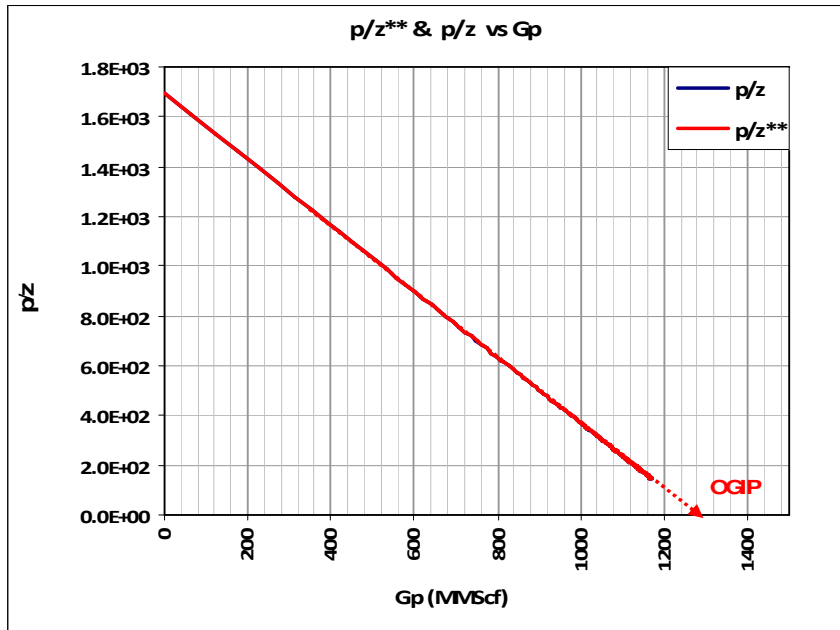


Fig. A.1 — Case 1:  $p/z^{**}$  and  $p/z$  vs  $G_p$  (% adsorbed = 0).

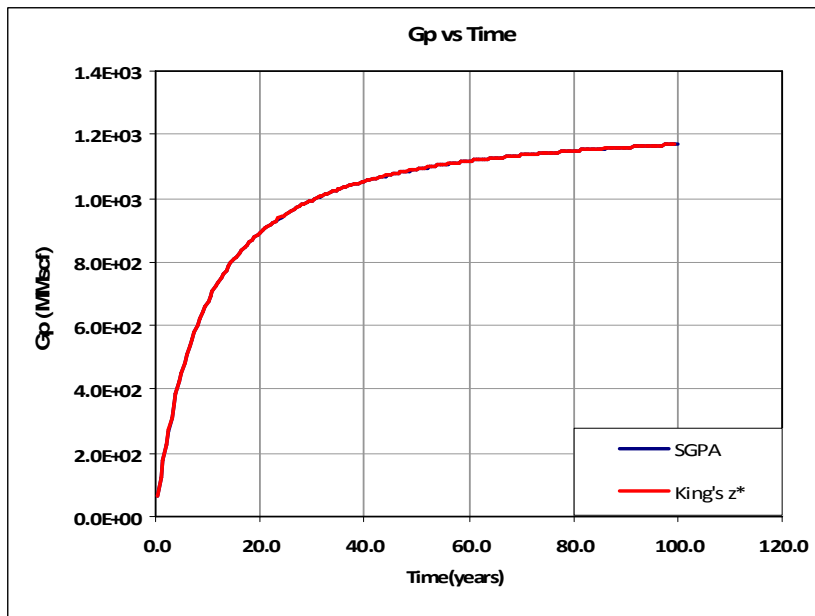


Fig. A.2 — Case 1:  $G_p$  vs time (% adsorbed = 0).

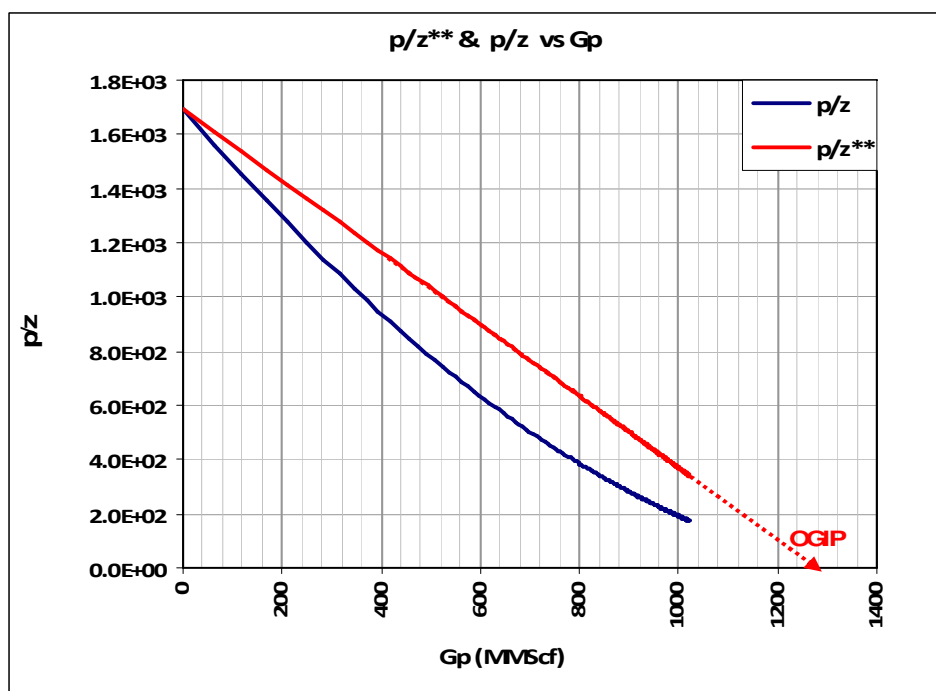


Fig. A.3 —Case 2:  $p/z^{**}$  and  $p/z$  vs  $G_p$  (% adsorbed = 50).

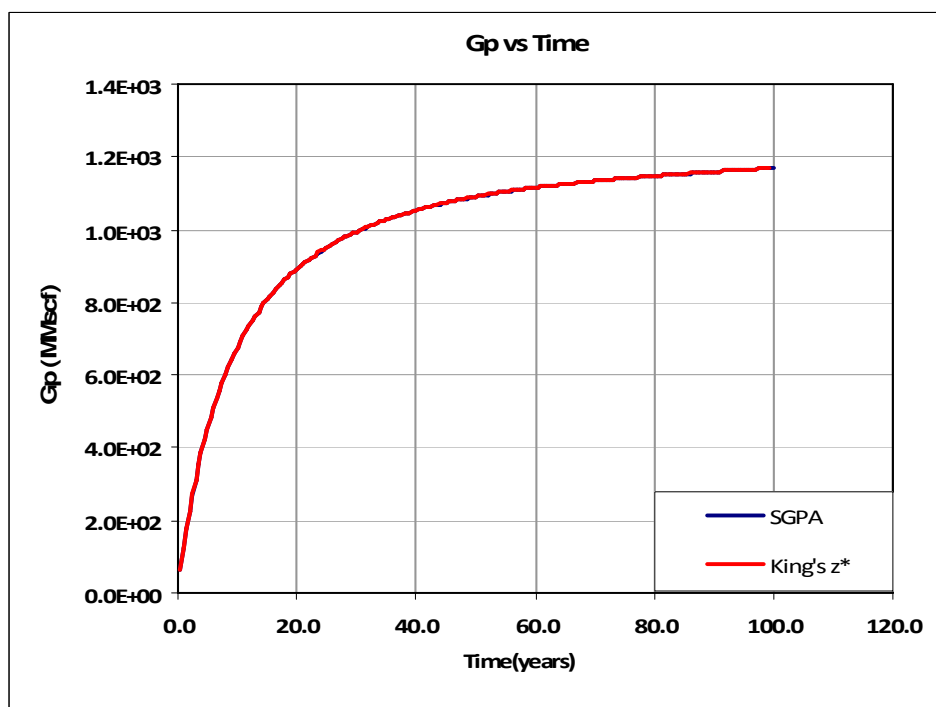


Fig. A.4 —Case 2:  $G_p$  vs time (% adsorbed = 50).

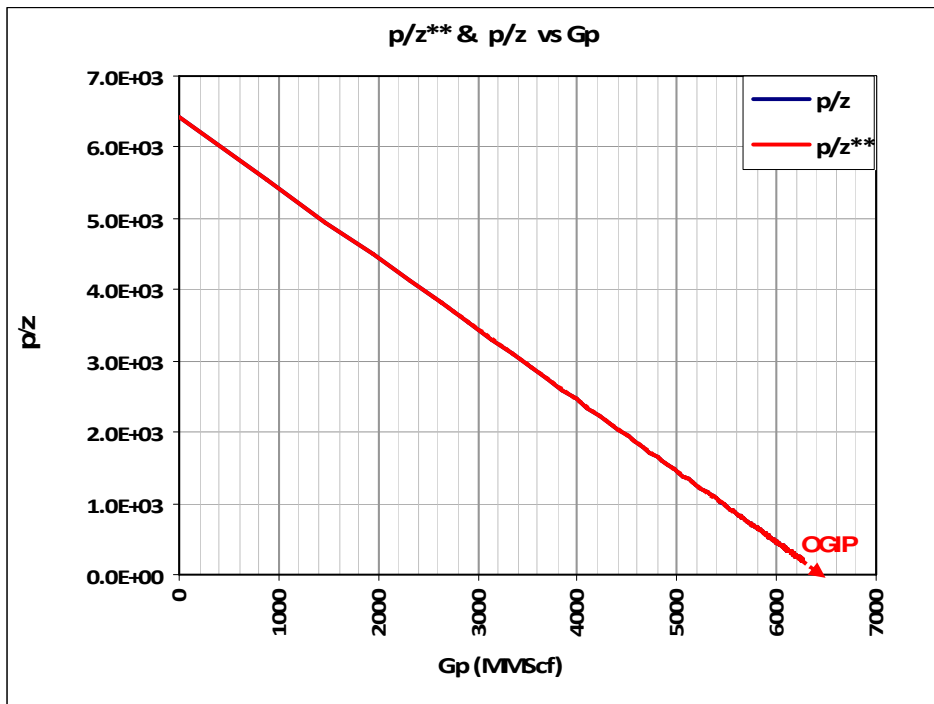


Fig. A.5 — Case 3:  $p/z^{**}$  and  $p/z$  vs  $G_p$  (% adsorbed = 0).

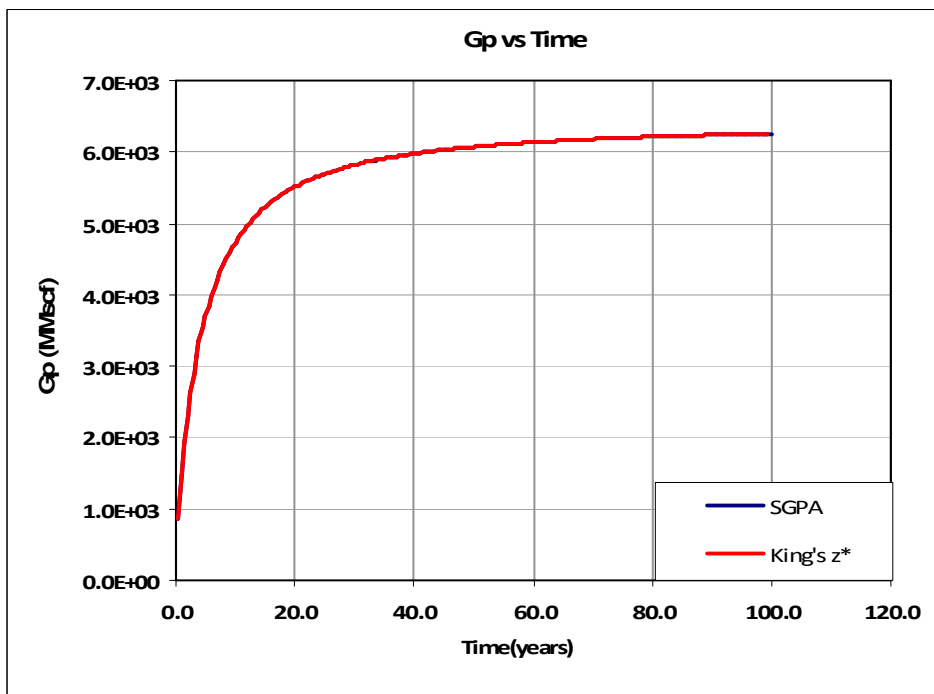


Fig. A.6 — Case 3:  $G_p$  vs time (% adsorbed = 0).

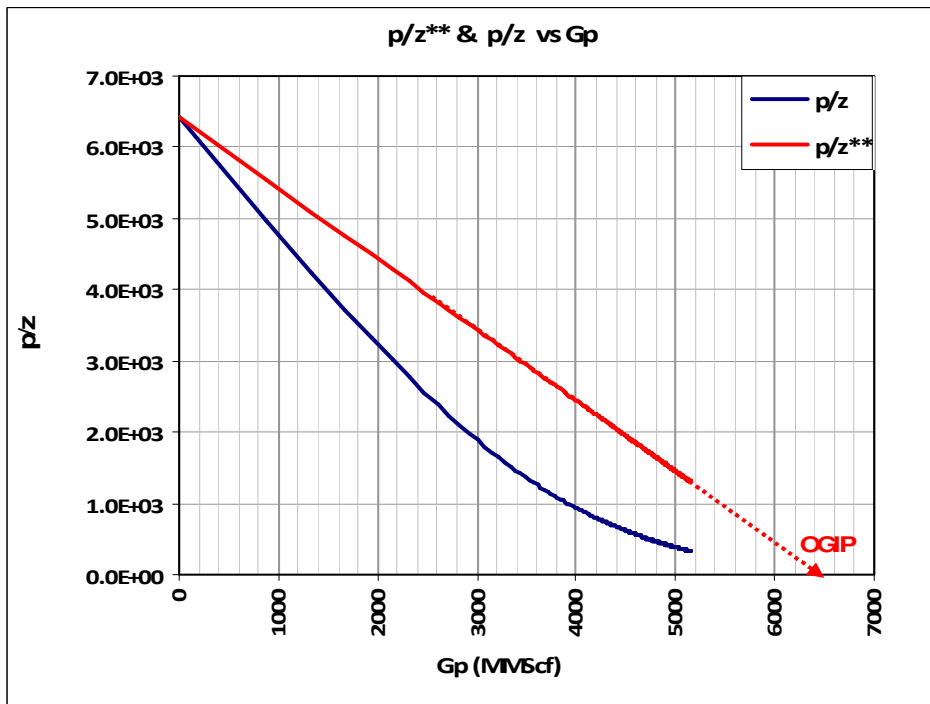


Fig. A.7 —Case 4:  $p/z^{**}$  and  $p/z$  vs  $G_p$  (% adsorbed = 50).

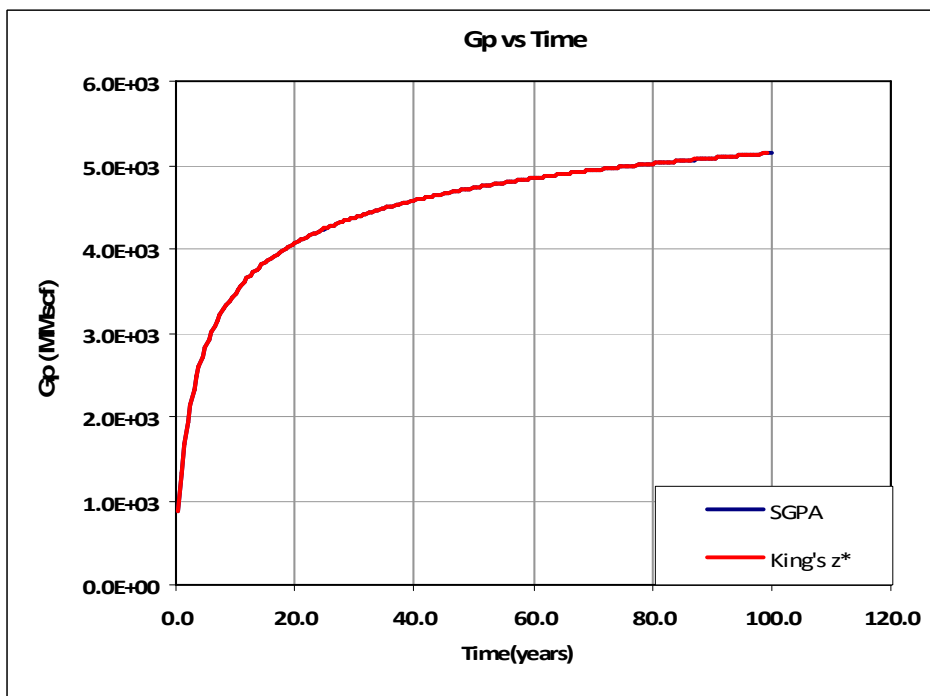


Fig. A.8 —Case 4:  $G_p$  vs time (% adsorbed = 50)

## APPENDIX B

### BUMB AND MCKEE'S COMPRESSIBILITY EXPRESSION FOR ADSORBED GAS AND COMPARISON WITH SGPA RESULTS

Bumb and McKee defined a compressibility expression for desorbed gas as

$$\frac{\rho_{gsc} V_L p_L}{\phi \rho_g (p_L + p)^2} = \frac{p_{sc} T \bar{z}}{\bar{p} T_{sc} \bar{z}_{sc}} \frac{V_L p_L}{\phi (p_L + \bar{p})^2} = \frac{B_g V_L p_L}{\phi (p_L + \bar{p})^2} \dots\dots\dots \text{B.1}$$

Total adsorbed and free gas volume is given by

$$G = \left[ \left( \frac{\phi V_B S_g}{B_{gi}} \right) + \left( 0.031214 \rho_B V_B V_m \frac{p_i}{(p_i + p_L)} \right) \right] \dots\dots\dots \text{B.2}$$

Assuming

$$HCPV = \phi V_B S_g, \quad \hat{V} = 0.031214 \rho_B V_B V_m \text{ and Substituting in Eq. B.2}$$

$$OGIP = \left[ \left( \frac{HCPV}{B_{gi}} \right) + \left( \hat{V} \frac{p_i}{(p_i + p_L)} \right) \right] \dots\dots\dots \text{B.3}$$

Also

$$G_p = \left[ OGIP - \left( \frac{HCPV}{\bar{B}_g} \right) - \left( \hat{V} \frac{\bar{p}}{(\bar{p} + p_L)} \right) \right] \dots\dots\dots \text{B.4}$$

Differentiating Eq. B.4 w.r.t to pressure we get

$$\frac{dG_p}{dp} = -HCPV \frac{d(1/B_g)}{dp} - \hat{V} \left( \frac{p_L}{(p + p_L)^2} \right) \dots\dots\dots \text{B.5}$$

Isothermal compressibility for free gas is

$$c_g = \left( \frac{1}{p} \right) - \frac{1}{z} \left( \frac{\partial z}{\partial p} \right)_T \dots\dots\dots \text{B.6}$$

Gas formation volume factor,  $B_g$  is given as

$$B_g = 0.0282T \frac{z}{p}$$

$$\frac{1}{B_g} = \frac{1}{0.0282T} \frac{p}{z} \dots\dots\dots \text{B.7}$$

Differentiating  $B_g$  w. r. t pressure we get

$$\frac{d(1/B_g)}{dp} = \frac{1}{0.0282T} \frac{d(p/z)}{dp}$$

$$\frac{d(1/B_g)}{dp} = \frac{1}{0.0282T} \frac{p}{z} \left[ \left( \frac{1}{p} \right) - \frac{1}{z} \left( \frac{dz}{dp} \right) \right]$$

$$\frac{d(1/B_g)}{dp} = \frac{1}{B_g} c_g \dots\dots\dots \text{B.8}$$

Substituting Eq. B.8 in Eq.B.5 we get

$$\frac{dG_p}{dp} = -HCPV \frac{1}{B_g} c_g - \hat{V} \left( \frac{p_L}{(p + p_L)^2} \right) \dots\dots\dots \text{B.9}$$

Putting values of  $\hat{V}$  and  $HCPV$  in Eq. B.9 we get

$$\frac{dG_p}{dp} = -\phi V_B S_g \frac{1}{B_g} c_g - 0.031214 \rho_B V_B V_m \left( \frac{p_L}{(p + p_L)^2} \right)$$

$$\frac{dG_p}{dp} = -\frac{\phi V_B S_g}{B_g} \left[ c_g + \frac{0.031214 B_g \rho_B V_m p_L}{\phi (1 - S_w) (p + p_L)^2} \right] \dots\dots\dots \text{B.10}$$

where

$$c_d = \left[ \frac{B_g V_L p_L}{\phi S_g (p + p_L)^2} \right] \quad \text{and} \quad V_L = 0.031214 \rho_B V_m$$

Substituting  $c_d$  in Eq.B.10 we get

$$\frac{dG_p}{dp} = -\frac{\phi V_B S_g}{B_g} [c_g + c_d] \dots\dots\dots \text{B.11}$$

As

$$q = \frac{dG_p}{dt} = \frac{dG_p}{dp} \frac{dp}{dt} \dots\dots\dots \text{B.12}$$

Substituting Eq.B.11 in Eq. B.12

$$q_g = -\frac{\phi V_B S_g}{B_g} [c_g + c_d] \frac{dp}{dt} \dots\dots\dots \text{B.13}$$

Stabilized flow equation in terms  $m(p)$  is given as

$$q_g = J_g [m(\bar{p}) - m(p_{wf})] \dots\dots\dots \text{B.14}$$

where

$$m(p) = \int \frac{2p}{z\mu} dp \dots\dots\dots \text{B.15}$$

Substituting Eq.B.15 in Eq. B.14 we get

$$q_g = J_g \left[ \int_{p_0}^{\bar{p}} \frac{2\bar{p}}{z\mu} d\bar{p} - \int_{p_0}^{p_{wf}} \frac{2p_{wf}}{z\mu} dp_{wf} \right] \dots\dots\dots \text{B.16}$$

As

$$\nabla m(p) = \frac{2\bar{p}}{\bar{z}\bar{\mu}} \nabla p \dots\dots\dots \text{B.17}$$

Substituting Eq.B.17 in Eq. B.16 we get

$$q_g = 2 J_g \left[ \frac{\bar{p}}{\bar{z}\bar{\mu}} dp - \frac{p_{wf}}{z\mu} dp_{wf} \right] \dots\dots\dots \text{B.18}$$

Differentiating Eq.B.18 w.r.t to pressure we get

$$dq_g = 2 J_g \frac{\bar{p}}{\bar{z} \bar{\mu}} d\bar{p} \dots\dots\dots \text{B.19}$$

Dividing B.18 by B.13 and integrating

$$\begin{aligned} \frac{dq_g}{q_g} &= \frac{2 B_g J_g \bar{p} d\bar{p}}{\phi V_B S_g \bar{z} \bar{\mu} [c_g + c_d] d\bar{p}} dt \\ \int_0^t \frac{dq_g}{q_g} &= - \frac{2 J_g}{\phi V_B S_g} \frac{B_g \bar{p}}{[c_g + c_d] \bar{z} \bar{\mu}} \int_0^t dt \\ \ln q_g - \ln q_0 &= - \frac{2 J_g}{\phi V_B S_g} \frac{B_g \bar{p}}{[c_g + c_d] \bar{z} \bar{\mu}} t \\ q_g &= q_0 e^{-\frac{2 J_g}{\phi V_B S_g} \frac{B_g \bar{p}}{[c_g + c_d] \bar{z} \bar{\mu}} t} \dots\dots\dots \text{B.20} \end{aligned}$$

<b>Table B.1— Match Cases: Bumb &amp; McKee’s Compressibility Expression Applied Results with SGPA Results</b>				
<b>Case #</b>	<b>Fig</b>	<b><math>p_i</math> (psi)</b>	<b>% Adsorbed</b>	<b>OGIP (MMscf)</b>
Case 1	B.1 & B.2	1500	0	1279
Case 2	B.3 & B.4	1500	50	1279
Case 3	B.5 & B.6	8000	0	6455
Case 4	B.7 & B.8	8000	50	6455

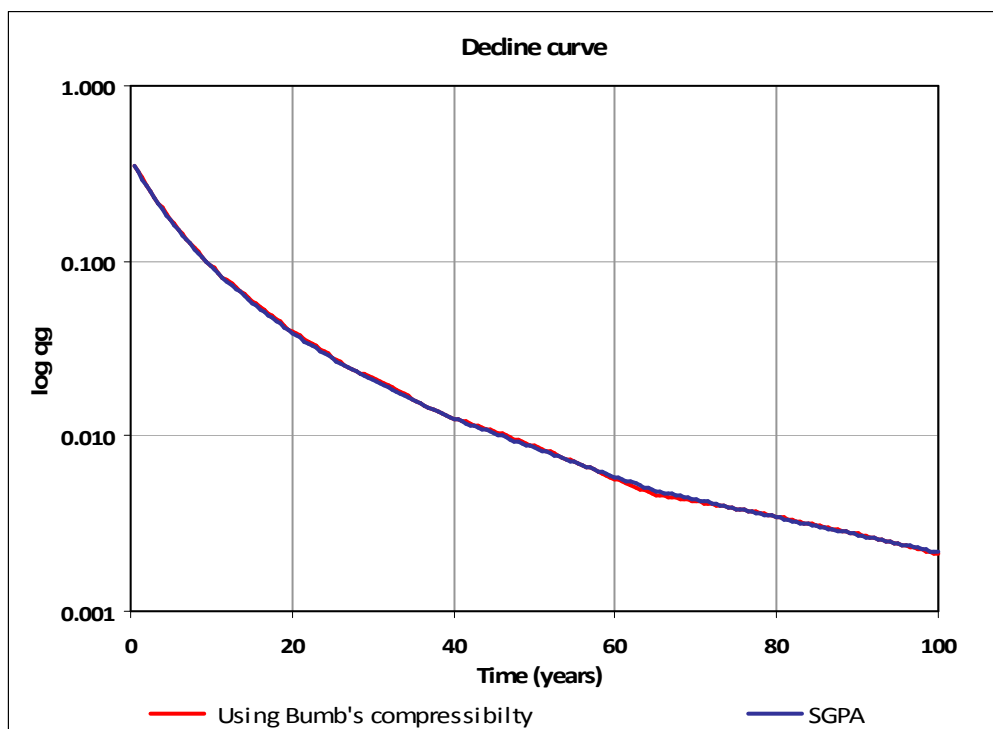


**Fig. B.1—Case 1: Decline curve (% adsorbed = 0).**

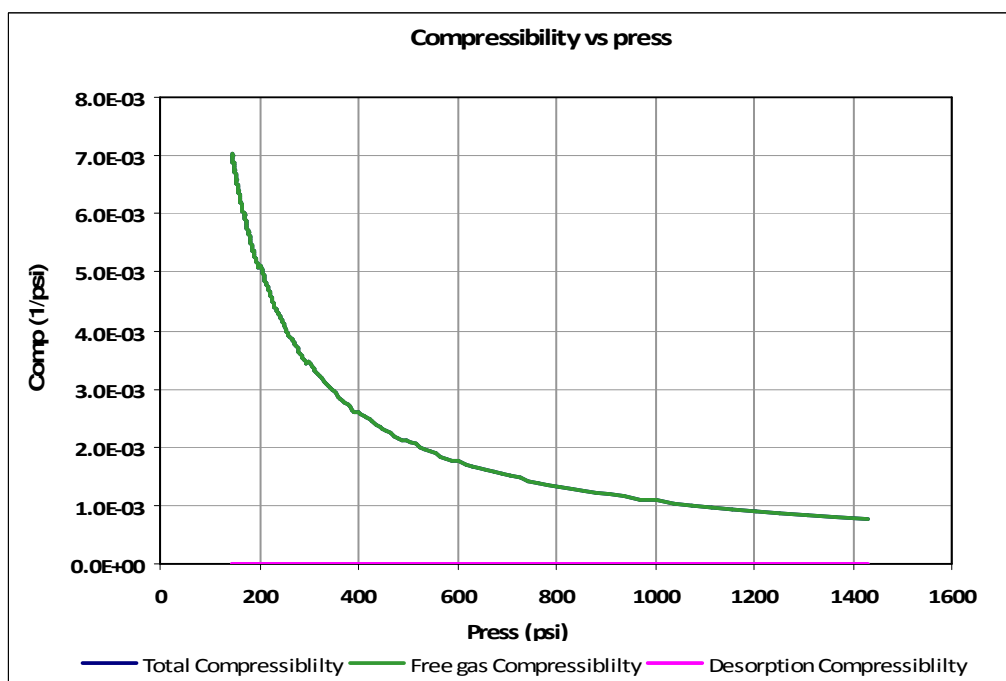


**Fig. B.2 —Case 1: Compressibility vs pressure (% adsorbed = 0).**

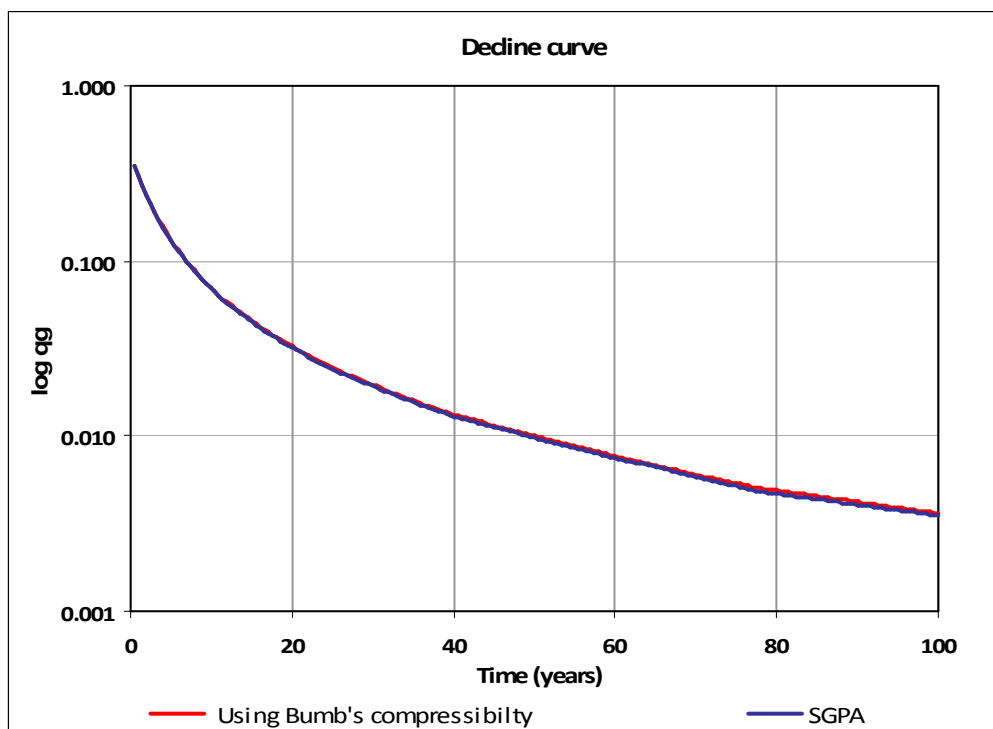


Fig. B.3 —Case 2: Decline curve (% adsorbed = 50).

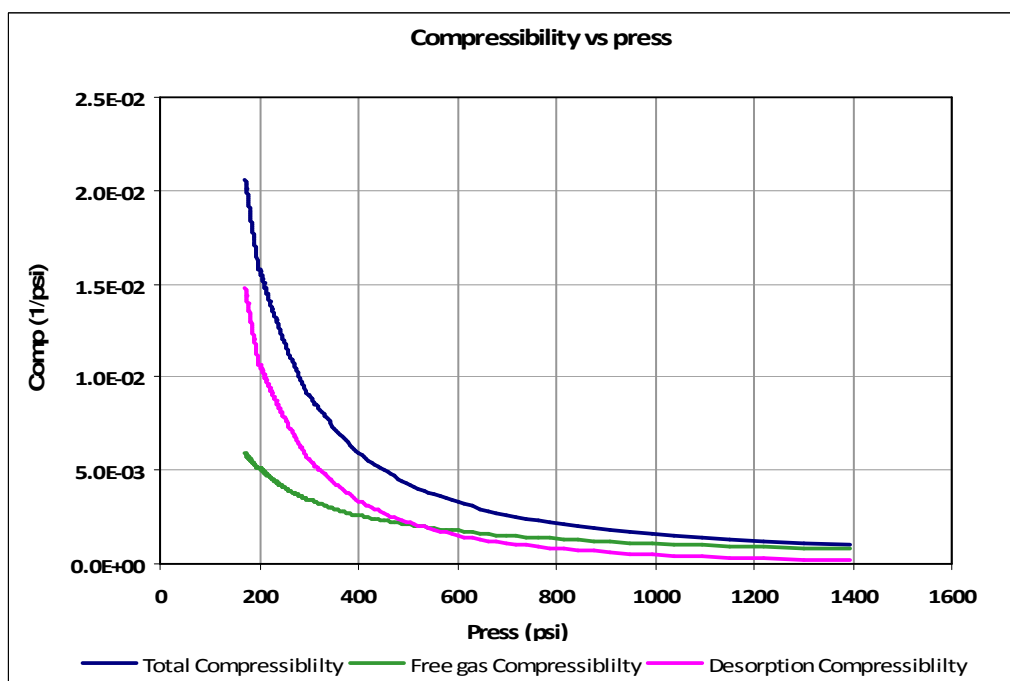


Fig. B.4 —Case 2: Compressibility vs pressure (% adsorbed = 50).

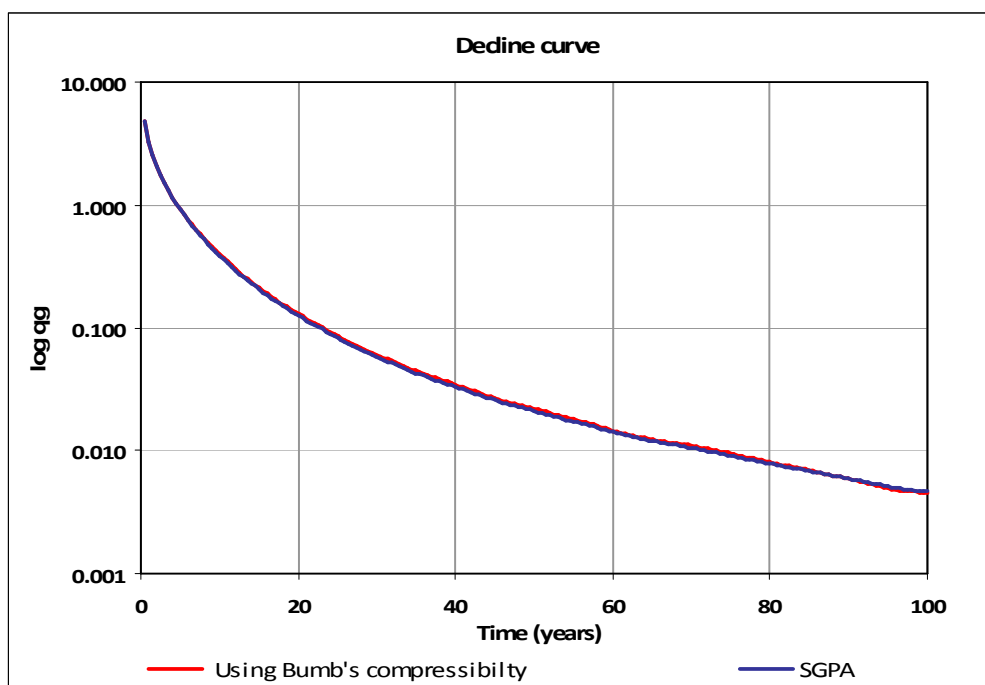


Fig. B.5 —Case 3: Decline curve (% adsorbed = 0).

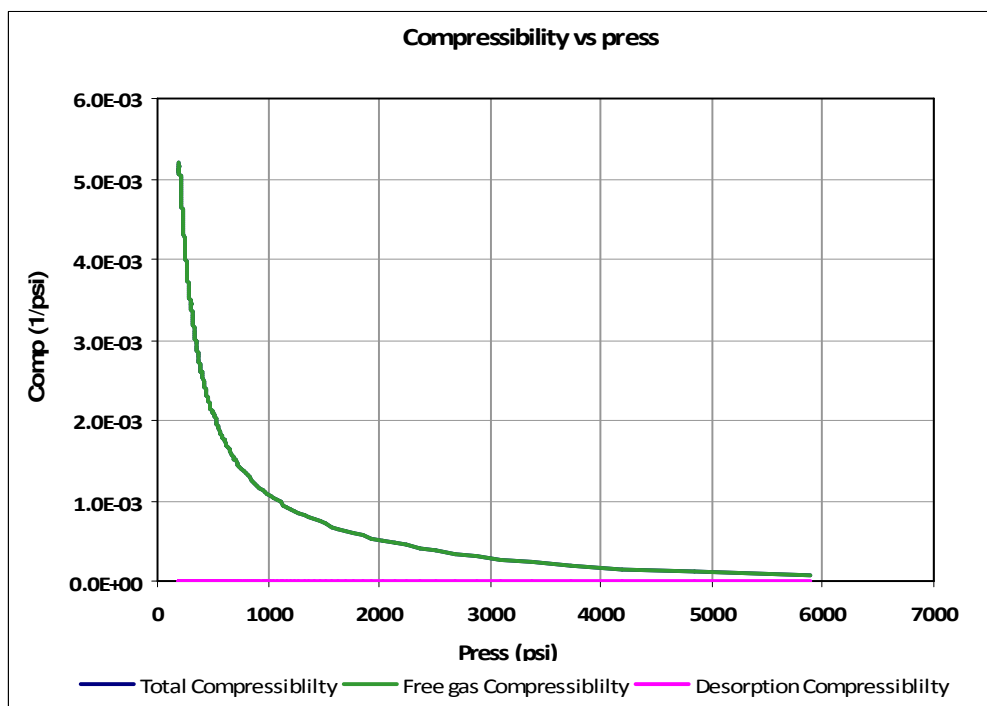
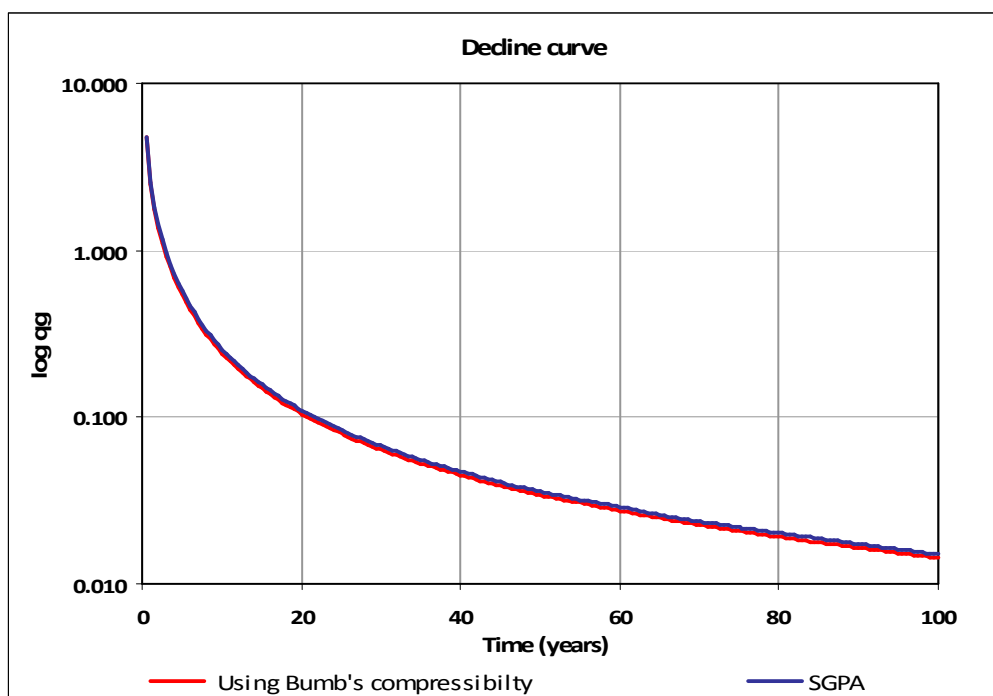
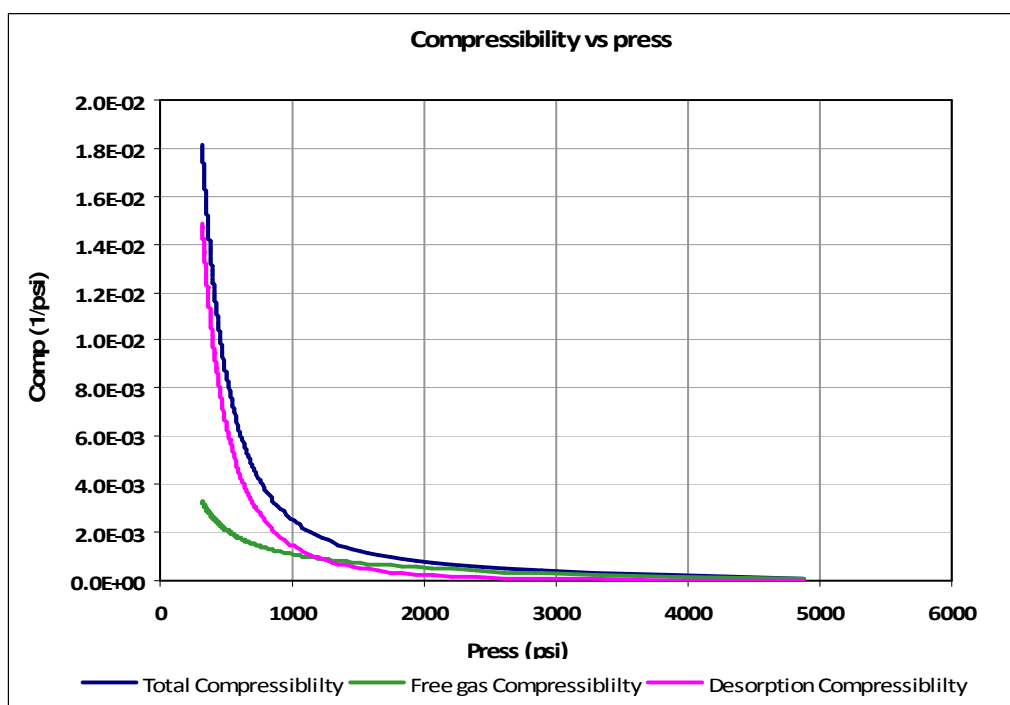


Fig. B.6 —Case 3: Compressibility vs pressure (% adsorbed = 0).



**Fig. B.7—Case 4: Decline curve (% adsorbed = 50).**



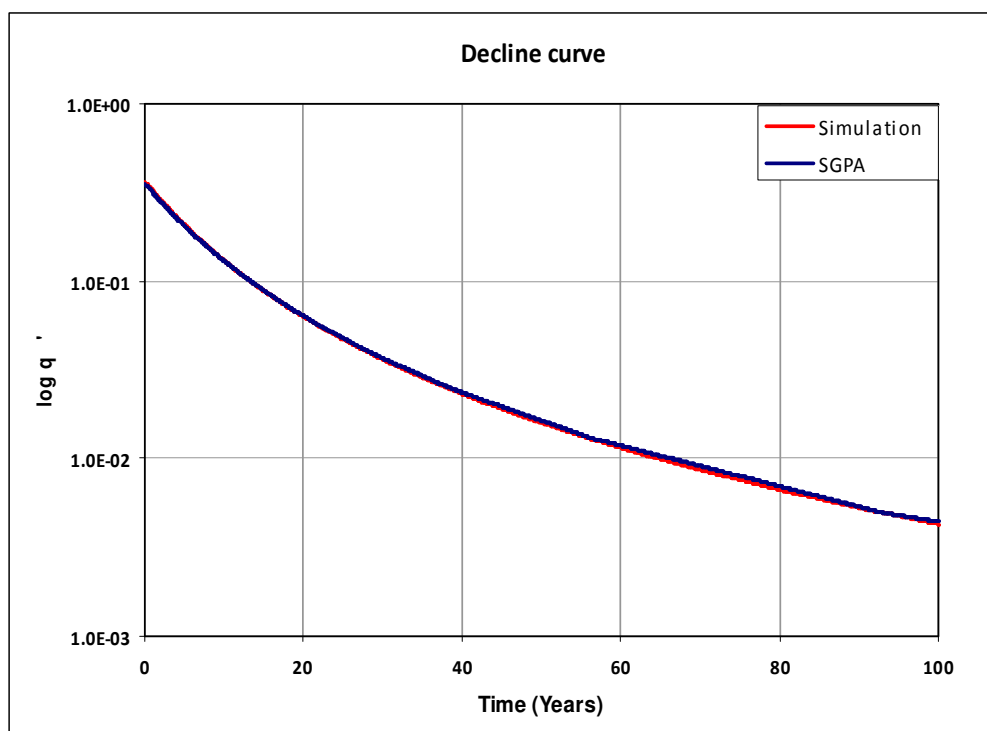
**Fig. B.8 —Case 5: Compressibility vs pressure (% adsorbed =50).**

## APPENDIX C

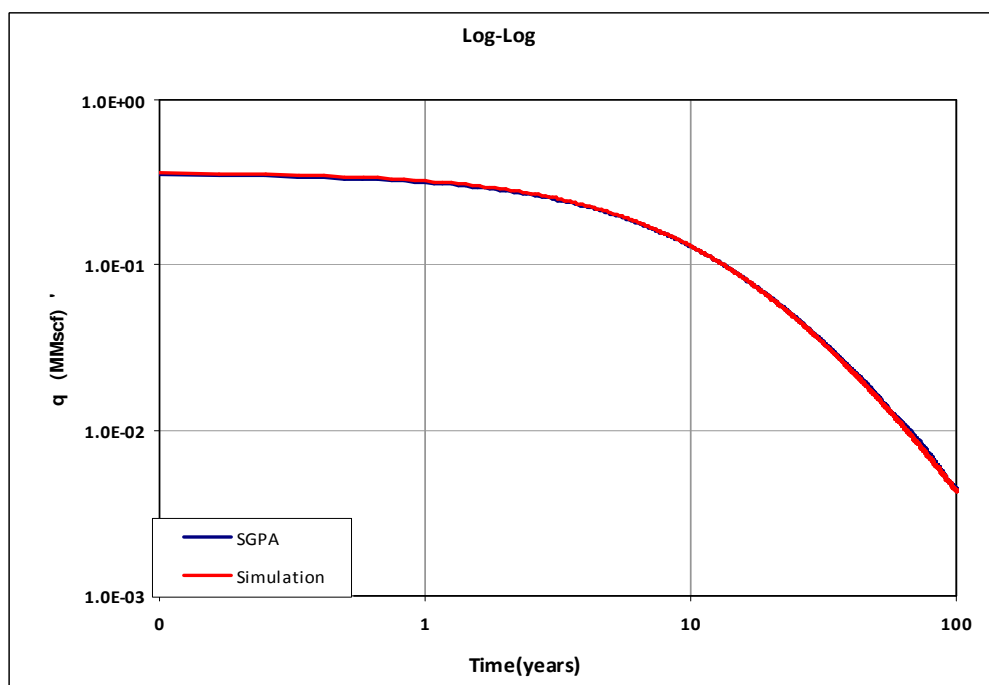
### COMPARISON OF SGPA RESULTS WITH NUMERICAL SIMULATOR (URS 01.2009)

Table C.1 shows the match cases for comparison of SGPA and URS 01 (2009) results followed by plots. To match different cases. Decline curves, log rate vs log time and  $G_p$  vs time plots were used.

<b>TABLE C.1— Match Cases: Comparison of SGPA and Numerical Simulator (URS 01.2009) Results</b>				
<b>Case #</b>	<b>Fig</b>	<b><math>p_i</math> (psi)</b>	<b>% Adsorbed</b>	<b>OGIP (MMscf)</b>
Case 1c	C.1, C.2 &..3	1500	0	1844.6
Case 2c	C.4, C.5 & C.6	1500	50	1844.6
Case 3c	C.7, C.8 & C.9	8000	0	6455
Case 4c	C.10, C.11 & C.12	8000	50	6455



**Fig. C.1—Case 1c: Decline curve (% adsorbed =0).**



**Fig. C.2 — Case 1c:  $\log q$  vs  $\log$  time (% adsorbed =0).**

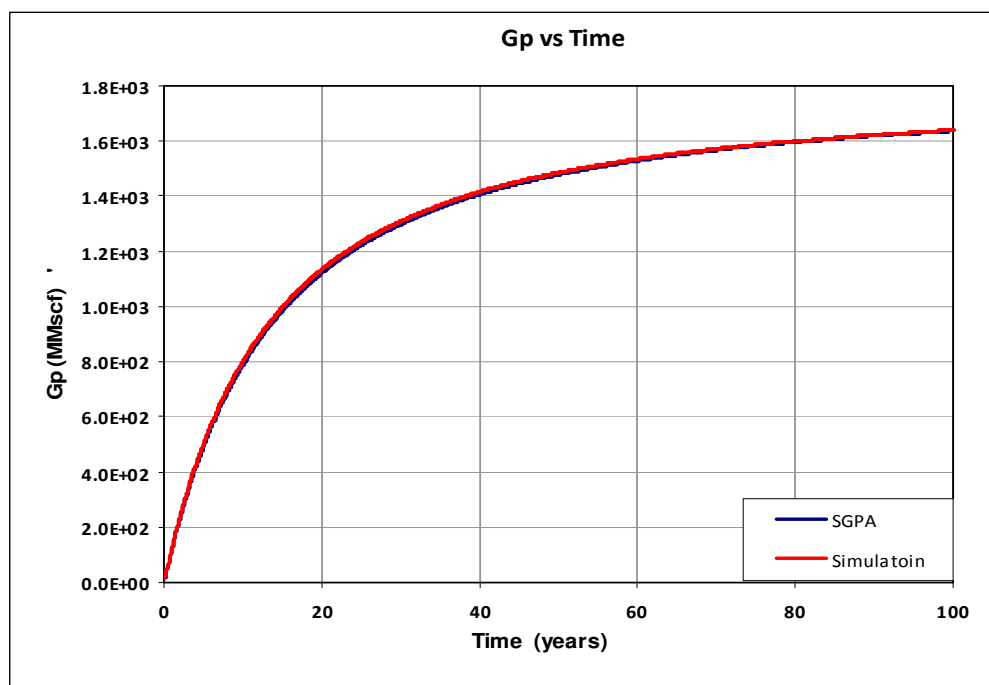


Fig. C.3 —Case 1c:  $G_p$  vs time (% adsorbed =0).

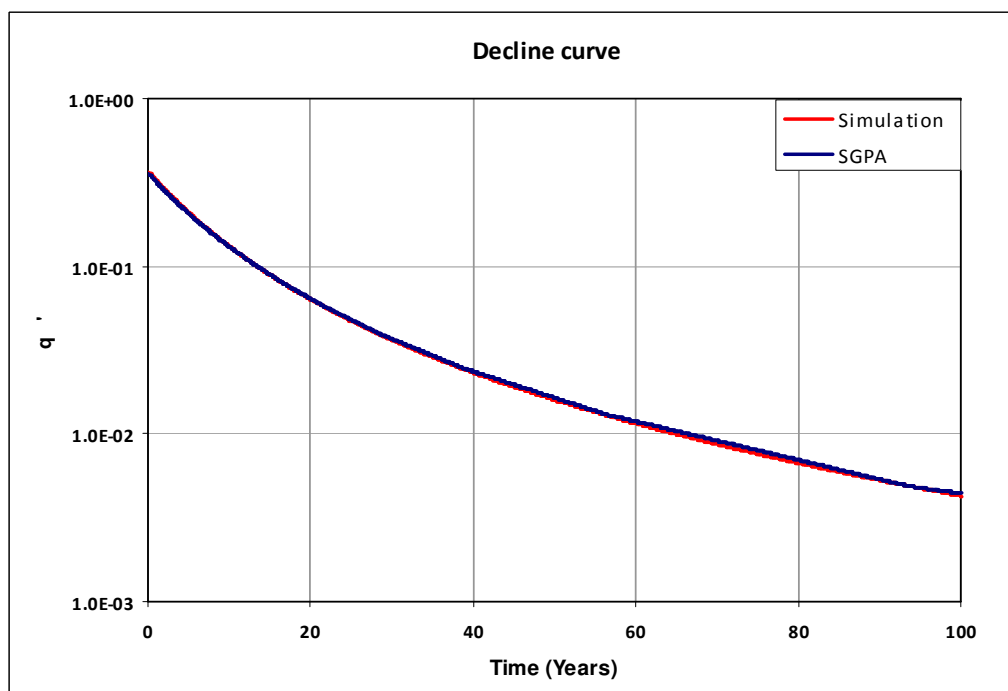


Fig. C.4 —Case 2c: Decline curve (% adsorbed =50).

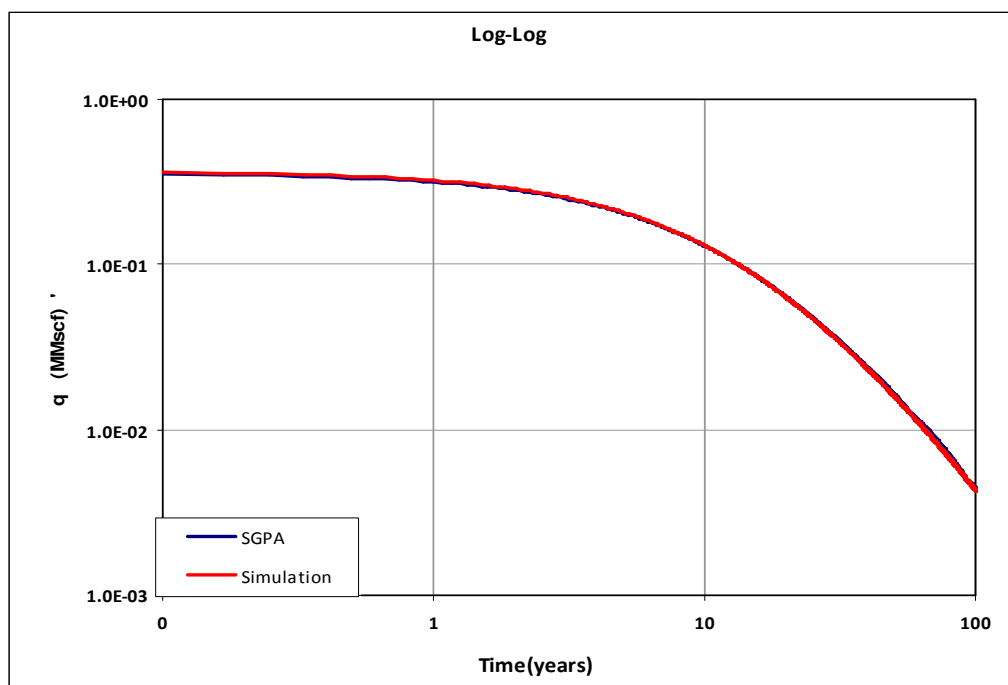


Fig. C.5 —Case 2c: log  $q$  vs log time (% adsorbed =50).

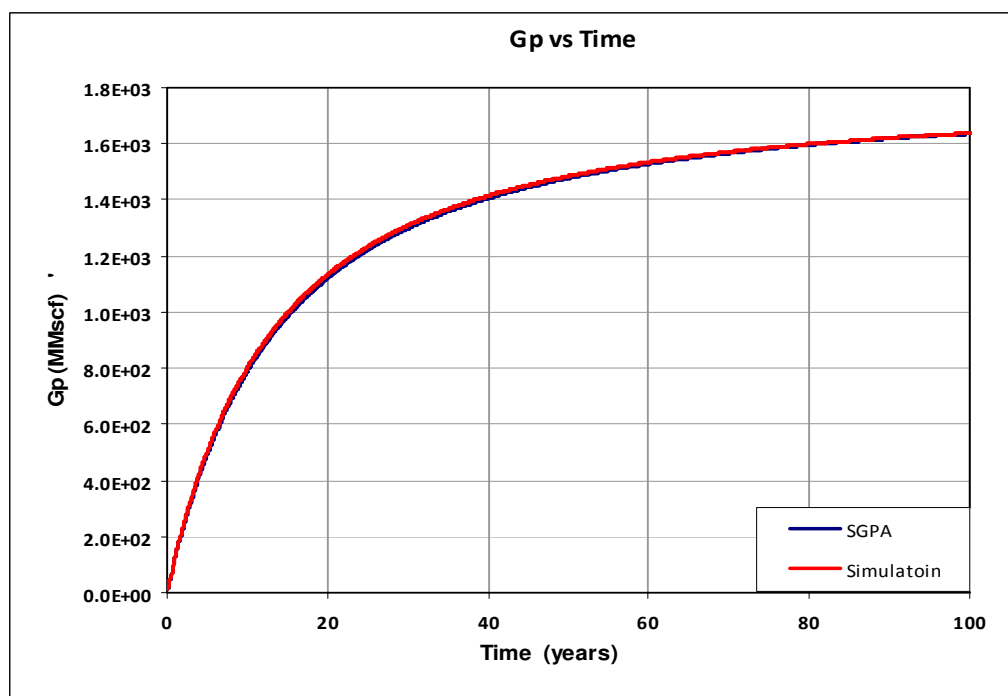


Fig. C.6 —Case 2c:  $G_p$  vs time (% adsorbed =50).

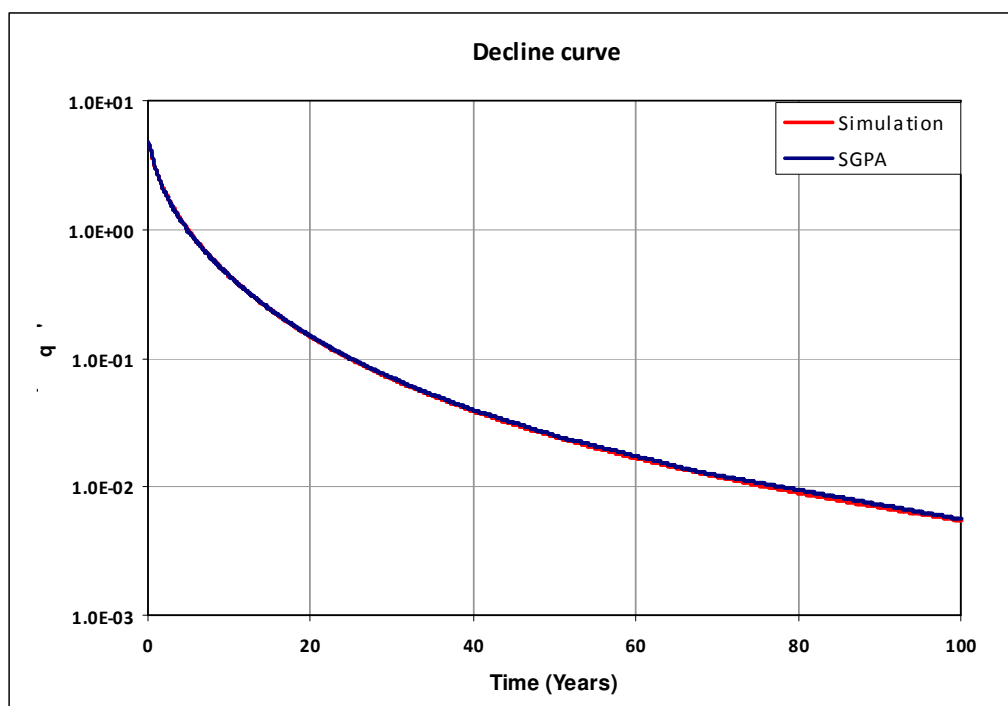


Fig. C.7 —Case 3c: Decline curve (% adsorbed =0).

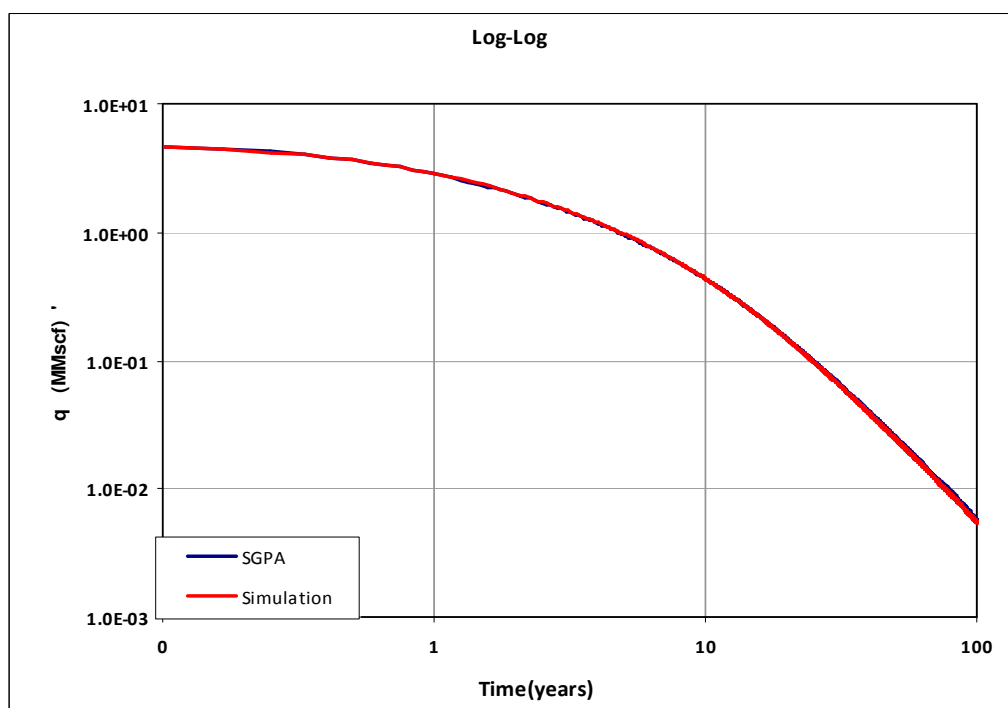
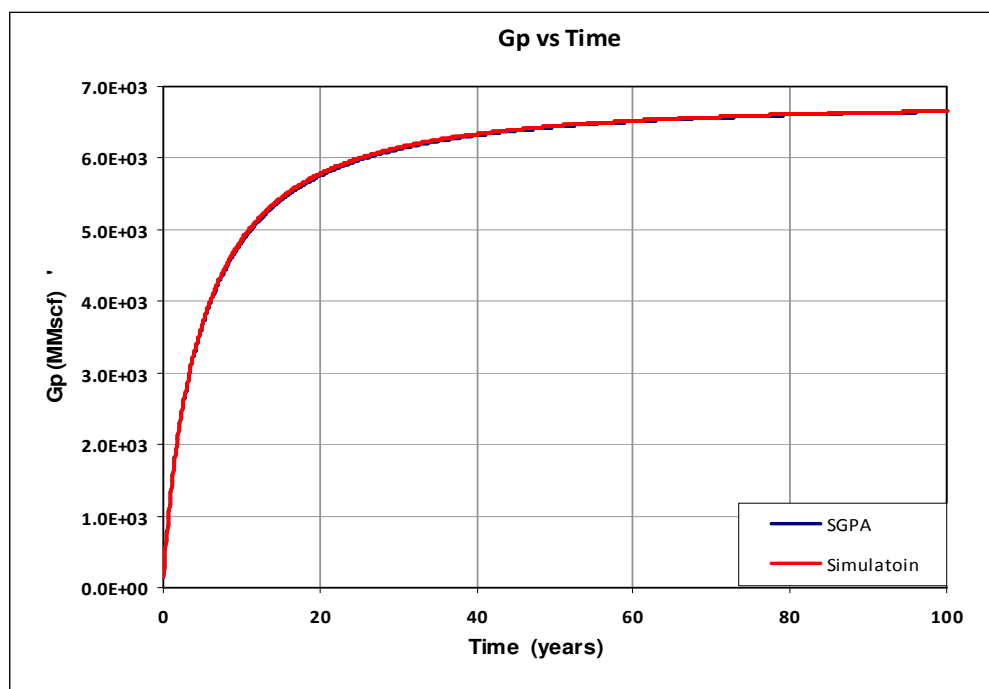
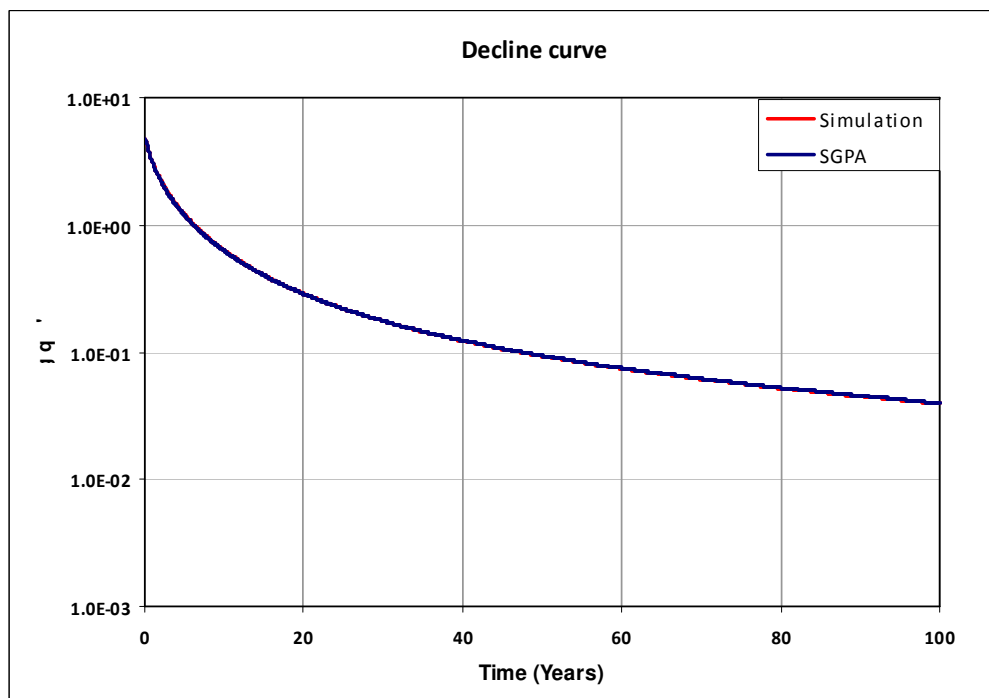


Fig. C.8 —Case 3c: log  $q$  vs log time (% adsorbed =0).



**Fig. C.9 —Case 3c:  $G_p$  vs time (% adsorbed =0).**



**Fig. C.10 —Case 4c: Decline curve (% adsorbed =50).**

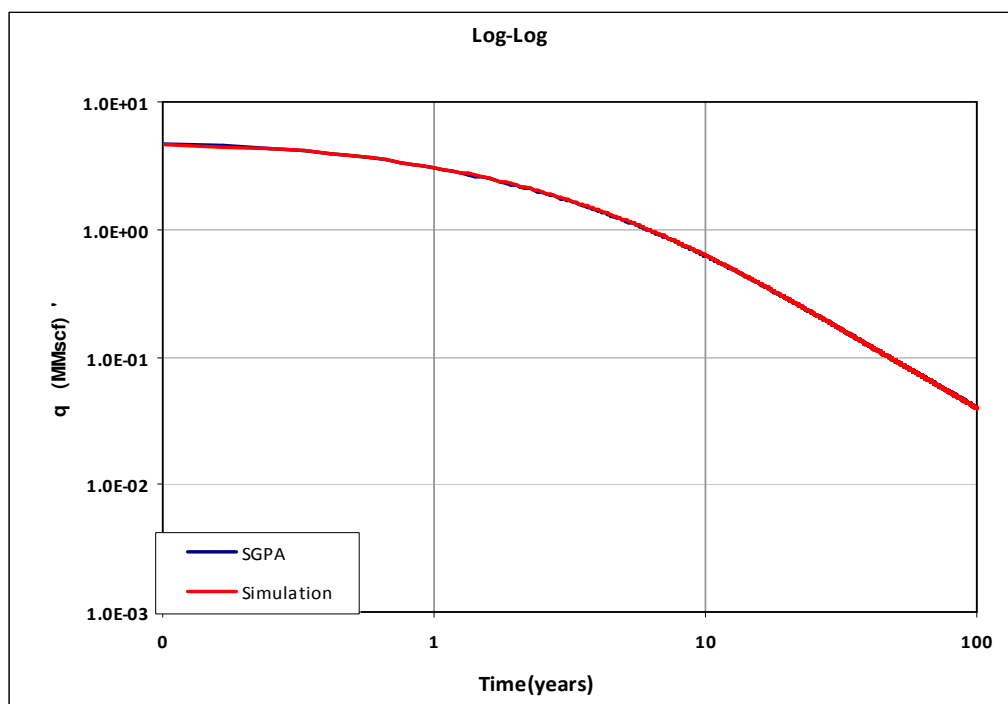


Fig. C.11 — Case 4c:  $\log q$  vs  $\log$  time (% adsorbed =50).

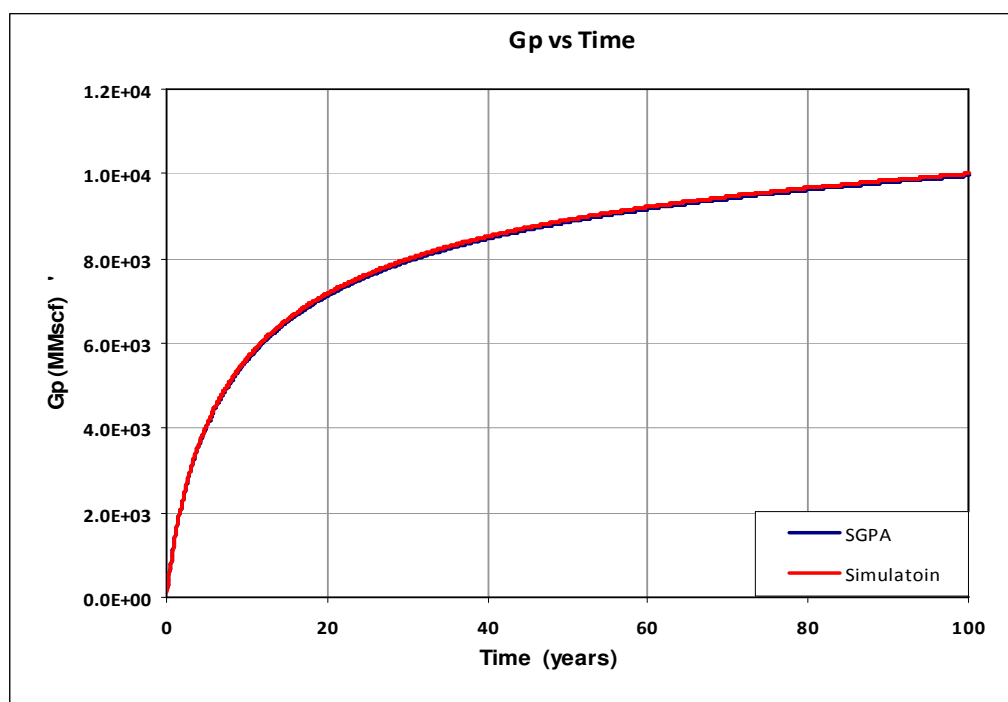


Fig. C.12 — Case 4c:  $G_p$  vs time (% adsorbed =50).

## APPENDIX D

### BOUNDARY DOMINATED FLOW METHODS

#### (INCLUDING ADSORPTION)

#### Liquid Material Balance (Constant Rate Depletion)

Assuming water saturation, formation volume factor to be constant and water / rock compressibilities to be negligible, the Material balance for single phase liquid is given as

$$N_p = OOIP - \left( \frac{V_p S_g}{B_o} \right) \dots \dots \dots D.1$$

Differentiating Eq. D.1 w. r. t pressure we get

$$\frac{dN_p}{d\bar{p}} = - V_p S_g \frac{d(1/B_o)}{d\bar{p}} \dots \dots \dots D.2$$

Substituting compressibility in Eq. D.2 which is given as

$$c_t = S_g c_o = -S_g \frac{1}{B_o} \left( \frac{dB_o}{d\bar{p}} \right) \Rightarrow \frac{d(1/B_o)}{d\bar{p}} = c_t \frac{1}{S_g B_o}$$

$$\frac{dN_p}{d\bar{p}} = - \frac{V_p c_t}{B_o} \dots \dots \dots D.3$$

$$\text{Also } q_o = \frac{dN_p}{dt}$$

$$dN_p = q_o dt \dots \dots \dots D.4$$

Substituting Eq. D.4 in Eq. D.3 and rearranging we get the volumetric expansion equation

$$\frac{d\bar{p}}{dt} = -\frac{q_o B_o}{V_p c_t} \dots\dots\dots \text{D.5}$$

Eq. D.5 is the Material balance equation for single phase liquid in terms  $q$ ,  $p$  and  $dt$ .

Productivity index equation for liquid is given as

$$q_o = J(\bar{p} - p_{wf}) \dots\dots\dots \text{D.6}$$

Differentiating Eq. D.6 w. r. t time (Assuming  $q_o$  to be constant) we get

$$\frac{d\bar{p}}{dt} = \frac{dp_{wf}(t)}{dt} \dots\dots\dots \text{D.7}$$

Substituting Eq. D.5 in Eq. D.7 and rearranging.

$$\text{Since } \frac{d\bar{p}}{dt} = \frac{dp_{wf}(t)}{dt} = -\frac{B_o}{V_p c_t} \dots\dots\dots \text{D.8}$$

Assuming  $q$  to be constant and Integrating Eq. D.5 we get

$$\int_{p_i}^{\bar{p}} dp = -\frac{q_o B_o}{V_p c_t} \int_0^t dt$$

$$\bar{p} - p_i = -\frac{q_o B_o}{V_p c_t} t \dots\dots\dots \text{D.9}$$

Subtracting  $p_{wf}(t)$  on both sides of Eq. D.9 and rearranging

$$\bar{p} - p_{wf}(t) = -\frac{q_o B_o}{V_p c_t} t + p_i - p_{wf}(t) \dots\dots\dots \text{D.10}$$

Substituting Eq. D.10 in Eq. D.6

$$q_o = -J \frac{q_o B_o}{V_p c_t} t + J[p_i - p_{wf}(t)]$$

$$\frac{q_o}{J[p_i - p_{wf}(t)]} = 1 - \frac{q_o B_o}{V_p c_t [p_i - p_{wf}(t)]} t \dots\dots\dots \text{D.11}$$

At initial rate ( $\bar{p} = p_i$ ) therefore Stabilized flow equation (Eq. D.7) at initial rate is

$$q_{oi} = J [p_i - p_{wf}(t)] \dots \dots \dots D.12$$

Substituting Eq. D.12 in Eq. D.11 and rearranging

$$\frac{q_o}{q_{oi}} = 1 - \frac{q_o B_o}{V_p c_t [p_i - p_{wf}(t)]} t$$

$$\frac{1}{q_o} = \frac{B_o}{V_p c_t [p_i - p_{wf}(t)]} t + \frac{1}{q_{oi}} \dots \dots \dots D.13$$

Multiplying both sides of Eq. D.13 by  $[p_i - p_{wf}(t)]$

$$\frac{[p_i - p_{wf}(t)]}{q_o} = \frac{B_o}{V_p c_t} t + \frac{[p_i - p_{wf}(t)]}{q_{oi}} \dots \dots \dots D.14$$

### Liquid Material Balance (Variable Rate Depletion)

Differentiating Eq. D.6 w. r. t pressure (Assuming  $p_{wf}$  to be constant) we get

$$\frac{dq_o(t)}{dt} = J \frac{d\bar{p}}{dt} \dots \dots \dots D.15$$

Substituting Eq. D.5 in Eq. D.15 and rearranging.

$$\frac{[dq_o(t)/dt]}{q_{oi}} = - \frac{J B_o}{V_p c_t} \dots \dots \dots D.16$$

Integrating Eq. D.16 with suitable limits we get

$$\int_{q_{oi}}^{q_o(t)} \frac{dq_o(t)}{q_o} = - \frac{J B_o}{V_p c_t} \int_0^t dt$$

$$\ln[q_o(t) - q_{oi}] = - \frac{J B_o}{V_p c_t} t$$

$$q_o(t) = q_{oi} e^{-\frac{J B_o}{V_p \bar{c}_i} t} \dots\dots\dots \text{D.17}$$

Eq. D.17 confirms that PSS constant pressure depletion (Single phase liquid) is equivalent to Arps's (1944) exponential decline.

$$q_o(t) = q_{oi} e^{-D_i t} \dots\dots\dots \text{D.18}$$

Recalling Eq. D.16.

$$\frac{J \bar{B}_o}{V_p \bar{c}_i} t = \frac{[dq_o(t)/dt]}{q_{oi}} = D_i \text{ where } D_i \text{ is Arps's (1944) initial decline rate.}$$

Taking inverse of Eq. D.17 and multiplying both sides by  $(p_i - p_{wf})$

$$\frac{(p_i - p_{wf})}{q_o(t)} = \frac{(p_i - p_{wf})}{q_{oi}} e^{\frac{J B_o}{V_p \bar{c}_i} t} \dots\dots\dots \text{D.19}$$

A plot of  $[p_i - p_{wf}] / q_o(t)$  vs  $t$  PSS constant pressure depletion for liquid is not linear unlike the constant rate case. Palacio and Blasingame in their work defined material balance time ( $t_c$ ) and showed that when  $t_c$  instead of time is used the resulting solution is corresponds to Arps's (1944) harmonic decline equation. Material balance time is defined as

$$t_c = \frac{N_p(t)}{q_o(t)} \dots\dots\dots \text{D.20}$$

Integrating Eq. D.16 with suitable limits we get

$$\int_{q_{oi}}^{q_o(t)} dq_o(t) = -\frac{J B_o}{V_p \bar{c}_i} \int_0^t q_o(t) dt \dots\dots\dots \text{D.21}$$

Substituting Eq. D.20 in Eq. D.21 we get.

$$q_o(t) - q_{oi} = -\frac{J B_o q_o(t)}{V_p c_t} t_c \dots\dots\dots D.22$$

Rearranging Eq. D.22

$$q_o(t) = \frac{q_{oi}}{\left[1 + \frac{J B_o}{V_p c_t} t_c\right]} \dots\dots\dots D.23$$

As  $\frac{J B_o}{V_p c_t} = \frac{[dq_o(t)/dt]}{q_{oi}} = D_i$  Eq. D.23 becomes

$$q_o(t) = \frac{q_{oi}}{[1 + D_i t_c]} \dots\dots\dots D.24$$

Eq. 24 is Arps's (1944) harmonic decline equation which confirms that PSS constant pressure depletion for liquid equivalent to Arps's harmonic decline when  $t_c$  is used.

Multiplying both sides of Eq. D.22 by  $[p_i - p_{wf}] / q_o(t)$  and dividing by  $q_{oi}$  we get

$$\frac{(p_i - p_{wf})}{q_o(t)} - \frac{(p_i - p_{wf})}{q_{oi}} = \frac{J B_o (p_i - p_{wf})}{V_p \bar{c}_t q_{oi}} t_c \dots\dots\dots D.25$$

Substituting Eq. D.12 in Eq. D.25 and rearranging we get.

$$\frac{(p_i - p_{wf})}{q_o(t)} = \frac{B_o}{V_p \bar{c}_t} t_c + \frac{(p_i - p_{wf})}{q_{oi}} \dots\dots\dots D.26$$

Eq. D.26 is similar to Eq. D.14 which validates that PSS variable rate depletion for liquid results in the same form as PSS constant rate depletion for liquid, provided that material balance time is used.

### **Gas Material Balance Including Adsorbed gas (Constant Rate depletion)**

Gas Material Balance, including adsorbed gas is defined by King as

$$\frac{\bar{p}}{\bar{z}^*} = \frac{p_i}{z_i^*} \left[ 1 - \frac{G_p}{G} \right] \dots\dots\dots \text{D.27}$$

where  $z^*$  for constant water saturation, (Neglecting water and rock compressibilities ) is defined as.

$$z^* = \frac{z}{S_g + \frac{V_L T p_{sc} z}{\phi (p + p_L) T_{sc} z_{sc}}} \dots\dots\dots \text{D.28}$$

Differentiating Eq.D.27 with respect to pressure

$$\frac{d(\bar{p}/\bar{z}^*)}{dp} = - \frac{p_i}{G z_i^*} \frac{dG_p}{dp} \dots\dots\dots \text{D.29}$$

Taking inverse of Eq.D.28 and Multiplying both sides by  $(p)$  we get

$$\frac{p}{z^*} = \left[ \frac{p}{z} S_g + \frac{V_L T p_{sc}}{\phi T_{sc} z_{sc}} \frac{p}{(p + p_L)} \right] \dots\dots\dots \text{D.30}$$

Differentiating Eq.D.30 w. r. t pressure we get (at average reservoir pressure)

$$\frac{d(\bar{p}/\bar{z}^*)}{dp} = \left[ \frac{d(\bar{p}/\bar{z})}{dp} S_g + \frac{V_L T p_{sc}}{\phi T_{sc} z_{sc}} \frac{d\left(\frac{\bar{p}}{(\bar{p} + p_L)}\right)}{dp} \right]$$

$$\frac{d(\bar{p}/\bar{z}^*)}{dp} = \frac{\bar{p}}{\bar{z}} S_g \left[ \left[ \frac{1}{\bar{p}} - \frac{1}{\bar{z}} \left( \frac{d\bar{z}}{d\bar{p}} \right) \right] + \frac{V_L T p_{sc} \bar{z}}{\phi S_g \bar{p} T_{sc} z_{sc}} \frac{p_L}{(\bar{p} + p_L)^2} \right] \dots\dots\dots \text{D.31}$$

Since Formation volume factor for gas, free gas compressibility and adsorbed gas compressibility (Bumb & McKee.1986) are given as

$$B_g = \frac{p_{sc} T z}{\bar{p} T_{sc} z_{sc}}, \quad \bar{c}_g = \left[ \frac{1}{\bar{p}} - \frac{1}{\bar{z}} \left( \frac{d\bar{z}}{d\bar{p}} \right) \right], \quad \text{and} \quad \bar{c}_d = \left[ \frac{B_g V_L p_L}{\phi (1 - S_w) (\bar{p} + p_L)^2} \right]$$

Eq.D.31 therefore will have the form

$$\frac{d(\bar{p}/\bar{z}^*)}{dp} = \frac{\bar{p}}{\bar{z}} S_g [\bar{c}_g + \bar{c}_d] \dots\dots\dots \text{D.32}$$

The total compressibility of the system can be given as  $c_t^* = S_g [c_g + c_d] + S_w c_w + c_f$ , where  $[c_g + c_d]$  can be called the total gas compressibility (adsorbed and free gas). Neglecting water and rock compressibilities results in  $c_t^* = S_g [c_g + c_d]$ . Eq. D.32 thus becomes

$$\frac{d(\bar{p}/\bar{z}^*)}{dp} = \frac{\bar{p}}{\bar{z}} \bar{c}_t^* \dots\dots\dots \text{D.33}$$

Substituting Eq. D.33 in Eq.D.29.

$$\frac{\bar{p}}{\bar{z}} \bar{c}_t^* = - \frac{p_i}{G z_i^*} \frac{dG_p}{dp} \dots\dots\dots \text{D.34}$$

$$\text{Also } q_g = \frac{dG_p}{dt}$$

$$dG_p = q_g dt \dots\dots\dots \text{D.35}$$

Substituting Eq. D.35 in Eq. D.34 results in

$$\frac{\bar{p}}{\bar{z}} \bar{c}_t^* = - \frac{p_i}{G z_i^*} q_g \frac{dt}{dp} \dots\dots\dots \text{D.36}$$

Introducing real gas pseudo pressure  $m(p)$ , given as

$$m(p) = \int \frac{2p}{z\mu} dp \dots\dots\dots \text{D.37}$$

Differentiating Eq.D.37 with respect to pressure and using chain rule will give.

$$\frac{dm(p)}{dt} \frac{dt}{dp} = \frac{2p}{z\mu} \dots\dots\dots D.38$$

Rearranging Eq.D.38 (at average reservoir pressure)

$$\frac{dt}{d\bar{p}} = -\frac{2\bar{p}}{z\mu} \frac{dt}{dm(\bar{p})} \dots\dots\dots D.39$$

Substituting Eq.D.39 in Eq.D.36 and Rearranging will give

$$\frac{dm(\bar{p})}{dt} = -\frac{2p_i}{G} \frac{q_g}{z_i^* \mu \bar{c}_t^*} \dots\dots\dots D.40$$

Normalized pseudo time  $t_n^*$  including adsorption to correct for gas properties can be defined as

$$t_n^* = \int \frac{\mu_i c_{ti}^*}{\mu \bar{c}_t^*} dt \dots\dots\dots D.41$$

Differentiating  $t_n^*$  w. r. t to time and Rearranging

$$\frac{1}{\mu \bar{c}_t^*} = \frac{1}{\mu_i c_{ti}^*} \frac{dt_n^*}{dt} \dots\dots\dots D.42$$

Substituting Eq.D.42 in Eq.D.40 results in

$$\frac{dm(\bar{p})}{dt_n^*} = -\frac{2p_i}{G} \frac{q_g}{z_i^* \mu_i c_{ti}^*} \dots\dots\dots D.43$$

Stabilized flow equation in terms of real gas pseudo pressure ( $mp$ ) is

$$q_g = J [m(\bar{p}) - m(p_{wf})] \dots\dots\dots D.44$$

Differentiating Eq. D.44 w. r. t to  $t_n^*$  (Assuming  $q_g$  to be constant)

$$\frac{dq_g}{dt_n^*} = J \frac{dm(\bar{p})}{dt_n^*} - J \frac{dm(p_{wf})(t)}{dt_n^*}$$

$$\frac{d m(\bar{p})}{dt_n^*} = \frac{d m(p_{wf})(t)}{dt_n^*} \dots\dots\dots D.45$$

$$\text{Since } \frac{d m(\bar{p})}{dt_n^*} = \frac{d m(p_{wf})(t)}{dt_n^*} = -\frac{2 p_i}{G} \frac{q_g}{z_i^* \mu_i c_{ii}^*}$$

Assuming  $q_g$  to be constant and Integrating Eq.D.43 with suitable limits

$$m(\bar{p}) - m(p_i) = -\frac{2 p_i q_g}{G z_i^* \mu_i c_{ii}^*} t_n^* \dots\dots\dots D.46$$

Subtracting  $m(p_{wf})$  on both sides of Eq. D.46 and rearranging we get

$$m(\bar{p}) - m(p_{wf})(t) = -\frac{2 p_i q_g}{G z_i^* \mu_i c_{ii}^*} t_n^* + m(p_i) - m(p_{wf})(t) \dots\dots\dots D.47$$

Substituting Eq. D.47 in Eq. D.44 and rearranging we get

$$q_g = J [m(p_i) - m(p_{wf})(t)] - J \frac{2 p_i q_g}{G z_i^* \mu_i c_{ii}^*} t_n^* \dots\dots\dots D.48$$

Rearranging Eq. D.48

$$\frac{q_g}{J [m(p_i) - m(p_{wf})(t)]} = 1 - \frac{2 p_i}{G z_i^* \mu_i c_{ii}^*} \frac{q_g}{[m(p_i) - m(p_{wf})(t)]} t_n^* \dots\dots\dots D.49$$

At initial rate ( $\bar{p} = p_i$ ) therefore Stabilized flow equation (Eq. D.44) at initial rate is

$$q_{gi} = J [m(p_i) - m(p_{wf})] \dots\dots\dots D.50$$

Substituting Eq. D.50 in Eq. D.49 and Multiplying both sides by  $[m(p_i) - m(p_{wf})]/q_g$

$$\frac{[m(p_i) - m(p_{wf})(t)]}{q_g} = \frac{[m(p_i) - m(p_{wf})(t)]}{q_{gi}} + \frac{2 p_i}{G z_i^* \mu_i c_{ii}^*} t_n^* \dots\dots\dots D.51$$

### Gas Material Balance Including Adsorbed Gas (Variable Rate depletion)

Differentiating Eq. D.44 w. r. t to  $t_n^*$  (Assuming  $p_{wf}$  to be constant)

$$\frac{dq_g(t)}{dt_n} = J \frac{dm(\bar{p})}{dt_n} \dots\dots\dots \text{D.52}$$

Substituting Eq. D.43 in Eq. D.52 and rearranging we get

$$\frac{dq_g(t)/dt_n}{q_g(t)} = -J \frac{2p_i}{Gz_i \mu_i c_{ti}} \dots\dots\dots \text{D.53}$$

Integrating Eq. D.53

$$\int_{q_{gi}}^{q_g(t)} \frac{dq_g(t)}{q_g(t)} = -\frac{2Jp_i}{Gz_i \mu_i c_{ti}} \int_0^t dt_n$$

$$\ln[q_g(t) - q_{gi}] = -\frac{2Jp_i}{Gz_i \mu_i c_{ti}} t_n$$

$$q_g(t) = q_{gi} e^{-\frac{2Jp_i}{Gz_i \mu_i c_{ti}} t_n} \dots\dots\dots \text{D.54}$$

Eq. D.54 confirms that PSS variable rate depletion ( gas) is equivalent to Arps's (1944) exponential decline.

$$q_o(t) = q_{oi} e^{-D_i t} \dots\dots\dots \text{D.55}$$

Recalling Eq. D.53.

$$\frac{2Jp_i}{Gz_i \mu_i c_{ti}} = \frac{[dq_o(t)/dt]}{q_{oi}} = D_i \text{ where } D_i \text{ is Arps's initial decline rate.}$$

Taking inverse of Eq. D.54 and multiplying both sides by  $[m(p_i) - m(p_{wf})]$

$$\frac{[m(p_i) - m(p_{wf})]}{q_o(t)} = \frac{[m(p_i) - m(p_{wf})]}{q_{oi}} e^{\frac{2Jp_i}{Gz_i \mu_i c_{ti}} t_n} \dots\dots\dots \text{D.56}$$

In order to extend the validity of Eq. D.56 for variable rate cases we need to introduce material balance time. Palacio and Blansingame material balance time is

therefore modified to correct for gas properties and include adsorbed gas to extend the validity of Eq. D.56 for variable rate gas (including adsorbed gas ) as well.

Normalized material balance pseudo time for gas is defined by N.M. Anisur Rahman et al. as

$$t_{ca} = \frac{G_{pa}(t)}{q_g(t)}$$

Normalized material balance pseudo time for gas including adsorbed gas  $t_{ca}^*$  can be defined as

$$t_{ca}^* = \frac{G_{pa}^*(t)}{q_g(t)} \dots\dots\dots \text{D.57}$$

where

$$G_{pa}^*(t) = \int_0^{t_n^*(t)} q_g(t_n^*) dt_n^* \dots\dots\dots \text{D.58}$$

Substituting Eq. D.42 in Eq. D.58

$$G_{pa}^*(t) = \int_0^{t_n^*(t)} q_g(t_n^*) \frac{\mu_i c_{ti}^*}{\bar{\mu} \bar{c}_t^*} dt \dots\dots\dots \text{D.59}$$

Substituting Eq. D.59 in Eq. D.57

$$t_{ca}^* = \frac{1}{q_g(t)} \int_0^{t_n^*(t)} q_g(t_n^*) \frac{\mu_i c_{ti}^*}{\bar{\mu} \bar{c}_t^*} dt \dots\dots\dots \text{D.60}$$

Integrating Eq. D.53 with suitable limits

$$\int_{q_{gi}}^{q_g(t)} dq_g(t) = - \frac{2J p_i}{G z_i^* \mu_i c_{ti}^*} \int_0^{t_n^*(t)} q_g(t_n^*) dt_n^* \dots\dots\dots \text{D.61}$$

Substituting Eq. D.58 in Eq. D.61

$$q_g(t) - q_{gi} = -\frac{2J p_i G_{pa}}{G z_i \mu_i c_{ti}} \dots\dots\dots D.62$$

Substituting Eq. D.57 in Eq. D.62

$$q_{gi} - q_g(t) = \frac{2J p_i q_g(t)}{G z_i \mu_i c_{ti}} t_{ca} \dots\dots\dots D.63$$

Rearranging Eq. D.63

$$q_g(t) = \frac{q_{gi}}{\left[ 1 + \frac{2J p_i}{G z_i \mu_i c_{ti}} t_{ca} \right]} \dots\dots\dots D.64$$

Substituting Eq. D.53 in Eq. D.64.

$$q_g(t) = \frac{q_{gi}}{[1 + D_i t_{ca}]}$$

Eq. 64 is Arps's harmonic decline equation which confirms that PSS variable rate depletion for gas (including adsorbed gas) is equivalent to Arps's harmonic decline when  $t_{ca}$  is used.

Multiplying both sides of Eq. D.63 by  $[m(p_i) - m(p_{wf})] / q_g(t)$  and dividing by  $q_{gi}$  we get

$$\frac{[m(p_i) - m(p_{wf})]}{q_g(t)} - \frac{[m(p_i) - m(p_{wf})]}{q_{gi}} = \frac{2J p_i [m(p_i) - m(p_{wf})]}{G z_i \mu_i c_{ti} q_{gi}} t_{ca} \dots\dots\dots D.65$$

Substituting Eq. D.50 in Eq. D.65 and rearranging we get

$$\frac{[m(p_i) - m(p_{wf})]}{q_g(t)} = \frac{2 p_i}{G z_i \mu_i c_{ti}} t_{ca} + \frac{[m(p_i) - m(p_{wf})]}{q_{gi}} \dots\dots\dots D.66$$

Eq. D.66 is similar to Eq. D.51 which validates that PSS variable rate depletion for gas (including adsorbed gas) results in the same form as PSS constant rate depletion for gas (including adsorbed gas), provided that  $t_{ca}^*$  is used.

## APPENDIX E

### SIMULATED DATA ANALYSIS

Synthetic data is used to create simulated data using unconventional reservoir simulator (URS 01.2009). The production data is then used in SGPA to generate results to estimate OGIP. The OGIP estimation methods discussed in previous chapters are used and results are then compared. This Appendix shows the synthetic data (Tables E.1 & E.2) used for simulation and SGPA results used to estimate OGIP with and without adsorption (Figs. E.1-E.4 & Tables E.3-E.5).

<b>TABLE E.1— Synthetic Data Used in Numerical Simulator (URS 01.2009) Without Adsorption.</b>			
OGIP, MMscf	2900	Gas Content, scf/ton	0
$p_i$ , psi	2950	Specific gravity, fraction	0.65
$p_{wf}$ , psi	500	Reservoir Temperature, °R	610
$\Phi$ , fraction	0.06	$c_t^*$ , psi <sup>-1</sup>	3.38E-04
$\rho_B$ , gm/cc	2.58	$z^*$ ,	0.859
$S_g$ , fraction	1	$Z^{**}$ ,	0.859
$\mu^*_{i,}$ cp	0.0203	$B_{gi}$ , scf/rcf	0.00503

<b>TABLE E.2— Synthetic Data Used in Numerical Simulator (URS 01.2009) with Adsorption.</b>			
OGIP, MMscf	4345	Gas Content, scf/ton	96
$p_i$ , psi	2950	$V_L$ , scf/rcf	7.72
$p_{wf}$ , psi	500	Specific gravity, fraction	0.65
$\Phi$ , fraction	0.06	Langmuir's pressure, psi	650
$\rho_B$ , gm/cc	2.58	Reservoir Temperature, °R	610
$S_g$ , fraction	1	$c_t^*$ , psi <sup>-1</sup>	3.05E-04
$\mu^*_{i,}$ cp	0.0203	$z^*$ ,	0.562
		$z^{**}$ ,	0.859

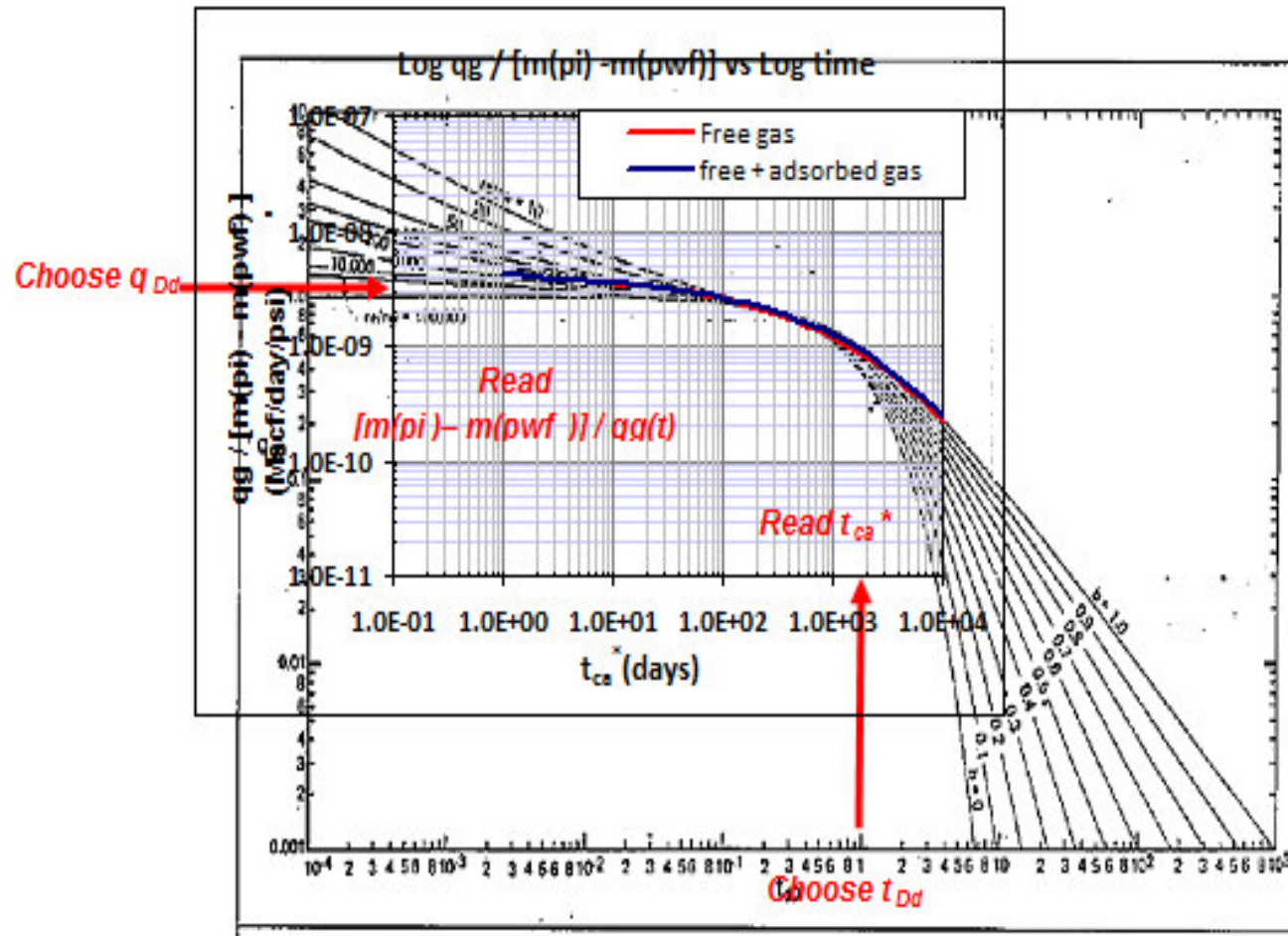


Fig. E.1—Matching plot of  $\text{Log } q_g / [m(p_i) - m(p_{wf})]$  vs  $\text{Log } t_{ca}^*$  on harmonic decline ( $b = 1$ ) stem of Fetkovich's (1980) Type curve to establish match points used to calculate OGIP with and without adsorbed gas by Palacio & Blasingame's (1993) method, simulated data.

**OGIP estimation with and without adsorbed gas from BDF Palacio and Blasingame's method**

Following match points can be read from Fig. E.1

<b>TABLE E.3— Match Points (M.P) from Fig. E.1</b>	
$t_{dD}$ , dimensionless	1
$t_{ca}^*$ , days	1080
$q_{dD}$ , dimensionless	1
$q_g / [m(p_i) - m(p_{wf})]$ , psi/MMscf/d	2.5 E-09

Calculate OGIP with and with adsorbed gas using Eq. 4.2.8

$$G = \frac{\left( \frac{q_g(t)}{[m(p_i) - m(p_{wf})]} \right)_{M.P.}}{(q_{dD})_{M.P.}} \cdot \frac{2 p_i}{z_i \cdot \mu_i c_{ii}} \cdot \frac{(t_{ca}^*)_{M.P.}}{(t_{dD})_{M.P.}} \dots\dots\dots 4.2.8$$

OGIP without adsorption:

$$G = \frac{2.5E-09 \times 2 \times 2950 \times 1080}{1 \times 0.859 \times 0.0203 \times 3.05E-04 \times 1} = 2990.5 \text{ MMscf}$$

OGIP with adsorption:

$$G = \frac{2.5E-09 \times 2 \times 2950 \times 1080}{1 \times 0.562 \times 0.0203 \times 3.38E-04 \times 1} = 4137.1 \text{ MMscff}$$

**OGIP estimation with and without adsorbed gas from BDF Ibrahim, Wattenbarger and Helmy / Anderson et al.'s method**

From Fig E.2 slope of BDF straight line without adsorbed gas =  $3.85E + 05$

And slope of BDF straight line with adsorbed gas =  $3.57E + 05$

Using slope we can calculate OGIP with and without adsorbed gas as follows.

OGIP without adsorption:

$$G = \frac{2 p_i}{m_{PSS} z_i * \mu_i c_{ti} *}$$

$$G = \frac{2 \times 2950}{3.85E+05 \times 0.859 \times 0.0203 \times 3.05E-04} = 2881 \text{ MMscf}$$

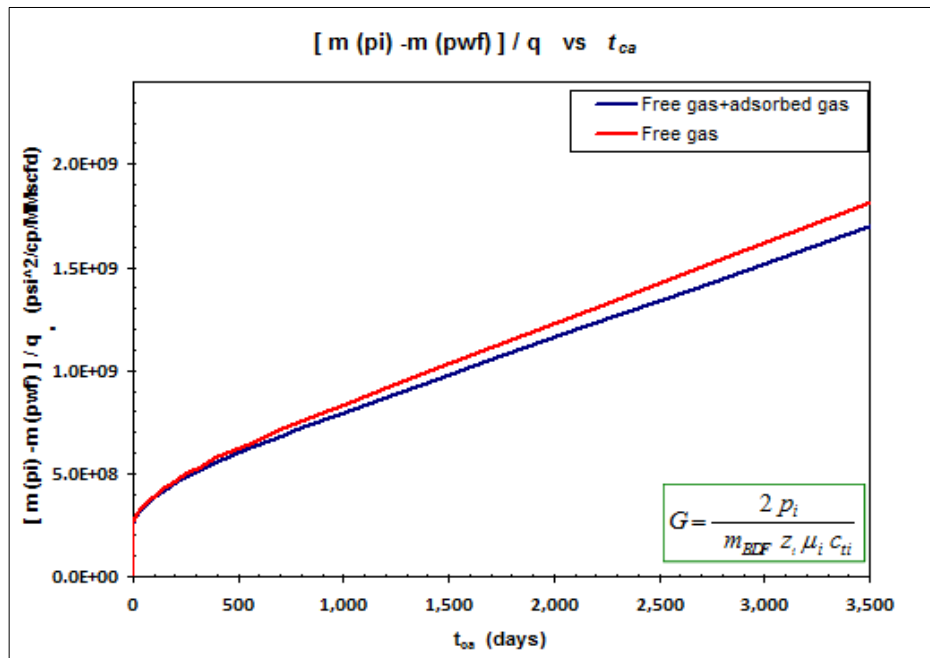


**Fig. E.2 —Plot of  $[m(pi) - m(pwf)] / q_g$  vs  $t_{ca}^*$  showing with and without adsorbed gas BDF with slope  $m_{BDF}$  used to calculate OGIP, simulated data.**

OGIP with adsorption:

$$G = \frac{2 p_i}{m_{PSS} z_i * \mu_i c_{ti} *}$$

$$G = \frac{2 \times 2950}{3.57E+05 \times 0.562 \times 0.0203 \times 3.38E-04} = 4290 \text{ MMscf}$$

From Fig E.3 estimated OGIP with and without adsorbed gas can be read directly on the x-axis as 2880 MMscf and 4300 MMscf respectively.

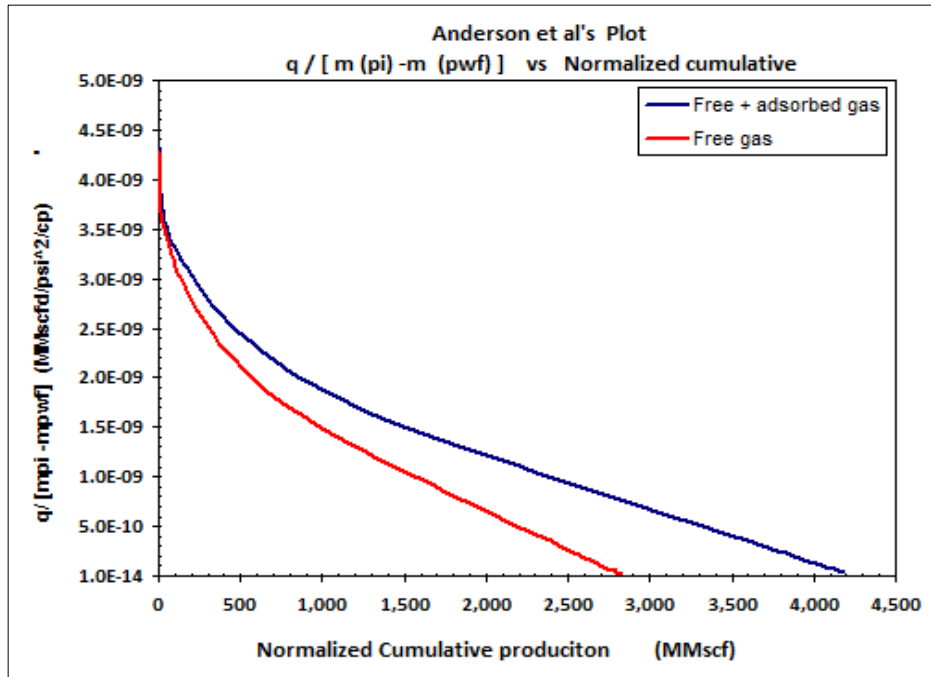


**Fig. E.3 — Normalized rate vs Normalized Cumulative with and without adsorbed gas showing OGIP on x-axis, Simulated data.**

#### OGIP estimation with and without adsorbed gas from Transient flow data.

From Fig. E.4 we can determine the following data.

<b>TABLE E.4— End of Transient Time and Slopes of Straight Lines Exhibited by Transient Flow Data With and Without Adsorbed gas.</b>			
<b>Without Adsorbed gas</b>		<b>With adsorbed gas</b>	
$t_{esr}$ , days	15.5	$t_{esr}$ , days	15.0
$m_{BDF}$ , slope	17777.8	$m_{BDF}$ , slope	15686.3

Data from Table E.3 is used in Eq. 4.5.3 to calculate OGIP

$$G = f_{CP} \frac{200.8 T}{\phi(\mu c_t^*)_i} \left( \frac{\sqrt{t_{esr}}}{\tilde{m}_{CPL}} \right) \left[ \left( \frac{\phi S_{gi}}{B_{gi}} \right) + \left( V_L \frac{p_i}{(p_i + p_L)} \right) \right] \dots\dots\dots 4.5.3$$

Calculate Dimensionless drawdown

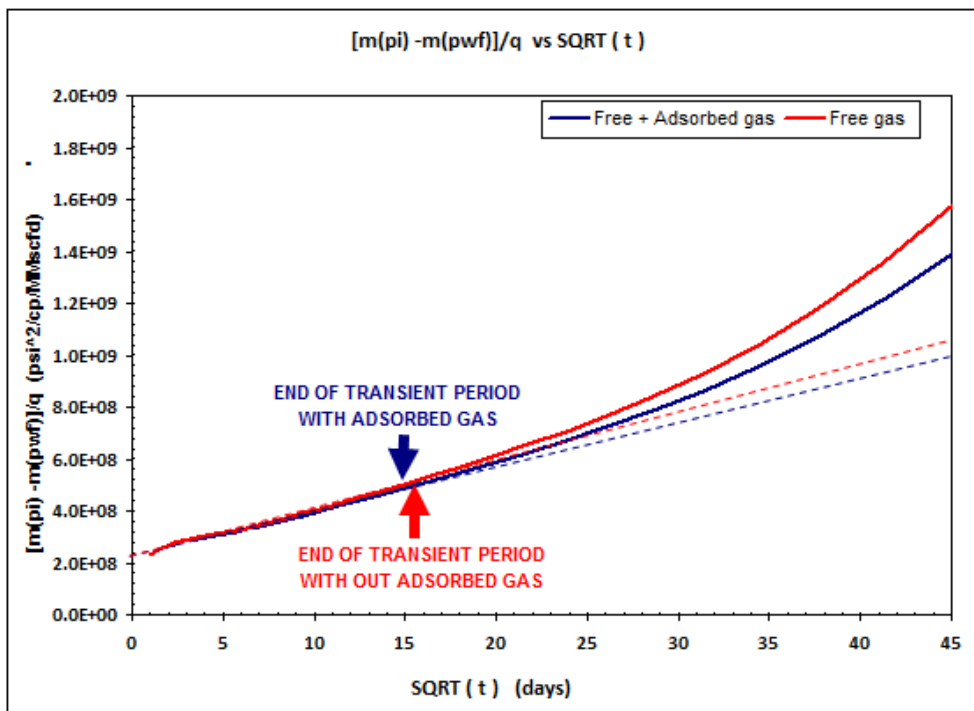


**Fig. E.4— Square of time Plot to determine end of transient time and slope of straight line exhibited by transient flow, simulated data.**

$$D_D = \frac{m(p_i) - m(p_{wf})}{m(p_i)}$$

$$D_D = \frac{(6.02E+08) - (2.47E+07)}{(6.02E+08)} = 0.96$$

$$f_{CP} = 1 - 0.0852(D_D) - 0.0857(D_D)^2$$

$$f_{cp} = 1 - 0.0852(0.96) - 0.0857(0.96)^2 = 0.84$$

OGIP with out adsorbed gas:

$$G = \frac{0.84 \times 200.8 \times 610}{0.06 \times 0.0203 \times (3.05E-04)} \left( \frac{15.5}{17777.8} \right) \left[ \left( \frac{0.06 \times 1}{0.00503} \right) + \left( \frac{0 \times 2950}{(2950 + 0)} \right) \right] = 2880 \text{ MMscf}$$

OGIP with adsorbed gas:

$$G = \frac{0.84 \times 200.8 \times 610}{0.06 \times 0.0203 \times (3.38E-04)} \left( \frac{15.0}{15686.3} \right) \left[ \left( \frac{0.06 \times 1}{0.00503} \right) + \left( \frac{7.72 \times 2950}{(2950 + 650)} \right) \right] = 4360 \text{ MMscf}$$

<b>TABLE E.5—Summary of OGIP Estimates</b>				
<b>OGIP, MMscf</b>	<b>Simulation</b>	<b>BDF: Palacio &amp; Blasingame</b>	<b>BDF: Ibrahim, Wattenbarger and Helmy</b>	<b>Transient flow data</b>
<b>Without adsorbed gas</b>	2900	2990	2881	2880
<b>With adsorbed gas</b>	4345	4237	4290	4360

## VITA

Name: Salman Akram Mengal

Address: Harold Vance Dept. of Petroleum Engineering  
TAMU, College Station TX 77843-3116.

Email Address: kohee888@ yahoo.com

Education: M.S., Petroleum Engineering  
Texas A&M University  
College Station, USA, 2010.

B.Sc., Petroleum Engineering  
University of Engineering and Technology  
Lahore, Pakistan, 2003.